Design and Analysis of Velocimetry for Supersonic Sled System

A thesis

submitted in fulfillment of the requirement

for the award of degree of

DOCTOR OF PHILOSOPHY

in

ELECTRONICS & COMMUNICATION ENGINEERING

by

Praveen Kumar Khosla

Supervisor

Dr Rajesh Khanna
Professor,
Electronics & Communication
Engineering Department, Thapar
University, Patiala,India

Supervisor

Dr Sanjay P Sood
Principal Design Engineer,
Centre for Development of
Advance -Computing (CDAC)
Mohali, Punjab, India

DEPARTMENT OF ELECTRONICS& COMMUNICATION ENGINEERING

THAPAR UNIVERSITY

PATIALA-147004 (INDIA)

Oct 2015

Certificate

I, **Praveen Kumar Khosla** hereby certify that the thesis entitled "**Design and Analysis of Velocimetry for Supersonic Sled System**" which is being submitted by me to **Department of Electronics & Communication Engineering, Thapar University, Patiala** in fulfillment of the requirements for the award of degree of "Doctor of Philosophy" is a record of bonafide research work carried out under the guidance and supervision of **Prof. (Dr.) Rajesh Khanna and Dr Sanjay P Sood**. The matter presented in this thesis does not incorporate without acknowledgment any material previously published or written by any other person except where due reference is made in the text.

(Praveen Kumar Khosla)

Reg. No.: 950906003 **Dated: 21st July, 2015**

This is to certify that the above statement made by the candidate is correct and true to the best of my knowledge and belief.

Dr Sanjay P Sood
Principal Design Engineer,
Centre for Development of
Advance Computing (CDAC)
Mohali, Punjab,
India

22/07

Dr Rajesh Khanna
Professor,
Department Of Electronics &
Communication Engineering,
Thapar University, Patiala
India

23/7/15

Abstract

Knowledge of precise velocity profile of aerospace bodies is essential in research programs-especially now when operating speeds are going much beyond supersonic regimes. Not much research has been reported on velocimetry of such systems. It was therefore considered essential to carry out in-depth study and research of various feasible techniques for high velocity measurements of bodies moving on rail system at supersonic speeds to give fillip to various research programs in defence and space domain. The research centre, where the testing of such systems is carried out, has a precision rail track on which the test articles such as parachutes, unmanned aerial vehicles, missiles and fuses etc are test run at required high speeds. It provides a unique environment for captive flight testing and enables experimentation at high velocities and accelerations for short durations. The research, elaborated in this thesis, was carried out at this facility.

While considering various techniques for determining velocity, it was realized that velocity could not be directly measured by any of the known techniques on the rail system. On the other hand, there were several techniques for velocity derivation from other parameters. Out of these, three such techniques were shortlisted for carrying out in depth studies. The identified techniques were based on different primary measurements of - position, acceleration and pressure-which, finally lead to the derivation of velocity.

Literature published half a century ago points to the use of position based measurements in rocket sled applications on the rails on which magneto inductive sensor were deployed. Thereafter, the field remained un-explored. It was found that magneto-inductive sensor output falls with the increase in velocity and it was not usable at speeds beyond 500 m/s. Simulation of such a system was carried out to understand the reasons for the problem. The outcome of the research was non-obvious. The study suggested reducing the number of turns of the inductive sensor, rather than increasing it, lead to increased amplitude at higher velocities. Based on the studies, the existing sensor was improved accordingly and experiments were conducted to validate the proposition.

The experiments were first conducted on a ground based rotor (figure 3.15) and then rail track. Relative error of the order of 0.046% was computed in one of the test configurations. The comparison between existing and proposed sensor, at feasible velocity of 303 m/s, indicated significant improvements in new design. Easy calibration of this system was feasible. The velocity derived from such a distance based techniques acted as a reference for other techniques.

It is well known fact that measurement of acceleration can lead to velocity. But its practical implementation leads to host of errors. Research also focused to quantify these errors. Two different solutions were worked out to measure velocity after mitigating these errors. Some of the methods employed included identification of improved method of integration, capping and filtering, bias correction, sensor mounting, reduction in RMS noise, position fix and the like. Under identical conditions, specially developed DSP processor based on-board measurement system included three accelerometers of different makes, which measured linear acceleration in the same direction. The result with one of the sensors was within 1.5% of reference values. These experiments were completed by the year 2014. Thereafter, a method of data fusion was developed which offered similar results. It obviated the use of position fix and the associated hardware.

Another technique involved was using pressure as primary measurement. Aircrafts use pressure transducer based Pitot tube to compute velocity. Study of its adaptation to rocket sled motion, associated challenges and its comparative performance was studied. Expression establishing relationship between Mach number or velocity with pressure were derived and were tailored to needs of rocket sled usage. Application specific Pitot tube, acquisition and logging system was developed so as to conduct experiments. Velocity was successfully measured in two different experiments. The challenges encountered in the process have been explained.

It was surmised that there is no single technique which has all the advantages over the rest of the techniques. It was also found that magneto-inductive system offers highest accuracy but its initial cost of installation is high. The acceleration based system is easy to deploy, inherently reduces noise, gives more number of measurement points and is economical. The comparative study of the three techniques is elaborated in the concluding section. The domain of velocimetry is vast and diverse. Challenges have been overcome in adopting technologies to a new application. The findings of this research would improve upon the knowledge base about this ever expanding field.

Acknowledgments

Firstly, I thank almighty for His blessings. It is through His strength that I could pursue a doctoral degree.

As I discover myself at the tail end of this work, I recollect many indispensable events that enabled its completion.

I am undoubtedly thankful to all those who were of help to me directly or indirectly, during the course of my research work. I owe them my gratitude.

I feel proud to be a student of Dr. Rajesh Khanna. With great pleasure and a deep sense of gratitude, I wish to thank for his continuous and invaluable guidance as well as his timely advice that contributed greatly to the completion of this dissertation. He allowed me to work on the topic of my interest. He cheerfully spared time beyond working hours and on holidays to review my work, speaks volumes about his active involvement. His profound technical insight, enduring effort and vision has helped to give the proper shape to this dissertation. But for his thought-provoking guidance and never-ending encouragement, this dissertation would not have been possible.

A big thanks to the co-supervisor Dr Sanjay P Sood for motivating me to take up the PhD programme, inspiring me from time to time, easy accessibility and helping me on "what next" decisions.

I would like to express my sincere gratitude for the entire administration and management of Thapar University for supporting me in achieving one of the most important goals of my life. I have great pleasure in expressing thanks to Director of Thapar University for his direct and indirect support. I greatly acknowledge Dr Sanjay Sharma, Head ECED, TU, my doctoral research committee members Dr. AK Chatterjee, DrRavinder Aggarwal and Dr OP Pandey, Dean Research for closely monitoring and sharing their valuable inputs in completing this work. Their watchful way of analytically promoting and monitoring research activities helped me immensely in completing my assignment.

I would like to acknowledge and express my sincere gratitude to Dr Manjit Singh, Director TBRL, Dr DR Saroha, Chairman, publications review committee, all Scientists and staff of RTRS for supporting me from time to time. My special thanks to Gp Capt GS Sandhu (Retd) for sparing valuable time to give me directions and carry out constructive and effective reviews.

I find no words to convey how happy and contended I feel to acknowledge my parents, Sh. SP Khosla and Smt. Raj Khosla, that it is only your blessings, continuous interest and confidence in me which made me what I am today and for instilling in me a love for learning. The moral and ethical values which you have imbibed in me always showed me a path of hardships.

Last but not the least, I understand and value all the cooperation, help and the sacrifices my wife, Ranjna, as well as my sweet daughters Ms. Prerna and Ria had to undergo. I also regret to say that I could not support Prerna in her studies where she needed my support so badly. I would like to thank my wife, Ranjna, for enduring a seemingly endless ordeal, for sacrificing some of her best years so that I could finally finish this research work. I wish to tell you something you know it is only now, I am able to complete my work because of your true love, support, patience and caring nature.

(PK KHOSLA)

CONTENTS

List of Figures

List of Tables

Acronyms and Abbreviations

Accel	Acceleration
ASIC	Application Specific Integrated Circuit
DSP	Digital Signal Processing
emf	Electro Motive Force
GAGAN	GPS Aided Geo Augmented Navigation
GPS	Global Positioning System
ILD	Inductive Loop Detector
INS	Inertial Navigation System
MEMS	Micro Electro Mechanical Systems
PIV	Particle Image Velocimetry
RTRS	Rail Track Rocket Sled
UAV	Unmanned Aerial Vehicle
WAAS	Wide Angle Augmentation System

Glossary of Symbols

Symbol	Glossary of symbols used in Chapter 3
B	Magnetic flux density
μ_0	permeability of free space in Tesla.metre/Amp
p	Pole strength
R_n	radial distance from north pole to the center of coil
R_s	radial distance from south pole to the center of coil
y_1	the vertical distance of the coil center from the two poles
B_y	Magnetic flux density along y axis
N_c	Number of turns in coil
R_L	ohmic resistance of load
L_c	Inductance of the coil
A_c	core cross-sectional area in m^2
e	induced emf
U	Sled velocity
Z_{sh}	impedance
R_S	line resistance
i	current through coil
R_{op}	output load resistance
v_{op}	output voltage
μ_c	resultant permeability of the core
l	Coil length
lc	core length
f_r	nominal frequency
Z_c	total impedance
C_i	Current coil
C_{i-1}	Coil before current coil
C_{i+1}	Coil after current coil
s_{i-}	distance between C_i and C_{i-1}

t_i	time of arrival of sled at C_i
t_{i-1}	time of arrival of sled at C_{i-1}
v_{av+}	Average velocity between C_{i+1} and C_i
s_{i+}	distance betweenC_i and C_{i+1},
t_i and t_{i+1}	time of arrival of sled at C_i and C_{i+1}
a_i	Acceleration at C_i
v_i	Velocity at C_i
S_{min}	minimum distance between two sensors
Δs	error in measurement of distance S_{min}
Δt	error in measurement of time T_{min}
T_{min}	minimum time between two pulses from inductive pickups

Symbol	**Glossary of symbols used in Chapter 4**
Δs	error in measurement of distance
S_{min}	minimum distance between two sensors
Δt	error in measurement of time
T_{min}	minimum time between two pulses from inductive pick up
C_f	capping factor
	correction coefficient
Sc	sensitivity constant
Ga	Gain

Symbol	**Glossary of symbols used in Chapter 5**
p_0	total pressure
p_s	static pressure
v	velocity of sled relative to flow
R	specific gas constant

T_s	ambient temperature
p_s	static pressure
ρ_0	density of fluid at point of stagnation
ρ_s	density of ambient air where trial is conducted
	Mach number
γ	specific heat ratio; it's value for air is 1.4

List of Publications

Published in SCI Listed Journal

[1] P. K. Khosla, R. Khanna and S. P. Sood, "Analysis of Magneto-inductive System for rocket Sled Velocity Measurement Beyond Mach 1.5", *Defence Science Journal,* vol. 64, no. 2, pp. 143-151, Mar. 2014.

[2] P. K. Khosla, R. Khanna and S. P. Sood, "Quantification and Mitigation of Errors in the Inertial Measurements of Distance", *MAPAN – Journal of Metrological Society of India*, vol. 30, no.1, pp. 49-57, 2015.

Published during the period of reported research with indirect relevance

[5] P. K. Khosla, S. P. Sood, R. Khanna *et. al.,*"Wireless Telemetry System to Expedite Thrombolytic Treatment" in *National Conf. on Emerging Medical Instrumentation from 11th May, 2010 to 12th May, 2010*, Chandigarh, pp. OP-3.6, 2010.
(Extracts of this paper appeared as a news in The Sunday Tribune of 16th May, 2010)

Chapter 1

1 Introduction

With the scorching pace of advancements in aircraft, missiles, rockets and aerospace systems designs - the operations are being progressively towards upper levels. The test and evaluation of their performance becomes critical and ever important. Airplane designs were earlier studied in flight testing by trial and error. But, these trials being too expensive and dangerous, wind tunnels were developed to investigate the performance of proposed airplane designs [1]. The requirements of dynamic testing grew beyond the aircraft testing. To bridge the gap between free flight testing and wind tunnel testing, Rail Track Rocket Sled (RTRS) facilities came into being in some of the countries such as USA, India, UK, France etc. Rocket sled testing has proven to be a useful tool for evaluating the functional performance of aerospace systems. Sled testing can be used to evaluate the performance of new prototype system designs as well as the performance degradation or design enhancement of existing systems, the latent design problems which percolate to the flight trials get detected when subjected to testing on the rail tracks.

Rail Track Rocket Sled, as shown in figure 1.1, is a National Test Facility in India, which offers possibilities of dynamic testing in short duration over large range of velocities and acceleration. The RTRS, is a precision, highly-instrumented facility which has found extensive use in the quantitative error evaluation of state-of-the-art systems under captive flight conditions. The sleds, carrying the unit under test and extensive monitoring instrumentation, which are subjected to a positive and negative acceleration profile tailored to both simulated missile environment, can be rigorously tested. While thrust is provided by rocket engines, deceleration has traditionally been accomplished by sand brakes. The Rail Track Rocket Sled National Test Facility is used for dynamic testing of parachutes, ejection seat of an aircraft, safety arming mechanism, ejectable components, impact studies, energy absorber for aircraft and a host of other aerospace applications.

Figure 1.1: Work centre for this research - Rail Track Rocket Sled facility

RTRS is the work centre for carrying out experiments on topic of this thesis. While the subject research was conducted, the track was concurrently augmented to penta rail supersonic track (figure 1.2). Further, development of measurement technology, similar to other technologies, is driven by the needs of potential users [1]. The accurate measurement of the distance travelled, velocity and acceleration at low velocities to supersonic speeds is an active area of research. The precise measurement of velocity is of utmost importance against which the performance of test articles can be evaluated. These test articles are un-manned aerial vehicles, parachutes, missiles and sub-systems of missiles etc. The item to be tested is mounted on a sled. The sled is propelled down the rail track using rocket motors. This thesis investigates the real-time, high velocity and acceleration determination using various techniques.

1.1 Importance and Need of Velocity Measurement

Velocity is a vital parameter of a moving body. Often the performance of the moving body is tested against such a parameter. All sub-systems of the moving body need to perform while moving in intended range of velocities. Thus, velocity measurement becomes an important parameter for evaluation of moving bodies. Lack of knowledge of velocity will impair the testability of moving bodies.

Figure1.2: The penta rail supersonic track which got augmented in the course of these studies

Therefore, it was found essential to study various feasible techniques which can be implemented on bodies moving on rails at high speed. With scientific development, the accurate velocity measurement of a fast moving object is drawing more and more attention [2]. These moving bodies encompass a scope of activities around us. These measurements range from measurement of velocity of blood flowing in the arteries [3] to the velocity of a missile coming from enemy territory. Each of these has its own importance and poses its own set of challenges. The ranges of velocities in the area of interest are low velocity (1-10 m/s), intermediate velocity (10-100 m/s) and high velocity (100-1000 m/s) [4]. The author of this thesis aims at measurement of high velocities.

There are varieties of fast moving objects. Some of these objects are used in on-board applications. Typical applications are in aircrafts, satellites, missiles, rockets and other mobile platforms. These products need to have high level of reliability as the cost of failure is many times more than the product itself. After the development of onboard products, these are lab tested. Thereafter, if these products are flight tested, any failure would jeopardize the mission and involve enormous cost. To bridge the gap between lab testing and free flight testing, captive flight testing of unit under test (UUT) is carried out at RTRS. The UUT is mounted on a sled. The sled is propelled down the rail track using rockets. To evaluate the performance of the UUT a number of parameters need to be monitored. The facility provides unique venue for conducting studies in capturing various parameter and communicating the same from mobile platform to static monitoring points. In this thesis development and implementation of velocimetry for supersonic sled has been carried out. The velocity so acquired will be communicated to ground using wired and wireless techniques. It would also involve addressing a host of issues that would crop up in measurement of velocity of high speed sled and especially, while communicating the parameter to ground based monitoring centre.

Requirement of Accuracy for measurement of velocity

For evaluation of physical phenomenon, the requirement of accuracy in the range of better than 1% is not there. But while evaluating the electronic units such as Inertial Navigation System (INS) which measure velocity with an accuracy of 1 m/s after travel time of 10 sec or a Digital Miss Distance Indicator working on the principle of Doppler radar, need to be evaluated against system capable of measuring velocity with accuracy of 0.1%.

1.2 Objectives

Research is a reasoned investigation to describe, explain and predict the observed phenomenon so as to increase the stock of knowledge and apply this knowledge to devise new applications. The research establishes facts and enables us to reach new conclusions. The objectives of the research were

a) To develop different techniques for measurement of velocity and communication of the same to distant location using wired and wireless technology. The development would keep in view the constraints of its implementation in Indian context.
b) Implementation of the concepts of velocimetry to new application - supersonic sled tests. Determining the limitations of the implemented techniques and proposing two best out of three for use in future.
c) To validate the techniques and provide for redundancy in real life operation using the experimental data so acquired.

1.3 Approach

Inductive methods were used to analyze the observed phenomenon and identify the general principles. Further deductive methods were used to verify the hypothesized principles through experiments. One was to develop explanations, and the other was to test the validity of the explanations. Often the research ends with the simulation, but we have gone on to realize the associated hardware and validated results of simulation by testing hardware, too.

1.4 Velocimetry

Rate of change of position of an object in a particular direction is called velocity andvelocimetry is the measurement of velocity of a moving body. Velocity is not directly measured. It is derived from another measured parameter. The primary measurement of following parameters can lead to measurement of velocity

- Position
- Acceleration
- Pressure - Pitot
- Frequency - Doppler
- Heat & Resistance - Anemometer
- Interference of light
- Optical – Fiber, camera

It was found that techniques based on measurement of position, acceleration and pressure are feasible options for rocket sled application. Therefore, a detailed study was carried out, which covered and not limited to, the primary measurements based on position, acceleration and pressure. The research so carried out identified the problems in the existing sensors and techniques, analysis of the same and proposed improvements to be carried out. The errors and noised reduction techniques associated with sensors and algorithms based on position, acceleration and pressure were also researched.

1.5 Importance of the Work Carried Out

The metrics of success or failure of outcome of the global research & development effort is based on the measurement of vital parameters. Velocity is the most important parameter when we evaluate for the objects in motion.

The RTRS facility, which is the work centre for this research, simulates the flight condition on the rail track. Cost of some of the test articles is as much as Rupees 40 million, the operation is single shot, i.e., they are destructive and would last only a single trial of few seconds. If the velocity is not measured, the trial has to be repeated and the expenditure incurred again!

For example, a brake parachute of an aircraft is used to slow down the aircraft while it lands. The drag offered by the parachute depends upon square of velocity. While testing it on the rail track rocket sled system, the parachute is deployed at the specified velocity, which is same as the velocity of aircraft while it lands. The structural integrity of the aircraft shows whether it is cleared for use on aircrafts. Here, the developers of parachute will gauge the success of their system by accurate measurement of velocity of the parachute system on sled.

Similarly, in some of the flight vehicles, the wing opens when it is in flight. The simulation on the ground demands the forces acting on wings should be same as the forces it experiences in flight. So, equivalent velocity on the ground is determined and the trial carried out. Here, the evaluation trial will not be a success if the velocity is not measured accurately.

Therefore, lack of accurate measurement of velocity can, in few seconds, result in a loss of millions of rupees.

1.6 Thesis Organisation:

The thesis is organized in five chapters which are briefly explained as below

1.6.1 Briefs of Chapter 1

Introduction to the research carried out is given in chapter 1. The importance of velocimetry, objectives of the research, approach to the studies, and importance of work centre and the work is described in this chapter.

1.6.2 Briefs of Chapter 2

To start with, in the second chapter a detailed description of various velocimetry techniques, which are feasible, are presented. Parallels are drawn from other diverse and tangential applications to explore its utilization in the current studies. Some of the topics explored include, but not limited to, domain of velocimetry are particle velocity, blood flow in the veins to velocity of bodies moving at supersonic speeds. Some of the examples include laser Doppler velocimetry, which is a technique used to measure linear velocity, and cover applications ranging from velocity of exhaust gases to blood flow[5].

1.6.3 Briefs of Chapter 3

Aligned to the objectives of research, this chapter contains the research carried out on one of the proposed techniques. This chapter explains how, the velocity of the sled moving along the track is determined by sensing the position where the sled reaches with reference to the time. At RTRS, the test articles to be evaluated are mounted on specially designed sleds, which slides and accelerates down the rail track, to the desired velocity using solid propellant rocket motors. The measurement of sled velocity at regular distances is carried out through a magnet and coil system. A U-shaped (or horse-shoe) magnet is mounted on the sled and inductive pickups are fixed along the rail track at 10 m separation from one another. Now as the sled moves along the track, the magnet on the sled passes over the coil on the ground. The emf pulse induced in the inductive pickup propagates to a computer at the monitoring point, which is up to 4.5 km away. The signal pulses propagate through the multiplexed cables. Although use of inductive pickups for measurement of sled velocity was reported more than 50 years ago as mentioned byBeutler[6] and [7], but even now the interest in these systems continues to grow. This is mainly because of the fact that the network of magneto-inductive sensors can be installed over distances of several kilometers and yet they give large signals without need of any excitation or signal conditioning and the feasibility of sensor being fabricated by user. Use of accelerometers in combination with coils has also been reported [8], are relevant in the present context. A feasibility study to measure velocity using interferometry [9] has been carried out but no further development has been reported. In this study the signal pulse from network of magnet and coil arrangement has to propagate distances as large as 4.5km. The advantage of proposed system is that the sensor is passive, that is, there is no excitation or active circuit and the arrangement is maintenance-free. The moving magnet, generates an approximately sinusoidal voltage signal in the pickup coil which is transmitted through a shielded twisted pair to record the corresponding 'instantaneous' event time in the data acquisition system. The sled velocity is computed from such recorded event intervals and the known separation distance between the fixed coils. The study helps the readers understand the limitations of pickup and how to improve it so as to capture faster phenomenon.

1.6.3.1 **The problem in the sensor and improvements carried out**

When experiments were conducted at velocities up to 500 m/s, it was found that the signal amplitude reaching recording device reduces with the velocity. The facility was being upgraded so as to attain velocities up to 1000 m/s. It was obvious that the existing arrangement will not work beyond 500 m/s. A detailed study was done to identify the problem and further improvements were carried out in the sensor. The experiments were also carried out on the improved sensors under the given constraints of maximum attainable velocities.

The detailed study pointed out that with increase in velocity, the induced emf increases. In open circuited coil, this indeed is the case. But problem is that when load is connected, the terminal voltage across load decreases. This is due to the fact that as the induced voltage causes current to flow which in-turn makes a back emf L di/dtto get developed. It also increases with the velocity. So, desirable component $e= N\, d\varphi/dt$ increases and undesirable opposing component $e_b=L\, di/dt$ also increases. The solution was worked out by reducing N, which reduced desirable component e, but undesirable e_b reduced more rapidly as $L\infty N^2$. Now the reduction in e_b is more than the reduction in e. This property is exploited in bringing about improvement in the sensor. If N is made ¼ the e will become ¼ but e_b will become 1/16. This results in increase in terminal voltage across load resistance.

The simulation results exploiting this property indicated significant improvement in amplitude of the signal acquired from pick up sensor. This was followed by the experiments at feasible velocities. The rotor (figure 3.15) based experimental set was rigged up which validated results at low velocity. Further, the experiments on rail track validated results at higher velocity. The findings of the simulation results which were validated by experiments have been elaborated in this chapter.

1.6.4 Briefs of Chapter 4

This chapter explains how the distance is derived from a number of accelerometers. It covers an accurate distance measurement method which was developed, tested and experimentally verified. This chapter describes accelerometers, with different noise density, identically moving, were chosen for sensing forward motion. A number of measures such as different mountings, bias correction, capping, digital filtering and position fix were tried in a practical implementation. To keep the measurement error within tolerable limits, a novel method of obtaining position fix was devised by using a pair of magneto-inductive sensors. The bias correction was applied in the position to derive corrected velocity and acceleration. To know the truthfulness of results and to validate the proposed methods, a system was developed to generate reference values for computation of error. This reference system had a relative error of 0.046% which was much better than reported in earlier study. After mitigation of various errors using proposed methods, an error within 1.5% was attained with one of the sensors used in trials. The work carried out helped in identification of the elements which contribute to errors, quantify the mitigated errors in some cases and highlights the measures which bring about significant improvement in error. It also suggested how to obtain more accurate results using economical Micro Electro Mechanical Systems (MEMS) based accelerometers.

This chapter further explains how the data fusion from three sensors is done so as to obtain results comparable to the ones explained earlier, without using the position fix and the associated additional hardware. Elimination of need of additional hardware is of immense importance in on-board applications.

1.6.5 Briefs of Chapter 5

This chapter explains the adaption of Pitot to supersonic sled applications. The measurements were carried out by measuring total pressure in a Pitot tube. In the context of sled motion, it explains that no single formula can derive velocity from pressure as the pressure that reaches the sensors gets modified due to the different flow regimes. The velocities of interest were divided into three different flow regimes and a formula was derived which explains the relationship between the mach number and the pressure. The Mach number is used for determining the velocity. It was identified that much of the errors in use of Pitot in aircraft applications are due to the error in

measurement of static pressure. In the application understudy the ambient pressure was recorded to act as the static pressure, thereby eliminating the static pressure transducer form Pitot, which is so essential in other applications of Pitot.
The chapter further explains how such a sensor can be realized which can measure pressure during sled motion. The details of experiments conducted in this regard, to validate what has been mentioned above, are described. Some of the limitations that emerged are also explained.

1.6.6 Briefs of Chapter 6

It compares the three techniques, namely, distance time based, acceleration based and the pressure based. The compliance to pre-defined objectives is mentioned in this chapter. Findings of each of these and the conclusions are drawn. The distance time based results are taken as reference values and the results of other two techniques are compared with it. The results are discussed. A fourteen point table brings out the comparative study of each technique. The conclusion of the research is written and the future scope is defined.

Chapter 2

2 Literature Survey

The work of velcoimetry is utilized by defence and civilian sectors of a country. Research work proposed in this thesis has got immense defence applications and has great thematic relevance when theme is self-reliance. However, not much work relevant to defence technologies is available in open sources. Although some work related to gouging, sled design, track alignment, sled vibration etc has been reported, which does not support present research, but there are hardly any publications directly relevant to velocimetry for rail track rocket sled facilities. On the other hand domain of velocimetry is vast and covers wide range of applications such as velocity of particles, flow of water, blood flow in the veins, bullet, vehicles, aircrafts, Unmanned Aerial Vehicle (UAV) and the like. Literature survey revealed that some work, which is tangential to this research, has been reported, but is of immense value to this study. Some of the techniques which were relevant to the topic of research are mentioned in section 1.4. The following sections elaborate the literature survey carried out in this regard.

2.1 Position Sensors

Variety of position sensing techniques are explained in [10] and the references there in, include induction loop detectors and the magnetic sensors. These are broadly used to count vehicles on the roads and are accompanied with the host of false alarms and misses for different category of vehicles.

The basic principles of inductive position sensors are explained in [11] and their utility in automotive, user interfaces, and utility metering using low cost sensors is claimed. The accuracy of the order of better than 1% of full scale is mentioned. The problem in hand targets accuracy better than these claims.

2.1.1 Magneto-Inductive Sensors

Magnetic sensors have helped mankind in sensing, analyzing and controlling thousands of functions for many decades. The use of such as sensor was reported half a century ago in research papers [6] and [7]. The research reported in chapter 3 of this thesis explains how the improvements in magneto inductive sensors brought about the measurement of supersonic velocities in the gamut of velocimetry. Authors of [12] have widely covered the field of magnetic sensors and their applications which are described in the following text.

Magnetic sensors can be classified according to whether these sensors measure the total magnetic field or the vector component of the magnetic field. The techniques used in both types of magnetic sensors fall in the domains of physics and electronics. Although magnetic tape drives using magnetic sensors are not in vogue, but it is still a popular technique of mass storage in data centers. Airplanes fly with high degree of safety standards due to high reliability of noncontact switching using magnetic sensors. Due to high reliability automobiles predominantly use magnetic sensors to determine position in places such as the engine crank shaft and wheel braking etc. Factories have higher productivity and maintainability because of the stability, repeatability and low cost of magnetic sensors. A common theme among all applications is that magnetic sensors provide a very rugged, reliable, and maintenance-free technology. These important advantages are also relevant to defence applications.

There are many ways to sense magnetic fields, most of these rely on the proximity between source of magnetic field and connection between magnetic and electric phenomenon. In the current research, the property of proximity has been exploited. Use of Coil and Magnet for sensing position in a similar application is mentioned in a report [13] - but, no technical details have been elaborated beyond the mention of usage.

2.1.2 Linear Induction Motor in High Speed Application

The author [14] does discuss the velocity regimes up to 1200 m/s and distances of the order of 3 km, which are similar to the case of this research. But the focus of the study was more on theory of possible utilization of linear inductions motor as a propulsion system in track testing of vehicles rather than velocimetry.

2.1.3 Inductive Loop Detector (ILD)

Basic traffic data is largely based on road sensors embedded in the pavement. Such sensors mostly use inductive loop detectors (ILDs) and are capable of measuring temporal traffic characteristics. The basic parameters needed by operational traffic engineer, such as traffic volume, occupancy and speed at a given point etc is detected by such systems. Other fixed sensors such as optical detectors, ultrasonic detectors were also developed and used for network surveillance. These fixed sensors are very useful, but such sensors fail in measuring spatial behaviour of traffic. In addition they suffer from their limited reliability, with their exorbitant cost in attaining significant coverage of the roadway network. A recent report [15] covers the use of ILDs signature technology to classify vehicles in a section of roadway. Since the ILDs are provide localized information, such as on a traffic light, it does not hold potential for longer length rail tracks.

2.1.4 Other Position Sensing Techniques

Some of the position sensing techniques such as electrically powered wire, computer vision, magnetic sensing, optical sensing, inertial navigation and global positioning systems (GPS) are mentioned in [16]. The author covers use of moving magnetic position markers and stationary sensors in vehicle and robot applications, which are expected to be operational in lower velocity regime.

2.2 Acceleration Based Techniques

Accelerometers and gyros are used in missiles to determine acceleration, velocity, position and trajectory [17]. Use of accelerometers has direct relevance whereas the use of gyro for correction due to rotations will not be required in the application under study as the test article moves along the straight line path of rails.

Looking for radically different approaches, on lower end of velocity spectra, walking velocity of humans was also studied [18].

Research community is actively working towards bridging the gap between the performance of low cost MEMS and the high performance accelerometers having prohibitive cost. This is a rapidly expanding domain. The research carried out concentrates on this class of sensor as a potential application.

2.2.1 Recent trends in MEMS based accelerometers

The trends given in [19] are elaborated in the following text. The impetus to growth of MEMS accelerometers was due its usage in cell phones for image rotation, pedometer and sensor based apps. These sensors have also found their way into pens, shoes, cattle, vehicles, pavements [20] and the like. Monitoring of chewing and eating habits of cattle has been reported in [67]. The accelerometer penetration in mobile phones is growing at the rate of 64%. There is explosive growth in consumer MEMS market. Acceleration sensors have helped it grow to multi-billion unit market. It is expected that the sensing nodes will grow to trillions by the turn of this decade. These pointers imply that the acceleration in this field should happen primarily due to a massive adoption of sensors, especially enabling the wireless and Internet connectivity.

Use of accelerometer for effective position estimation is given in [21]. The paper further proposes a system of calibration. It also gives a procedure for evaluation of accelerometer in terms of sensitivity, accuracy and data reliability. Suitability of the accelerometer for short duration distance measurement [22] has been claimed.

2.2.2 Data Fusion

Information from multiple sources of data is combined so as to provide a better inference [23]. Data fusion is applied in diverse fields in civilian and military applications such as surveillance and reconnaissance, wildlife habitat monitoring, and detection of environment hazards [2–5]. Several methodologies have been proposed in the literature for the purpose of multi-sensor fusion and aggregation under heterogeneous data configurations. Due to the different types of sensors that are used and the heterogeneous nature of information that needs to be combined, different data fusion techniques are being developed to suit the applications and data. These techniques were drawn from a wide range of areas including artificial intelligence, pattern recognition, statistical estimation, and other areas. Since this research proposes to use variety of techniques, data fusion holds a good promise for its application in the current problem.

2.3 Pressure Based Measurements

Various techniques for measurement of velocity of flow of water have been appraised in [27] and the use of Pitot tube for such applications has been explained. Use of sound pressure level to study the property of liquid sheets is also reported [28]. Two co-linear water jets, whose velocity can be varied, form thin planar liquid sheets. It is excited by the acoustic wave, whose frequency and sound pressure level is changed to see the threshold at which the sheet remains unaffected.

The basics of Pitot tube are explained in [29], which describes how velocity of air flow can be determined using differential pressure transducers. It further mentions ways to improve accuracy of measurement of velocity. Some of these measures can be implemented by knowing the relative humidity, temperature, barometric pressure and placement of Pitot tube. Its calibration in a wind tunnel will also improve accuracy. The findings of the paper are useful for the present research, but the author recommend use of a computer which can handle data from variety of sources such as temperature, humidity etc. The study for rocket sled application requires motion of sensors and data acquisition system along with the sled. Chapter 5 elaborates utilization of Pitot tube research on pressure based velocimetry.

It has been reported [30] that velocity of projectile can be measured by using a pressure sensor. If the velocity of projectile is supersonic, a shock wave travels ahead of projectile. It has been found that the velocity can be computed by measuring pressure profile of the shock wave using piezo-electric pressure sensors. The limitation of such a technique is that it will measure pressure only at location of sensor and that the sub-sonic velocities cannot be measured. Wherever pressure transducer is used, a signal conditioner, excitation and transmission will also be required at every point.

2.4 Other techniques

As there are wide varieties of applications that demand measurement of velocity, so are the techniques to meet the demand. Details of some of these techniques are mentioned in the following sections.

2.4.1 Laser based Measurements

Measurement of velocity using Laser Doppler velocimetry techniques have been extensively studied by several authors. The technique Laser Doppler velocimetry is used to measure linear velocity in applications ranging from velocity of exhaust gases to blood flow [24]. It is also used in studies of turbulence, measurement of wind speed and combustion [5]. These authors discuss principles of laser optics and give attention to the Doppler shift, the differential Doppler technique, signal processing techniques etc. A non contact method based on laser sheet, which determines the velocity of a projectile has been reported [4]. The projectile blocks and unblocks the laser as it progresses in the path. Mathematical formulation has been developed to determine the velocity of projectile.

LASER curtain based velocity measurement techniques have also been developed. The system of measurement is that the projectile passes through two laser curtains or screens which are distant apart [31]. The shadowgraphy is used at frame rates of 1 million frames / sec [26].

The technique can measure the velocity of rocket sled, too. But, it is suitable for measurement of velocity at one or two points only. Moreover, the system is proposed for small caliber projectiles, whereas the sled is a large object whose velocity needs to be determined. The rocket sled travels a distance of 4 km and velocity needs to be measured at at least 400 points. So this technique does not address the requirements of our study. The changes in the track bed conditions in the present application would cause error [25]. Further, the reflections from allied items of rail track and plume of the rocket would compound the problem and therefore this method was ruled out for further studies.

2.4.1.1 Laser Interferometer

Displacement and high velocity can be measured using laser interferometers. The basic theory of all fiber displacement interferometer is explained [2]. The application is useful in the study of shock and detonics.

2.4.2 Particle Image Velocimetry (PIV)

It is a Lagrangian technique explained in section 2.4.7.2. Here a tiny particle in a flow is illuminated by a double pulse laser beam. Illuminated particle appears as a bright spot in the photograph because of the flash of the laser light. Image processing software is called upon to measure the displacement between the bright spots. This displacement and the time difference between laser pulses gives the velocity.

Advances and advantages of using multi frequency in echo PIV in an application [3] have been highlighted.

2.4.3 Light Gates

In this technique the velocity of a projectile fired from gun can be measured using light gates of narrow width. In this case the interval between the light interruptions and the distance between the two is used to find the velocity. To measure the velocity of projectile in the range 200m/s to 500m/s, the use of light gates at muzzle has been reported [32]. Further, the same author also mentions use of images taken by high speed camera to measure the velocities between 400 m/s to 700 m/s on impact [33]. Both these methods operate in the velocity regime of our interest. But, both the methods can measure velocity when phenomenon is localized in an area of interest. In the application under study, velocity needs to be measured over distances of 12 km in three different dual rail tracks in open field. Although the principle of former method can be exploited, the techniques, as such, are not suitable.

2.4.4 Velocity Using Mobile Phones

Work has also been done to find the velocity of movement of mobile phones. Analytical models have been developed to find distance and velocity by utilizing knowledge of directional movement of mobile phones [34]. The same authors have also suggested the use of movement of pixels and arrive at position, velocity and acceleration in a computer game [35]. Further work on establishment of independence or dependence of present velocity of a mobile node in a network on previous time step is also reported [36]. The work of this nature lacks hard real time capability, which is one of the requirements of the application under study in this thesis.

2.4.5 Modulated Waves

Some studies have been carried out on measurement of velocity of medium through which wave travels and the distance travelled by the moving object using frequency modulated sound or ultrasound. A mathematical model has been proposed to extract information about distance and medium velocity from electrical signal [24]. The method is useful for small distances and medium velocities. This study does not explain the measurement of high velocities over larger distances, which are of our interest in this study. But velocity of medium such as air is of importance in determining velocity of vehicle moving on rails while using Pitot tube.

2.4.6 Measurement of Velocity of Trains

Trains as well as rocket sleds have similarity in the sense that both move over rails. Odometers are used for measurement of velocity of trains. The velocity is determined by counting wheel increments and measuring the corresponding period. The wheel slips over the rails and its radius changes due to worn tread [25]. This causes errors in the measurement. As no wheels are used in rocket sled, this method was not found suitable for research.

2.4.7 Additional Velocimetry Techniques

2.4.7.1 Linear Velocity Transducer

It consists of a rod of permanent magnet, called core, over which two coils are wound. The output of the two coils is proportional to the velocity of the core. The range is limited to few mm. So it was not found suitable for rocket sled application.

2.4.7.2 LagrangianVelocimetry

It is used to measure velocity of fluid. A fluid particle is identified and its displacement is tracked. It is assumed that velocity of particle and fluid is same, that is, it is tiny particle which is seeding the flow. Time derivative of displacement leads to velocity.

2.4.7.3 Eulerian Velocity

In Eulerian velocity measurement, the marked fluid particle is not tracked. Instead, a probe or a sensor is projected inside the fluid flow. Velocity is determined as function of time.

2.4.7.4 Hot wire anemometer

It works on the principle that rate of convective heat transfer from a hot object to the surrounding fluid flow is proportional to the speed of the fluid flowing around the object. Wind tunnels utilize this type of velocimetry. But, its suitable for lower end of velocity range, that is, less than 30 m/s only.

2.4.7.5 **Rotating velocimeter**

It is like a cup anemometer used to measure the velocity of wind by weather stations. In such devices open side (concave) of the cup experiences higher drag than the closed side (convex).Thus when wind blows, the shaft rotates. By measuring the rotation rate of turbine, the velocity can be inferred.

2.4.7.6 **Electromagnetic velocimeter**

Such devices are used to measure the velocity of conducting fluids. In such devices, a magnetic field is applied to the conducting fluid, such as sea water or molten metals. It causes induced emf and the resulting induced current to flows. Two electrodes are immersed in the fluid, the current carrying and moving fluid induces voltage into the electrodes. The velocity of fluid can be inferred from induced voltage.

2.5 Safety while conducting experiments

The present research heavily relies on experimental results. Conducting such tests involves deployment of rockets for propulsion of the sled. It required due safety procedures to be followed and some of the references in [37] formed the basis of the same. Before a trial is conducted, a standard operating procedure is developed and all operating personnel appraised of the same, for adherence.

2.6 Research Gaps

The rail track rocket sled testing facilities exist in countries like USA [38], UK, Japan[39], France, Russia and India etc. A magnet and coil based velocity system and a hybrid system was reported in 1957 and 1958 in [6][7]. Ever since there has not been any reported activity in the domain of velocimetry in such an application. This research has picked up threads from there. There has been wide spread activity in tangential applications [38]. There have been developments in use of Pitot tubes in aircrafts and continuous developments in Inertial Navigation Systems (INS) [40] for determining position in aircrafts and missiles. Therefore, there is scope of adoption of the technologies in these systems to the application under study. Keeping in view such developments, the techniques which emerged for further studies include distance, acceleration and pressure based techniques. The following three chapters cover studies based on distance, acceleration and pressure respectively.

Chapter 3

3 Improved Magneto-Inductive System for Velocity Measurement of High Speed Sled

3.1 Introduction

The velocity of sled is a vital parameter against which the performance of the test article mounted on the sled is to be evaluated. It is imperative to measure the velocity accurately in every trial. In the conventional method of measurement of velocity, the position of arrival of sled at a fixed marked distance is sensed and the time of arrival at each position is noted to calculate the velocity. In the conventional method the position marker is generated by a magnet which is mounted on the sled and a pickup coil mounted on the track at predetermined positions as shown in Figure 3.1. The time of arrival is logged by a timer in a specially designed card.

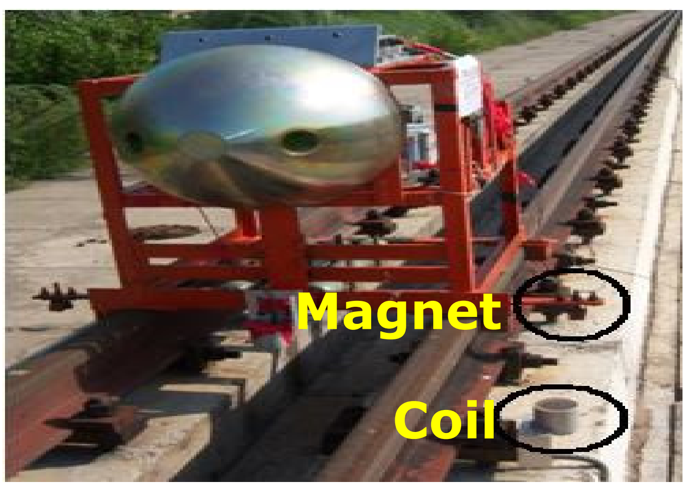

Figure 3.1: Arrangement of magnet on movable sled and sensor on stationery rails

It is believed that the operating principle of pickup coil sensors is known and is one of the oldest. But, it is also claimed that it is known only to the specialists [41]. There are commercially available Application Specific Integrated Circuit (ASIC) which can sense magnetic fields with a resolution of 10nT [42] and give inherently digital output which oscillates. The component has not been found suitable for use in the current application as the specific shape of induced pulse precludes an accurate time reference. Further it will require development of an ASIC based circuit with power supply and deploy 1200 such boards in the field. Instead, the study focuses on rugged and field deployable solution such as an inductive pickup which does not require power to operate it. The proposed sensor is just a magnetic pickup coil which is ruggedized for use in field.

Although inductive pickups for measurement of sled velocity have been in use for more than 50 years [22-23], even now improvements in these systems continue to grow. This is due to the fact that the network of magneto-inductive sensors is amenable to use in the field and can be installed over distances of several kilometers. They give large signals without any need of excitation or signal conditioning and can be fabricated very easily. Use of accelerometers in combination with coils has also been reported [8], which are forgotten but are relevant in the current context. A feasibility study to measure velocity using interferometry has been reported in [9], but we have not come across any further development. The proposed sensor is passive, that is, there is no excitation or active circuit and the arrangement is maintenance-free. These are the desirable features for deployment in the field.

Magneto-Inductive sensor is the topic of this chapter. The term Magneto-Inductive sensor, sensor, coil are used interchangeably.

3.2 Conventional System for Determining Velocity by Sensing Position

Over several decades, there has been a scientific controversy whether the field due to permanent magnet is like a wave or it moves like a body [43][44]. The emf induced in a circuit is influenced by it. The recent as well as fairly old literature [22-24] dwells on the topic. The moving magnet generates an approximately sinusoidal voltage signal in the pickup coil. This chapter focuses on the real life application of magnet and pick up coil system. The sled with magnet slides over the rails at supersonic speeds [45]. The permanent magnet passes over a number of stationary magnetic pickups coils which are fixed along the track at predetermined distances.

In the application under study, the signal pulse from network of magnet and coil arrangement has to propagate distances as large as 4.5 km. In the conventional system these are transmitted through a coaxial cable. The arrival time of these pulses is recorded in the data acquisition system. The sled velocity is computed from such recorded event intervals and the known separation between the fixed coils. This study helps us to understand the limitations of magneto-inductive pickup and also elaborates means to improve it so as to capture faster phenomenon.

The sled with magnet slides over the rails at supersonic speeds [45]. The permanent magnet passes over a number of stationary magnetic pickups which are fixed along the track at predetermined distances, say every 10m, as shown in Figure 3.2. These pickups are connected to the cables, which are multiplexed to save the length of cable used. The arrangement is shown in figure 3.2. Although inductive pickups for measurement of sled velocity have been in use for more than 50 years [6][7], even now the interest in these systems continues to grow.

The moving magnet generates an approximately sinusoidal voltage signal in the pickup coil. In the conventional system these are transmitted through a coaxial cable. The arrival time of these pulses is recorded in the data acquisition system. The sled velocity is computed from such recorded event intervals and the known separation between the fixed coils. This study will help the readers understand the limitations of magneto-inductive pickup. It also elaborates means to improve it so as to capture faster phenomenon.

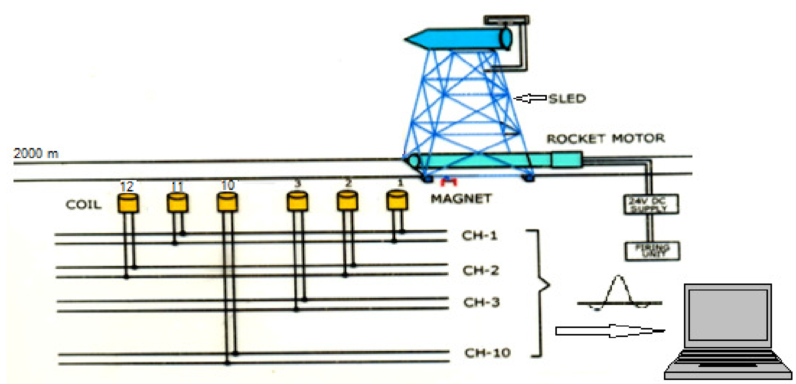

Figure 3.2: Schematic of existing magneto-inductive system with multiplexed scheme of array of sensors

The output of pickups coils are connected to the cables, which are multiplexed to save the length of cable used. The multiplexing arrangement is shown in figure 3.2.

3.3 Problems faced due to limitations of existing approaches

The existing magnet-coil velocity measurement system, which was installed nearly 25 years ago, has served the intended purpose. Its overall precision and consistency needs to be significantly improved to meet the current and futuristic challenges, albeit with some shortcomings. A problem in the magneto inductive system surfaced by chance when trial was being conducted in the rail track facility. Due to higher drag in the upper portion of the sled than the design value, the sled got truncated while it was running on the track. The lower parts of the sled, where magnet was fitted, remained intact. It resulted in attaining the maximum velocity of 500 m/s against an estimated value of 300 m/s. On close observation of the recorded signals, it was found that the peak amplitude of the signal reduces with the increase in velocity. This was contrary to the known facts, that is, with increase in velocity the rate of change of flux and hence the induced emf in the coil should increase. The value at serial no 6 in Table 3.1 is erroneous and may be due to relatively large separation between magnet and sensor. As the facility was being upgraded to achieve velocity up to 1000 m/s, the observed limitation was too serious to be ignored.

Table 3.1: Experimental Data of track testing with conventional sensor

Sl No	Velocity (m/sec)	Maximum Amplitude (V)
1.	106	3.44
2.	173	3.29
3.	266	1.87
4.	312	1.57
5.	368	1.02
6.	413	0.59
7.	459	0.75
8.	500	0.73

The variation of amplitude of pulse induced with velocity is plotted in figure 3.3. Signals acquired at velocity of 106, 312 and 500m/s in an experiment on rail track of 2Km are shown in figure 3.4. A distortion in the signal pulse shape with increasing sled velocity is observed in figure 3.4.

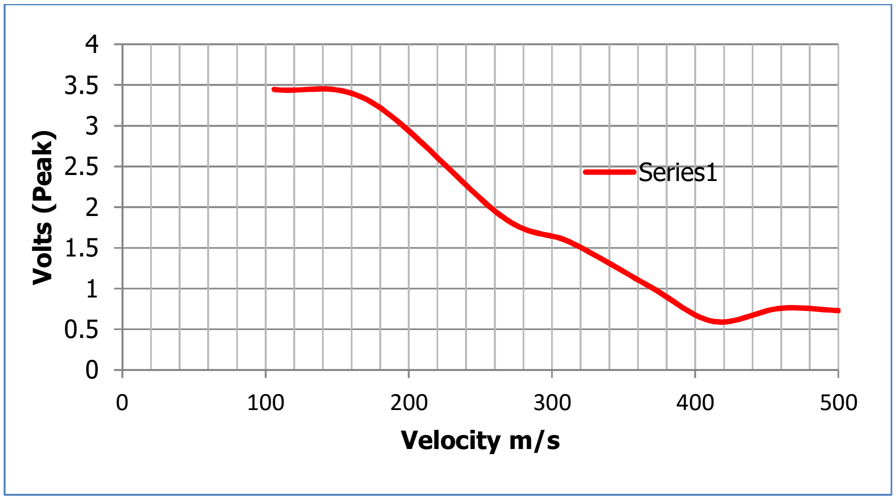

Figure 3.3: Variation in maximum amplitude of the signal pulse with velocity

The present analysis of the existing velocity measurement system was undertaken with the objective of improving its detection beyond Mach 1.5 and to remove the known shortcomings. A major challenge which needed to be addressed was thesignificant attenuation in signal at higher sled velocities. The attenuation was

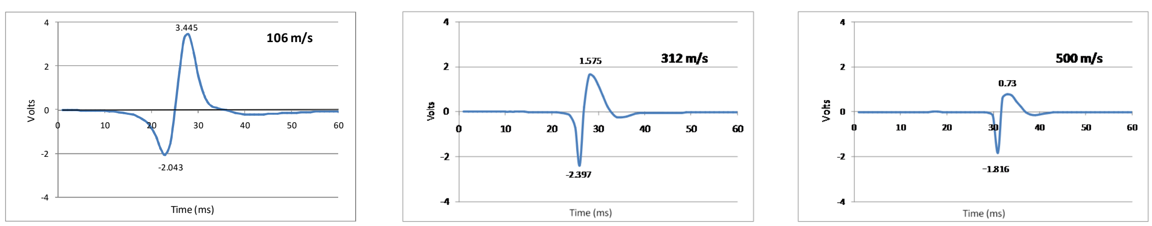

Peak amplitude 3.4 V at 106m/s

Peak amplitude 1.6 V at 312m/s

Peak amplitude 0.7 V at 500m/s

Figure 3.4: Signals acquired at velocity of 106, 312 and 500m/s in an experiment on rail track

so high that the signal would not be detectable at higher velocities, that is, beyond Mach 1.5. The signal will further attenuate when more coils will be added in parallel as the track length is going to increase. There are problems in estimating the instantaneous velocity of sled from distorted pulse shape due to shifting of reference point. To solve such a problem, there is a need to understand and analyse the problem. This is addressed in the next section and subsequent section will propose the improvements.

3.4 Interactions of the magneto inductive system

This section derives an expression for distribution of resultant flux due to a U shaped magnet, which is independent of velocity. Further, this study is expanded to explain the expression for the emf that is induced when magnet moves over the coil at a given velocity.

3.4.1 Distribution of flux density

A schematic representation of the existing magneto-inductive system is shown in figure 3.5. The size of each pole face of the U shaped magnet mounted on the sled

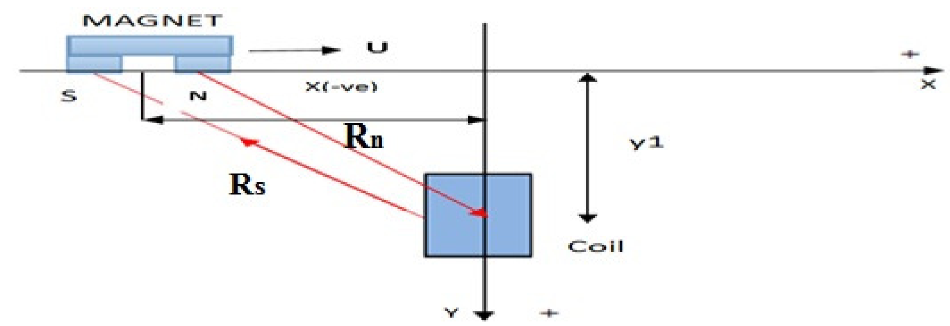

Figure 3.5: Schematic representation of magnet moving over the coil.

is of 11.5 mm X 30 mm area. The distance d between the two pole faces is about 32 mm. The Specified maximum magnetic field strength (B_0) is about 1500 Gauss (0.15 Tesla), which corresponds to an equivalent pole strength (p) of about 80 Ampere metre (Am). Such an equivalent magnetic pole can be assumed to be located around 6 mm (half a pole width) inside the pole face. On the basis of equivalent magnetic pole strength (+ve for North and –ve for South pole), the effective magnetic flux density B, at a distance r from the pole (along r vector), can be expressed as,

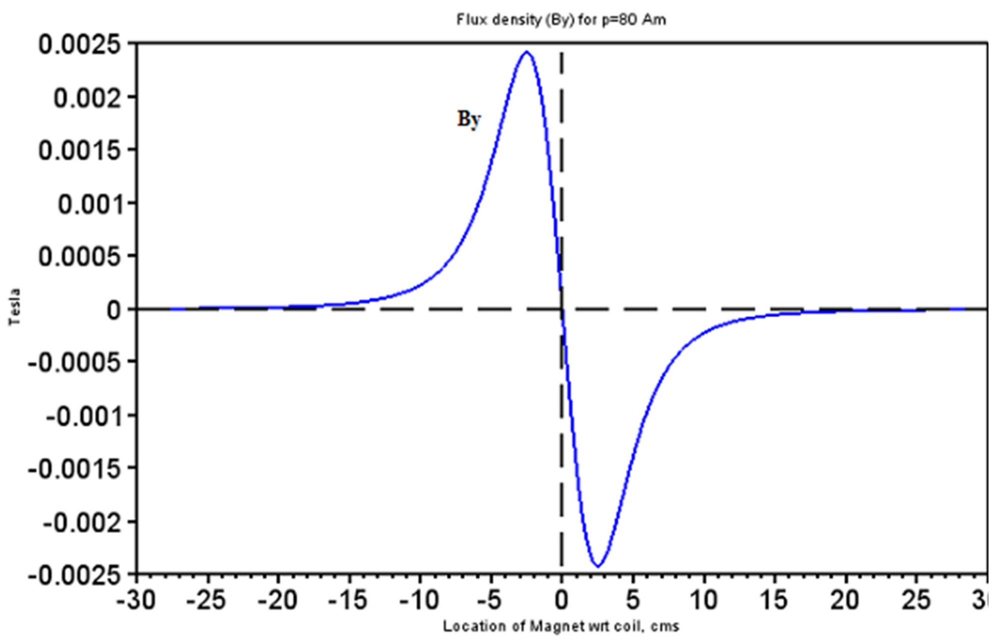

Figure 3.6: Variation of Magnetic flux density B_y from relative location of magnet wrt coil

$$B = \frac{\mu_0 p}{4\pi r^2} Tesla \tag{3.1}$$

Where μ_0 is the permeability of free space in H/m

R_n is the radial distance from North Pole to the center of coil and R_s is the radial distance from South Pole to the center of coil. Let y_1 be the vertical distance of the coil center from the two poles (figure 3.5). The downward component, along Y axis, of resultant magnetic flux density B_y due to the combined effect of two poles is given by

$$B_y = \frac{\mu_0 y_1}{4\pi}\left(\frac{1}{{R_n}^3} - \frac{1}{{R_s}^3}\right) \text{ Tesla} \tag{3.2}$$

A graph of magnetic flux density, B_y (equation 3.2) for various positions of the magnet on the X-axis is given at Figure 3.6. The variation of flux density B_y along X-axis is obviously independent of the sled velocity.

3.4.2 Induced emf due to velocity

We need to find out an expression for the induced emf as a function of velocity of sled, so as to analyse the problem. As shown in Table 3.2, existing sensor coil consists of 10,000

Table: 3.2 Specifications of conventional sensor

Sl no	Specifications	Value
1	Wire	36 SWG enameled Copper
2	Resistance	650Ω ± 5%
3	Inductance	2500 mH
4	Core	Soft Iron
4	Coil Dia	18 mm
5	No of turns	10,000
6	Casing material	Aluminum

turns (N_c) of fine copper wire, wound around 18 mm diameter soft iron core of 38 mm length. The ohmic resistance R_L of the coil is 650 Ω and the inductance L_c of the coil is 2.5 Henry. Let A_c denote the core cross-sectional area in m^2, then the total magnetic flux in the core will be given by $B_y.A_c$ in Webers. The expression for induced emf will be

$$e = -\frac{d}{dt}(N_c B_y A_c)$$
$$= -N_c A_c \frac{d}{dx}(B_y) \cdot \frac{dx}{dt}$$
$$= -U.\, N_c A_c \frac{d}{dx}(B_y) \quad (3.3)$$

Therefore, when the magnet moves over the fixed coil at velocity U along the X-axis, the induced emf e in the coil of N_c turns can be found from equation (3.3). This equation shows that the induced emf e increases with the velocity. But experimental findings show (figure 3.3) that the output signal reduces with the velocity. Usually, one tends to think that with the increase in velocity the rate of change of flux increases and therefore, the maximum amplitude of the induced pulse would increase. The experimental findings are contrary to the general belief.

3.5 Analysis and simulation of variation of induced emf and output signal pulse with velocity

The result of section 3.4 has been in line with Faradays law of electro-magnetic induction. However, we need to find an answer as to why the output falls with velocity. The gap in our understating between the induced emf and the output pulse needs to be bridged. This section explains the theory of this gap. Here we explain how we carried out simulation of the induced emf and the output signal pulse as a function of velocity. The description does not take into account any marginal effects of a lossless transmission line through which the signal pulse propagates. No mathematical system model is perfect; it only depicts the characteristics of direct interest [46]. A model, that was developed depicting sensor and load, is shown in figure 3.7. At the load end, which is a recording device, the signal pulse voltage output of the sensor coil can be estimated from an equivalent circuit diagram. The impedance Z_{sh} of the other sensors which are connected in parallel (figure 3.2) will increase with the velocity and the line resistance R_S is negligible. Both have been ignored for simplicity. Here, the magnet induced emf *e* of equation 3.3 in the coil drives a current *i* through coil of resistance R_L, inductance L_c and the output load resistance R_{op}. Applying Kirchhoff's voltage law for the voltage drops across various elements in the current loop, we get the following relationship.

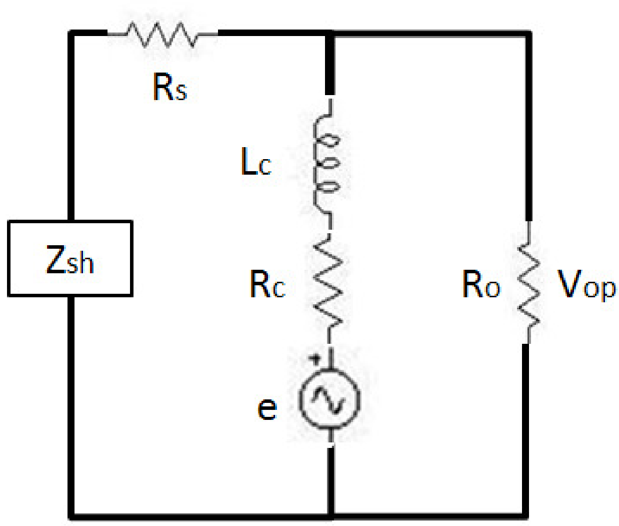

Figure 3.7: Equivalent circuit of the Magneto-Inductive velocity measurement system at RTRS

$$\mathrm{e} - iR_L - L_c \frac{di}{dt} - iR_{op} = 0 \tag{3.4}$$

$$\frac{di}{dt} = \frac{1}{L_c}(e - i(R_c + R_{op})) \tag{3.5}$$

The value of e from equation 3.3 was substituted in the equation 3.5. Further equation 3.5 was solved as a function of x or t using improved Euler method of numerical integration, to obtain an i pulse corresponding to the e pulse of equation (3.3).

The signal across R_{op} is the output voltage $v_{op.}$ The output voltage (v_{op}) pulse is then obtained from $v_{op} = iR_{op}$. The $R_{op}$is set 4.7 k ohm during track testing and 1.8 k ohm while testing on the rotor (figure 3.15). The value was chosen so that the sensor output remains within +/-5V input range of the PC based data acquisition card. The rotor based test setup is explained in section 3.8.2.1.

The three simulated signal pulses for e and v_{op} at velocities of 100, 300, 1000 m/s were obtained using SCILAB 5.4.0 application package. The results of simulation are shown in figure 3.8. These simulation results explain the answer we were looking for, that is, fall in signal level with the velocity. The red coloured graph shows the induced emf e increases with velocity and is at much higher level than blue coloured graph of output voltage v_{op}which reduces with the velocity.

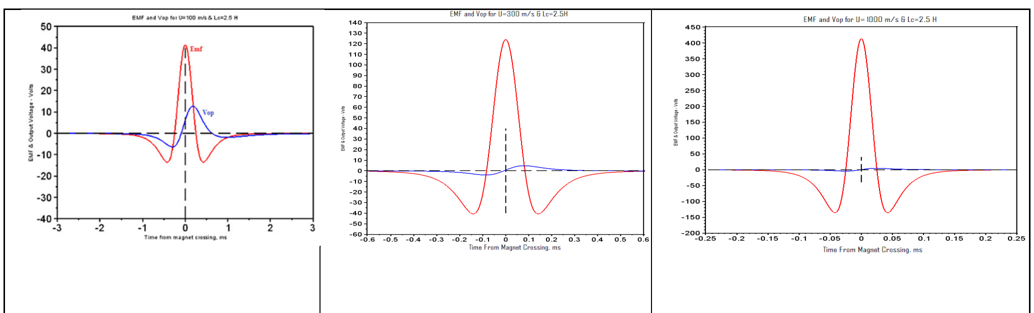

Figure 3.8: Variation of induced emf and the output terminal voltage with respect to magnet crossing over the magneto-inductive sensor at 100, 300 & 1000 m/s velocity and with soft iron coreand Lc=2.5H.

3.6 Explanation of fall in output signal with velocity

It was identified in section 3.3 that the output signal diminishes as the velocity increases. This is the problem we wish to correct. It can be inferred from simulation results of the previous section 3.5 that although the induced emf increases, the output signal continues to reduce with the velocity. The findings are a step in the desired direction and answers the problem projected in section 3.3.

The equations (3.3) & (3.4) show that induced emf e is desirable but large L_c is undesirable, which increases the opposing self induced emf. As long as the load is not connected across the inductive pickup, no current flows through it. So no self induced emf develops. Open circuit voltage will increase with the velocity. As the load of recording device is connected across the sensor, the current flows through its coil and an opposing self induced emf gets developed. Secondly, the output is not taken directly across the coil, but it propagates through the transmission line of several km and the resulting current passes through the input R_{op} of recording device. The current also has to overcome the inductive reactance of the sensor coil. This inductive reactance of sensor increases with the frequency. The frequency in-turn increases with the velocity. Therefore, it can be inferred that it is this opposing self induced emf which increases with velocity and is primarily responsible for making the output signal fall with the velocity.

Now having understood the cause of problem, the focus turns to improving the sensor.

3.7 Suggested improvements in the sensor

The experimental data of figure 3.3 and the simulation data of figure 3.8 suggest that in the existing sensor, the output signal falls with increase in velocity. Having identified the cause of problem in the previous section, the next logical step was to improve the output of the sensor so that the signal obtained at higher velocity has higher amplitude than the output of existing sensor. Further, equation 3.4 shows that the e should be high and L_c should be low so as to obtain high level of signal pulse.

Here desirable component $e \propto N$

and undesirable component $L \propto N^2$

These are the key parameters considered for bringing about improvements in the sensor.

3.7.1 Parameters modified

In order to improve the sensor, inductance L needed to be reduced. The number of turns N_c of the coil were reduced, with result both the desirable and undesirable components reduced. With this change the reduction in undesirable component would be higher than the reduction in desirable component. This was the property exploited to bring about improvement in the sensor. Reduction in L is accompanied with reduction in R, which improves the low frequency response [12].

Further, the inductance L_c of the sensor coil is high because of its soft iron core, which also adversely affects the high frequency response. It may be noted that the coil inductance is directly proportional to the relative permeability μ_r of the core material. However, in the present set up the magnetic flux density B linking permanent magnet and the inductive sensor was nearly independent of μ_r of the core material. Hence the provision of soft iron core in the sensor coil merely increased the value of inductance L_c without increasing the total flux or the induced emf in the coil. Therefore, it is proposed that the soft iron core be eliminated. The review paper [41] reports that the non-linearity of coil with core can be removed by changing it to air cored sensors and gives following empirical formula for inductance.

$$L_c = N_c^{\,2} \frac{\mu_0 \mu_c A_c}{l_c} \left(l / l_c \right)^{-3/5} \qquad (3.6)$$

Where μ_c is the resultant permeability of the core and is much lower than the permeability of the material, *l* and *lc* are the coil and the core length respectively.

Further, if the number of turns is halved, the emf would also become ½ as per equation (3.3) but the inductance will reduce by ¼. An attempt was also made with turns reduced to 1/4th, but results were better when turns were reduced to ½ (shown at C3 in Table 3.5) in case of isolated Lc. Further, experiments and studies were done using the proposed sensor along with the existing sensor, so as to have evaluation with identical magnet to coil gap and identical velocity for comparison. Preliminary design was arrived at by using equation 3.6. Since these sensors will be manufactured in large numbers, appropriate discrete values were chosen for study. The inductive pickups were having 10,000, 5000, 4000 and 2500 turns. Except existing coil of 10,000 turns, which was the conventional sensor, remaining all were air core coils. The results obtained with 5000 turns sensor were found to be superior as is explained in subsequent sections. Reducing number of turns further would reduce the output signal at lower velocities.

The parameters modified in the inductive pickup to bring about the improvement were number of turns and the core. Further studies were carried out to determine the impedance offered by existing and proposed sensor and the comparative output of the two at different velocity.

3.8 Comparison of impedance offered by existing and proposed sensor at different velocities

It is the internal impedance of inductive pickup which attenuates the output voltage with increase in velocity. This impedance also plays a role when several such sensors are connected across the transmission line; comparison of impedances of existing and proposed sensors was undertaken. The signal pulse produced in the sensor coil, is transmitted to the output load (R_{op}) of about 4.7×10^3 ohm, through a coaxial cable of more than 2 km length. The cable used in conventional system at RTRS is a twin coaxial cable (RG 58C) of characteristic impedance (Z_0) 50 ohm, line capacitance 100pf/m and line inductance of 2.4×10^{-7}H/m with a velocity factor of about 68 percent. In the kHz frequency range of the signal pulse, the coaxial cable acts as a lossless transmission line. As such a high impedance output load (R_{op}) is used in the present case for monitoring the signal pulse. Consequently, a part of the signal power does get reflected from the output end of the cable. Presently the output impedance is 4.7 kΩ. If terminated with a matched impedance of 50 ohm, it will be fully absorbed at the far end of the cable.

Further, it is not feasible to match the sensor coil impedance with the characteristic line impedance of the cable since the inductive reactance of the coil keeps increasing with the velocity of the rocket sled. Therefore, under the circumstances, full power of the signal pulse does not get transferred to the transmission cable. The power transfer from the induced signal pulse in the sensor coil to the coaxial cable can however be maximized by minimizing the inductive reactance of the coil by minimizing its inductance [45].

To calculate the impedance, nominal frequency (f_r) of the induced emf pulse can be computed from the time period of the pulse as seen in figures 3.8 above. In table 3.3, total impedance Z_c of the coil with inductance L_c and internal resistance R_L is calculated using,

$$Z_c = \sqrt{\left(R_L{}^2 + (2\pi f_r L_c)^2\right)} \tag{3.8}$$

Since frequency f_r of the pulse increases with sled velocity, total impedance of the coil will also increase with the velocity. The corresponding total impedance of the coil with iron core and air core is given in Table 3.3 for different values of the rocket sled velocity.

Table 3.3: Simulated studies of parameters of existing and proposed sensors

S.no	Sled Velocity U (m/s)	Nominal Frequency f_r (Hz)	Impedance Z_c (kΩ) of existing sensor for L_c =2.5H, R_L=650Ω	Impedance Z_c (kΩ) of proposed sensor for L_c=0.284H R_L=250Ω
1.	50	0.559×10^3	9.284	1.081
2	100	1.179×10^3	18.531	2.118
3	200	2.358×10^3	37.045	4.215
4	300	3.538×10^3	55.578	6.318
5	400	4.717×10^3	74.097	8.420
6	500	5.896×10^3	92.616	10.523
7	600	7.075×10^3	111.135	12.627
8	700	8.255×10^3	129.670	14.732
9	800	9.434×10^3	148.190	16.836
10	900	10.06×10^3	166.662	18.934
11	1000	10.17×10^3	185.198	21.039

As is evident from figure 3.7 and table 3.3 the lower impedance of the proposed sensor would be beneficial in realizing sensor with higher amplitude signal output.

However, low impedance can have effect on shunting of the sensor by the other sensors on the same line. It is possible to overcome such a disadvantage by connecting a diode in series with each inductive pickup.

3.9 Comparative estimation of variation of output voltage with velocity

The parameter of interest in proposed sensor is the signal voltage appearing across the impedance of the recording device and not the induced emf due to magnet. The self-induced emf in the inductive pickup is in opposition with the emf induced due to permanent magnet. That is the reason for output voltage v_{op} available across load R_{op} to get reduced considerably in comparison with the induced emf, as the magnet induced emf has to overcome the self induced emf.

Comparison of maximum values of this output voltage for the soft iron core (L_c=2.5) and for air core (L_c=0.284H) versions of the sensors is given in Table 3 [45]. It is observed that the voltage output from proposed sensor is higher for any given velocity. It may be noted that these values are for isolated sensors. They will become part of a network of parallel sensor during implementation and the output, in that case, further reduces. As the experimental data of table 3.1 shows that in case of existing sensor it becomes so less that the output is not detectable. In case of proposed sensor the output remains appreciably high even at higher velocities, as reported by author of this research in table 3 [45], and can be detected by data acquisition card.

The sensor impedance is much more than the characteristic line impedance of the coaxial cable. Therefore, the amplitude of the output voltage is likely to get further attenuated because the full power of the induced pulse cannot get transferred to the transmission line due to impedance mismatch. The signal pulses for e and v_{op} obtained for the soft iron core inductive pickup of Lc of 2.5H and air cored coil with L_c of 0.284 Henry are given below in Figure 3.9 as red and blue graph respectively. Simulation results of variation of induced emf and the output terminal voltage with magnet crossing over the coil at 100, 300 & 1000 m/s respectively using existing sensor having soft iron core are shown in Figure 3.9. It is abundantly clear from the simulation results presented in the graph, that in case of existing sensor the emf induced due to magnet increases and the signal output voltage falls with the increase in velocity.

Whereas in case of proposed sensor the emf induced due to magnet increases and the signal output voltage also increase with the velocity in the velocity regime of interest.

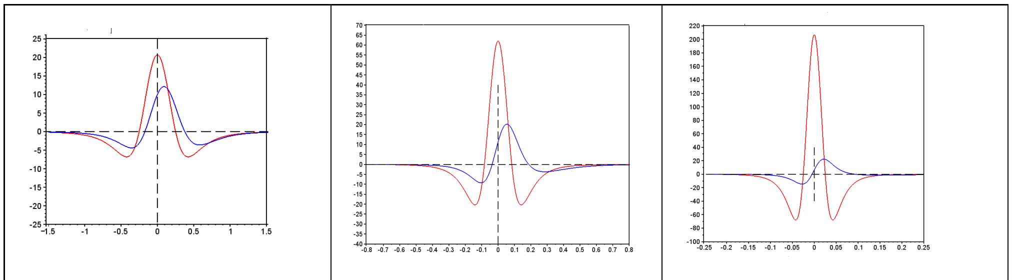

Figure 3.9: Variation of induced emf (in red) and the output terminal voltage (in blue) with respect to magnet crossing over the inductive pickup at velocity of 100, 300 & 1000 m/s and with proposed air core sensor having Lc=0.284 H.

As seen from these graphs, the distortion in the output voltage pulse noted with soft iron core gets minimized with the use of air core. This is due to the corresponding reduction in coil impedance.

3.10 Implementation

If the benefit of successful development has to reach the intended purpose, it should be translated in to a product which can be realized in large numbers and deployed in the field. The specifications of proposed sensor were developed keeping in view the manufacturability and are briefed in Table 3.5. A total of 1200 numbers of sensors were fabricated to these specifications.

3.10.1 Derivation of velocity of sled from average velocity

As the sled slides along the rail track at high velocity, the emf is induced in the inductive sensors. The induced pulses are conditioned and digitized. The time of arrival of these pulses is recorded. Knowing the distance between the sensors and the interval between the incoming pulses, velocity can be calculated. But this will be average velocity between the sensors. The distance and time are measured and specified when the magnet is on the sensors. The distance is specified in meter to third decimal place, i.e., in mm. So to correctly tabulate the result the average velocity between the sensors needs to be converted to the velocity on the sensor. The equations given below convert the average velocity between the sensors to the velocity on sensor.

Assuming the sled has crossed over the sensor coils C_{i-1}, C_i and C_{i+1}progressively.

Average velocity between$C_i$and $C_{i-1}$is $$v_{av-} = \frac{s_{i-}}{t_i - t_{i-1}} \quad (3.9)$$

Where s_{i-} is the distance between C_i and C_{i-1},

and t_i & t_{i-1} are the time of arrival of sled at C_i and C_{i-1}

Average velocity between C_{i+1} and C_i is $$v_{av+} = \frac{s_{i+}}{t_{i+1} - t_i} \quad (3.10)$$

Wheres_{i+} is the distance betweenC_i and C_{i+1},

and t_i and t_{i+1} are the time of arrival of sled at C_i and C_{i+1}

Acceleration at C_i $$a_i = \frac{v_{av+} - v_{av-}}{(t_{i+1} - t_{i-1})/2} \quad (3.11)$$

Thus Velocity at C_i $$v_i = v_{av-} + (v_{av+} - v_{av-})2 \quad (3.12)$$

Thus equation3.12 gives us the velocity at the point where magneto-inductive sensor is installed and signal from each sensor is available. In case signal from some of the sensors is not received, following equation will give better results

$$v_i = v_{av-} + a_i\ (t_i - t_{i-1})/2 \quad (3.13)$$

Further, two different types of systems were built to acquire signals from the moving sled. These are described in the next section.

3.10.2 Realisation of sensor

The inductive sensors can be directly manufactured by users [41]. These are the best sensors when dimensions are not a constraint, as is the case in the application under study. Keeping in view the simulation studies of section 3.7.3, two different sensors were realized. The parameters of one of the sensors are given in table 3.4. Manufacturability in large numbers and adaptability to existing system was also kept in view.

Table: 3.4 Specifications of realized sensor

Sl no	Specifications	Value
1	Wire	36 SWG enameled Copper
2	Resistance	230Ω ± 5%
3	Inductance	200 mH
4	Core	Air
5	Coil ID	12 mm
6	No of turns	5000
7	Casing material	Aluminum

3.10.3 Onboard system

In this system inductive pickup and hardware were on the sled and magnets

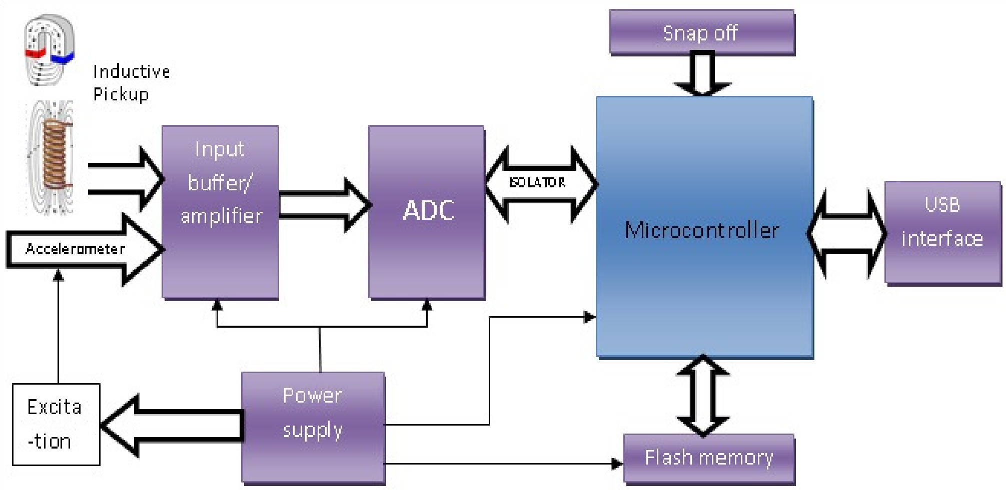

Fig 3.10 : Simplified block diagram of onboard velocity measurement and logging system

were fixed on the ground. These magnets were separated by nearly 1 m distance. The pulse picked up by the inductive pickup was buffered and digitized. Microcontroller latched the time of arrival of the pulse. The block diagram of this system is shown in figure 3.10 and the corresponding photograph of the hardware is shown in figure 3.11. This time was recorded in the onboard flash memory. This system acquired the signals at 50 kHz sampling rate. The data could be retrieved after the trial through USB port. The worst case relative error in this arrangement is given by equation 3.14.

$$Relative error = [(\Delta s/S_{min}) + (\Delta t/T_{min})] \, X \, 100 \;\; \% \qquad (3.14)$$

Here, Δs is error in measurement of distance S_{min}, S_{min} is the minimum distance between two sensors, Δt is the error in measurement of time T_{min}, T_{min} is the minimum time between two pulses from inductive pickups. The precision of the system when recording onboard was found to be 0.046%.

The velocity measured using such a system in two different experiments is shown in figure 3.12.

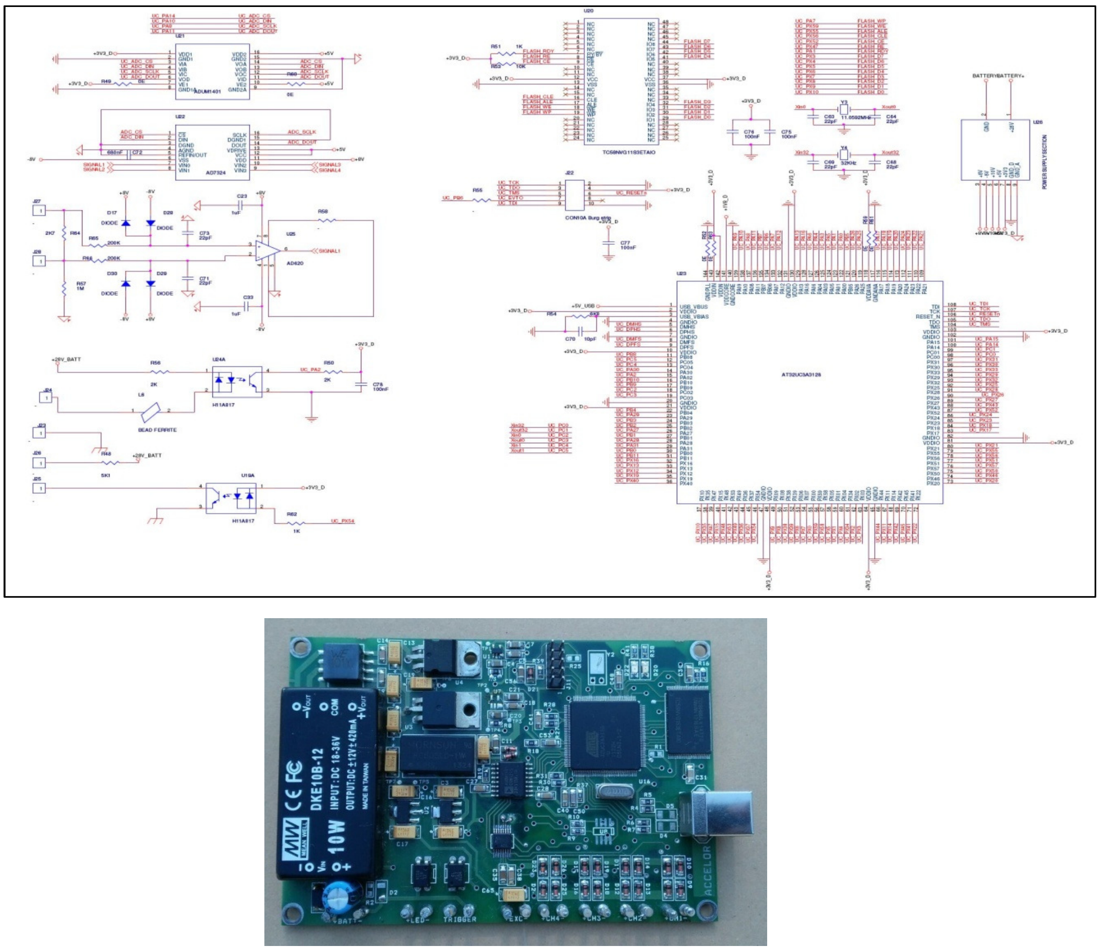

Figure 3.11: Microcontroller based card developed for implementation of the onboard system

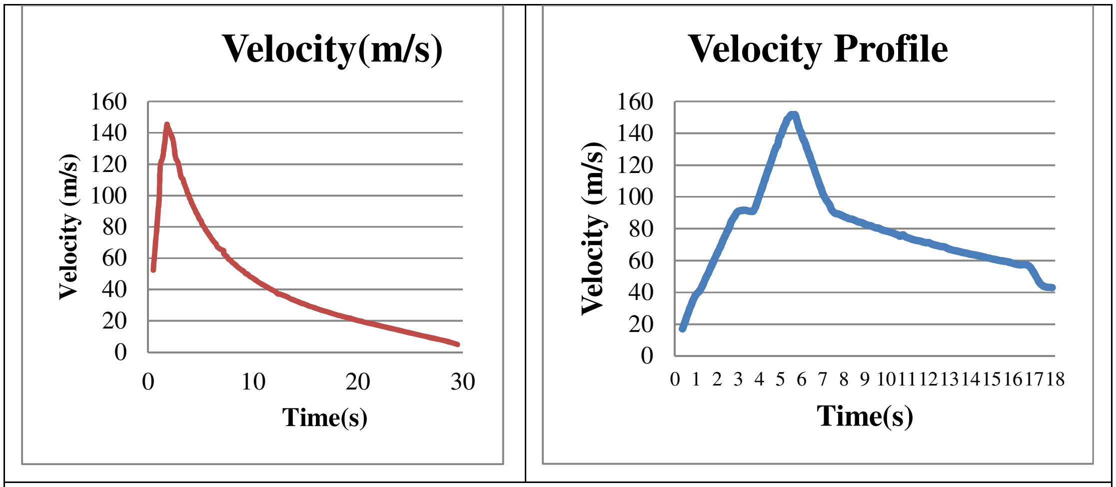

Figure 3.12 : Velocity measured by onboard system in two different experiments

The major advantage of such a system was that no long distance transmission lines were required. High sampling rate could be implemented due to smaller number of channels as compared to the ground based system. This resulted in higher precision, too. The disadvantage of this system was that the information was available off line after the experiment, setup time for each trial was more and the onboard system had to be rugged. The system could not be deployed in the trials where test article will leave the track and impact on the target.

Effect of variation of LCR of sensor

In the proposed sensor only inductance has been varied. The signal frequency varies with the velocity. The sensor impedance changes with change in frequency. If sensor impedance matches the impedance of transmission line, maximum power transfer will take place. It can be achieved by adding capacitance in parallel with the sensor. However, practical problem is that all 1200 sensors will be different. Moreover, velocity over the sensor will be different in different experiments. So solutions will not practical.

3.10.4 Ground based system

In the 2nd system the magnet was mounted on the moving sled. Inductive pickups were on the ground. These sensors were deployed along the track covering a stretch of 12 km.

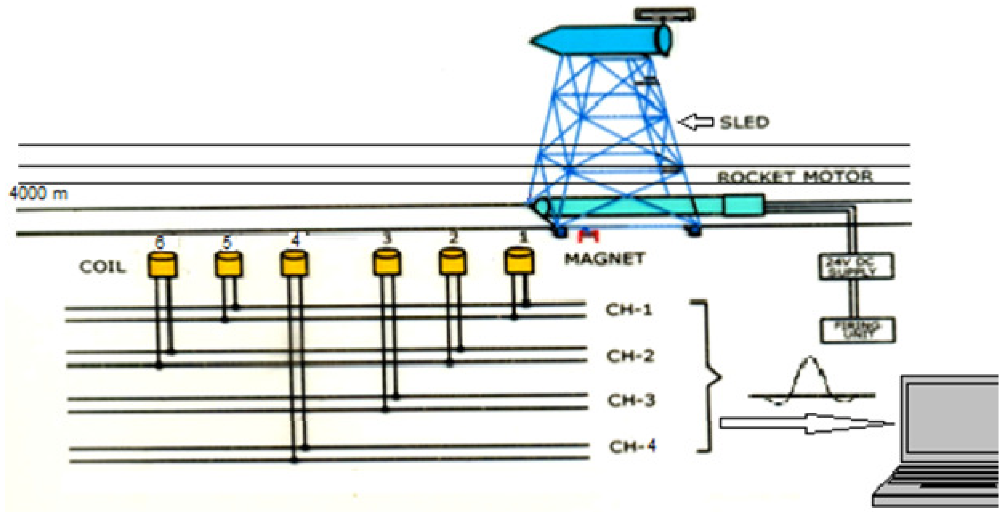

Figure 3.13: Ground based system showing magnet on the moving sled and the array of inductive picks on stationery rails. The sensors are multiplexed into 4 channels

As the signallevels attained were higher (figure 3.13), four multiplexed channels were used in this system (figure 3.13) instead of 10 channels used in the conventional system depicted in the figure 3.2. This scheme resulted in saving of 72 km of cables as compared to the conventional system. The signals propagated to PC based data acquisition card. The distance between the sensors was entered in the program. The velocity was calculated using interval recorded and the pre-programmed distances. The velocity so obtained was average velocity at the middle point between sensors. It was recalculated to arrive at the velocity on coil where measured distances were available. The equation 3.12 above was used for this purpose. The velocity obtained with this system in an experiment is shown in figure 3.14. It's a rising graph as the sled was to go beyond the track after attaining maximum planned velocity. So it was not possible to record the falling velocity.

The advantages of such a system are the arrangement is static, there is no overhead on the sled borne system and signals are available in real time. Onboard quality hardware need not be implemented as the system is ground based. The precision was calculated using equation 3.8. The attained value was 0.24%. The value was higher than the onboard system due to lower available sampling rate of the data acquisition card. The disadvantage is that the transmission lines attenuate and distort the signal as impedance matching with sensors is not feasible. The performance capabilities of these sensors will manifest themselves as the operations at RTRS are gradually scaled up. The results obtained in figure 3.14 are acquired in such a setup.

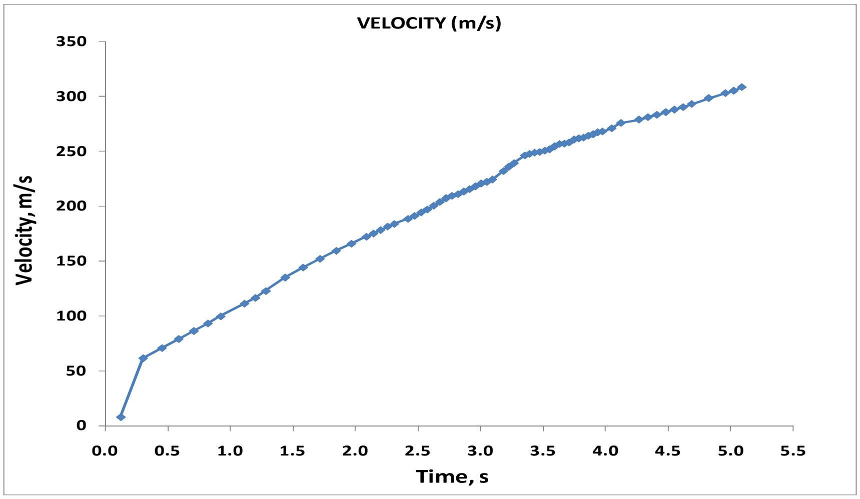

Figure 3.14: Velocity recorded by ground based system in an experiment of sled run.

3.11 Experiments conducted to validate improvements

A number of experiments were planned and conducted to understand the effect of improvements in the sensors and its performance vis a vis the conventional sensors. The feasible velocities were up to 62 m/s per second in the static tests in a rotary system. The feasible velocity in case of the dynamic tests on the rocket sled were up to 303 m/s second. The following sections describe the test setup, the experiments conducted and the results.

Figure 3.15: Test setup of rotating magnet.

3.11.1 Test setup for comparison of experimentally acquired signals from realized sensor versus the conventional sensor

There was need to conduct several experiments to validate the findings of simulation. The RTRS facility for conducting experiments was under augmentation. Moreover, it was not viable to conduct rocket sled tests on and off, due to prohibitive cost requirement of other resources. Some of the requirements of these experiments were to conduct tests with identical magnet to sensor gap and identical velocity for existing and proposed sensors so as to successfully compare the performance and hence the improvements. To meet the requirements, a test setup was rigged up. A rotating fan with radius of 1 m was improvised (see figure 3.19). The fan was rotated by a three phase motor. Entire setup was enclosed in the Pendine blocks to prevent accident in case a fragment or a magnet breaks away. The magnets were fixed on both ends of the fan shaped arm. The sensor coil was stationary and opposite the magnet.

The gap between magnet and coil was kept 33 mm so as to have a signal within ±5 V range of data acquisition card of National Instruments (NI) which was used for this purpose.

3.11.2 Experimental results

The results of three types of coils were used in three different experiments so as establish comparative values and consistency.

Table 3.5: Comparison of amplitude at 36 m/s

Core	Turns		Expt 1 +vepk (V)	Expt 2 +vepk (V)	Expt 3 +vepk (V)
C1: Soft Iron	10000	Set 1	3.15	3.2	3.15
		Set 2	3.72	3.66	3.76
C2: Air Core	5000 (Prop.)	Set 1	5.0	4.9	5.0
		Set 2	5.0	5.0	5.0
C3: Air Core	2500	Set 1	3.12	3.2	3.22
		Set 2	3.27	3.16	3.24

The waveforms captured with such a system are shown in figure 3.16. It shows the peak amplitude is higher for 5000 turn coil as compared to 10,000 turn and 2500 turn coils. The sensor C1 is the existing sensor and C2 is the proposed sensor. Initially a velocity of the order of 36 m/s could only be achieved and results are shown in table 3.5. This table lists the 3 sensors used in experiment and its comparative data.

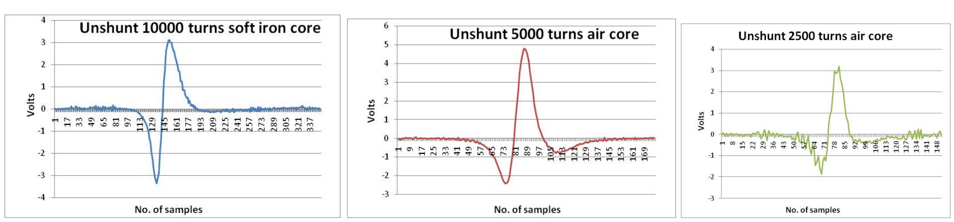

Figure 3.16: Experimentally acuired signals captured at 36 m/s velocity using rotor.

The data set wastaken again on another day with recording as set 2 so as to have adequate data and check for consistency of trend in results. As per results of simulation, reducing the inductance would improve the high velocity response of the sensor. However, reducing inductance should not be so much that it reduces the induced emf e below threshold at low velocity. Table 3.5 shows that the sensor C2 higher output and is proposed as a choice for further work involving larger quantity of sensors. Further, improvements were carried out in the rotor apparatus (figure 3.15) so as to attain higher velocity and to check validation at range of velocities. The results are shown as comparison of existing and proposed sensors at different velocity when tested on rotor as shown in Table 3.6. Magnet to sensor gap was kept at gap of 34mm. The gap was kept fixed as we had focused on relative performance.

Table 3.6:Comparative output of existing and proposed sensor when tested on rotor.

Sl No	Vel (m/s)	2.5 H	0.284 H
		C1(V)	C2(V)
1.	24.19	3.35	3.27
2.	30.70	3.511	3.71
3.	37.16	3.592	3.913
4.	42.05	3.592	4.033
5.	47.00	3.672	4.234
6.	52.35	3.712	4.274
7.	57.25	3.712	4.475
8.	61.68	3.672	4.515

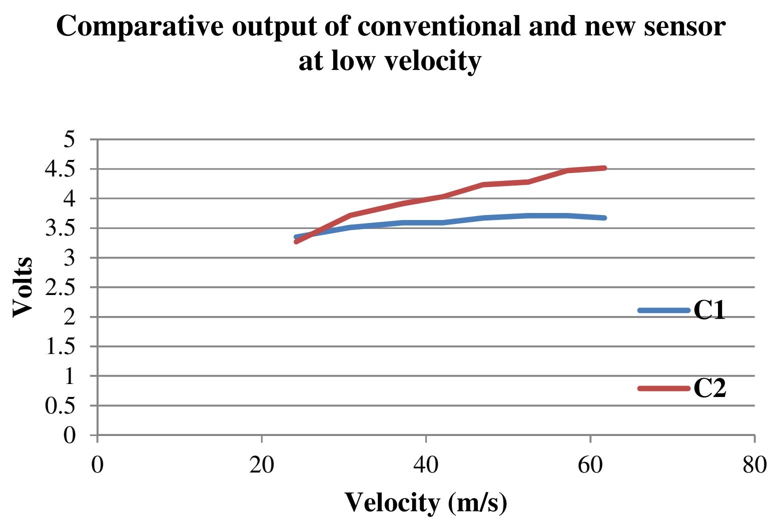

Figure 3.17: Change in peak amplitude of existing sensor C1 and proposed sensor C2 for low order velocities recorded at improvised rotor experimental setup.

The focus of study has been the comparison of amplitude and shape of signal pulse for the existing and proposed sensors rather than the comparison of absolute values of amplitude. It reduces the efforts in experimentation as the gap between magnet and pickup need not be changed. The load resistance in this case had to be reduced to meet the requirement of within ±5V range of data acquisition card. It is found that the amplitude is higher and distortion is less in case of air core based sensor with Lc = 0.284 H and it validates the findings of simulation results, too.

It had emerged in simulation studies that the proposed sensor will have higher output for supersonic velocities as compared to the conventional sensor. At lower velocities the improvements were not expected much. However, the trend available from figure 3.17 shows that even at lower velocities the proposed sensor C2 begins to show an upward trend. This sensor is recommended for use in establishing network of sensors along the rail track. The experiments at higher velocity will be feasible thereafter.

In much later stages, after the publishing of paper [45]and when the RTRS facility had become operational, it became feasible to achieve a velocity of 303m/s. Evaluation at high velocities is cost prohibitive. The trial in which the signal were acquired at 303m/s involved cost on rockets alone to the tune of Rs 4.8 million.

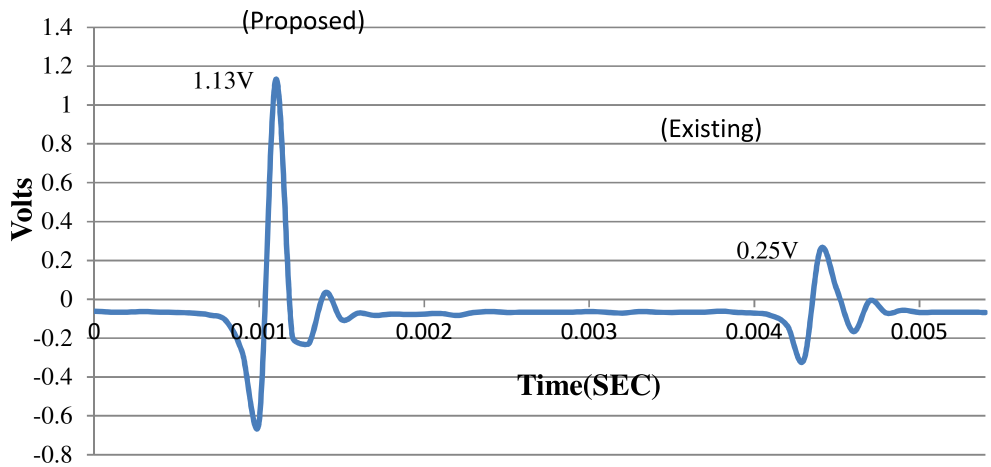

Figure 3.18: Experimental output of proposed and existing sensor at high speed of 303 m/s (**1091km/h**)

Testimony of successful research is the outcome depicted in figure 3.18. It shows the comparative result of existing and proposed magnetic-pickup in an experiment in which sled attained velocity of 303m/s. Under identical conditions and identical gap between sensor and the magnet, the proposed sensor recorded an output of 1.13V against 0.256V in conventional sensor, The experimental result validates our findings that with increase in velocity the output of proposed sensor will give higher output.

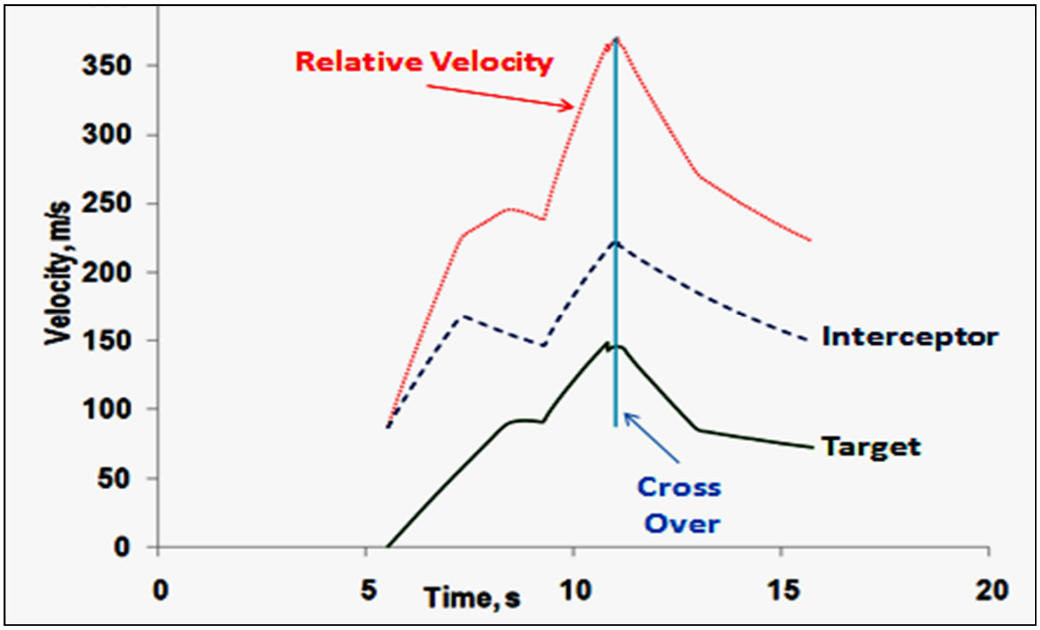

Figure 3.19: Ground based (on Target) and onboard systems (on Interceptor) systems being simultaneously used in opposite directions in an experiment.

An experiment was conducted in which ground based velocity system was used in a sled moving in the forward direction and onboard system was used in a sled moving in opposite direction on an adjoin rail track, thereby giving higher relative velocity. The results of experiment are plotted in figure 3.19. This also demonstrates the successful implementation of the finding of our research.

3.12 Summary of Chapter

It is found that the existing inductive sensor has limitation of output amplitude at higher velocity. When the signal level falls below the threshold level of 0.7V at Mach 1.5, it could not be detected due to noise in the long distance transmission lines. Moreover, the 2nd negative peak attenuates significantly thereby distorting the signal and shifting the reference. The study carried out by us first simulates and recreates the problem faced. Further, an improved sensor is proposed, its simulation results, which show the improvement, are presented. The proposed sensor is air core based, has lesser inductance and has lesser resistance. These changes result in higher output voltage for any given velocity. Two different types of implementations were developed and experiments conducted. The implementation with onboard hardware had a precision of 0.046%. In the ground based system the precision available was

0.24%. Further, experiments were conducted at feasible velocity to validate the results of simulation. The results of experiments were in agreement with the finding of simulation. With these improvements, unlike existing sensor, the signal can be detected for measurement of velocity beyond 500 m/s. The distortion in the signal is also considerably lower. In this process the sensor has become capable of being used at higher velocities.

This chapter has covered how an inductive pickup sensorwas successfully improved. For further studies, the next chapter discusses the measurement of velocity with acceleration as the primary measurement.

Chapter 4

4 Quantification and Mitigation of Errors in the Inertial Measurements Leading to Velocity

4.1 Introduction

In chapter 3 the primary measurement was distance which lead to the measurement of velocity. In this chapter the primary measurement is acceleration. The focus of research has been to find the distance travelled from primary measurement, that is, acceleration. The distance is derived from acceleration by double integration. As stated in chapter I, the velocity is not directly measured but derived from other primary measurements. The velocity is computed form the corrected distance versus time profile. The advantage of operating in distance domain is that it is possible to obtain reference values in distance domain with high level of accuracy. Further, the correction can be applied to get improved values of velocity.

The topic of position sensing is ages old. The sense of position-movement was originally described in 1557 by Julius Caesar Scaliger as a "sense of locomotion"[47]. The distance travelled and velocity of interest ranges from experiences of human / robotic motion to supersonic speeds of bullets, which is the subject of this paper. In the recent past accelerometers have been deployed for sensing motions [48]. The advent of MEMS based technology and devices have drastically reduced the prices of accelerometers, although with reduced specifications. These devices have opened a very wide range of applications covering pen to remember what is being written, computer mouse, shoe which can measure gait and pattern of walk, heartbeat, estimation of motion of robot to missiles and rockets etc. [49-52]. Such accelerometers are also used in a wrist band to know the level of physical activity of a person. The use of accelerometers in devices like pen and shoe etc. has become possible as MEMS based technology has made the accelerometers available at low prices. The extensive use of accelerometers in inertial navigation systems (INS) is reported in a large number of papers including the sensing of ground borne vibration [49-52]. The information from INS is of immense value in moving from one location to the next. INS houses three accelerometers oriented in three orthogonal directions to determine the position and velocity [51]. Gyroscopes are used to determine the angular velocity and deploy rate gyros for the purpose. Gyroscope free all accelerometer solutions are also proposed by some authors [54].

The challenges in meeting the requirements of newer applications have been due to noise in the accelerometers and long time integration errors in deriving the position. As stated earlier the distance is derived from acceleration by its double integration. The error in measurement of distance increases as the time of integration increases. The small errors in the measurement of acceleration are integrated into progressively larger velocity errors, which are compounded to still greater errors in position. Since the new position is calculated based on previously calculated position and the measured acceleration, these errors accumulate roughly proportional to the power of time since start of integration time. The RMS error estimates for numerical double integration of noisy stationary accelerometer signals has been published [49]. In case of Global Positioning System (GPS) aided INS, the error is corrected by taking a fix from GPS. The focus of research community has moved to using economical accelerometers by bridging the gap between available specifications and the requirements of the applications.

It is also pointed that long-term integration of accelerometer signals to achieve velocity and position signals has been largely unsuccessful due to integration of small DC offsets resulting in linear and quadratic errors in velocity and position, respectively. In a recent paper, method to detect motion stops in human motion, has been reported so that integration is done only during motion thereby reducing the errors due to double integration [55]. That is, the integration time is reduced by not integrating when actual motion is not there. Further, the characteristics of strap down inertial navigation sensors, namely accelerometers and gyroscopes are explained and their error models are described in [56]. One of the studies proposes use of inertial measurement unit in conjunction with Global Navigation Satellite System [44]. There is a thermal bias drift with time in accelerometers and errors so accumulated in velocity and distance are also reported [35]. Nevertheless, there is a lack of consensus regarding how errors behave with integration time[55].

Inertial measurements obtained using accelerometers are discussed in this chapter and the terms accelerometer, acceleration sensor and sensor are used interchangeably throughout the text of this chapter.

Sources of errors in accelerometers

The captive flight at Rail Track Rocket Sled (RTRS) facility provides a unique environment for kinematic testing at supersonic speeds. Using RTRS facility, the experiments conducted for this work were meant to measure kinematic parameters such as distance traversed, velocity and acceleration attained. It plays a vital role in evaluating missiles, UAVs, fuses and parachutes etc. and triggering events during the sled run test. The error in calculated position becomes significant and needs to be periodically corrected by obtaining fix from some other type of navigation system such as GPS or a novel method proposed in this chapter. In India, a previous study mentions that the GPS offers poor accuracy and Indian Space Research Organisation took up a project GAGAN (GPS aided Geo Augmented Navigation) to improve this accuracy so as to be usable in the air traffic control application [57]. The project GAGAN is reported to have achieved an accuracy of 1.5 meter [58]. Such a system will be put into operation by end of 2014 [59]. A US based Wide-Angle Augmentation System (WAAS)-enabled Global Positioning System is reported to have achieved sample to sample variation in position of 110mm [60]. The system proposed in chapter 3 is recommended as the reference system in this study and offers an accuracy of 4.6 mm (0.046%) while measuring a distance of 10 m, which is the requirement in application under study. It is pertinent to add here that while GPS (although with poor precision) could have been imperfectly deployed in the proposed application, but proposed reference system cannot be used in most applications where GPS is deployed. A study has also been carried out to for fusion of data from different sensors. It is explained that matching performance can be achieved even without position fix.

The work published in [45] focused on quantifying the errors which can be improved by taking various measures.

4.1.1 Sources of Errors

The identified sources of errors in accelerometers are listed below.

- Bias error

- Scale factor non-linearity
- Misalignment of sensitive axis
- Cross coupling error
- Temperature sensitive error
- Mounting error
- Vehicle dynamics error
- Vibration induced error
- Integration errors

4.1.2 Issues Addressed in this Study

The primary measurement described in this chapter is the acceleration. In the course of measurement of acceleration and its derivation to accurate distance, a number of problems were encountered. This study discusses following solutions to the problems encountered in using accelerometers as sensors.

- Methodology in arriving at correct values of kinematic parameters such as displacement or distance, velocity and acceleration.
- Generation of reference readings using a novel method to validate results. The method described in the chapter 3 is used as a reference system in this chapter.
- Quantification of improvement's measures to mitigate errors. Identification of the measures which reduce errors, which have significant effect and also the ones which have very little effect. Instead of studying individual errors, the present study focuses on gross improvements by removing or adjusting the errors to minimum.
- Mitigation of the error due to mounting of sensors as in this application sensors have high level of vibration.
- Accurate method of generation of position fix which is better than the GPS based and reasons for applying fix in position and not the velocity or acceleration.
- Bringing out contribution of previously studied and highlighted noise in stationary accelerometer, which is found to be very little [49].
- Discussion of issues and challenges in conducting experiments

4.1.3 An Alternate Ground Based System and its Shortcomings

At the outset it can be stated that the objectives of the research have been to study more than one technique. A technique for measurement of velocity was proposed, implement and explained in chapter I. The technique mentions about a network of ground based magneto-inductive sensors which can be used for measurement of distances. The system is elaborated by us in previous publication [61].

In the augmented track at RTRS, it requires setting up sensors all along 3 tracks of length 12 km. The requirement of deployment of cables and sensors increases the cost of implementation. Unlike the system proposed in this chapter, this earlier proposed scheme cannot generate triggers for various events based on the kinematic parameters, which are required for onboard operations.

4.1.4 Approach

A methodology was developed in which acceleration was the primary measurement. . The study begins by developing a system which could measure acceleration during sled motion. A system with more than one acceleration sensor was required to carry out the studies. The cycle of development followed is shown in figure 4.1. Further, such a system was subjected to a high level of acceleration. The acceleration so measured was subjected to bias correction for the processing to be meaningful. The distance was derived from measured acceleration by double integration. The derived values of distance were compared with the reference values to determine errors. In this process several elements of error are identified and the measures are taken to reduce the errors before obtaining the corrected kinematic parameter.

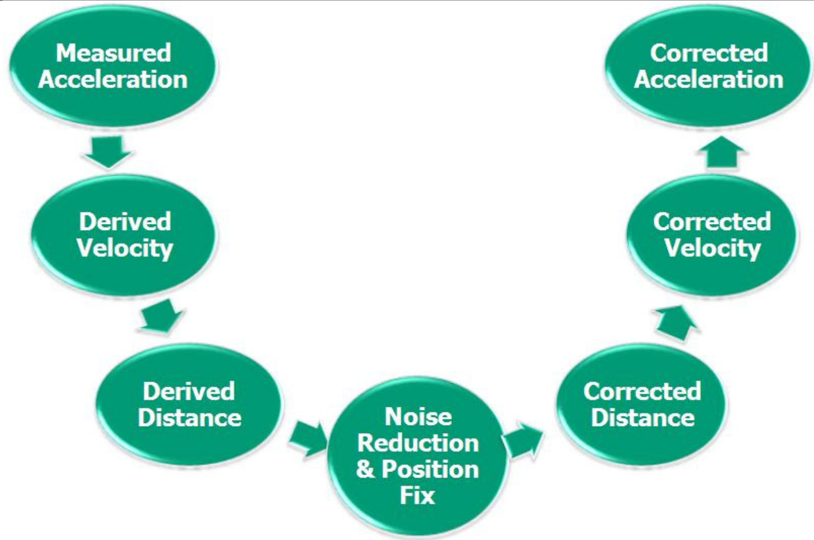

Figure 4.1: The approach followed in improving upon the signals acquired using accelerometers.

4.2 Measurement of Acceleration

The aim of conducting experiment was to measure the acceleration and distance. The corrected distance leads to velocity and acceleration of sled. The measurement of these parameters is of utmost importance in evaluation of performance of test article and also for generating event triggers. The sled is propelled down the rail track by rockets. In a typical trial it traverses a distance of about 2 km in 20 sec. The maximum velocities recorded on this track reach a level of 500 m/s. In this regard following sections describe the onboard system developed for measurement of various parameters, the selection of sensors and method of generating reference reading, applying the bias correction and plotting results of distance obtained in first iteration. It helps in identifying errors and correcting them in the subsequent sections.

4.2.1 Development of Onboard System

To measure and determine the variation of kinematic parameters like acceleration, velocity and distance with time, a DSP based onboard system was developed. The DSP processor TMS320C6748 based designed board could acquire

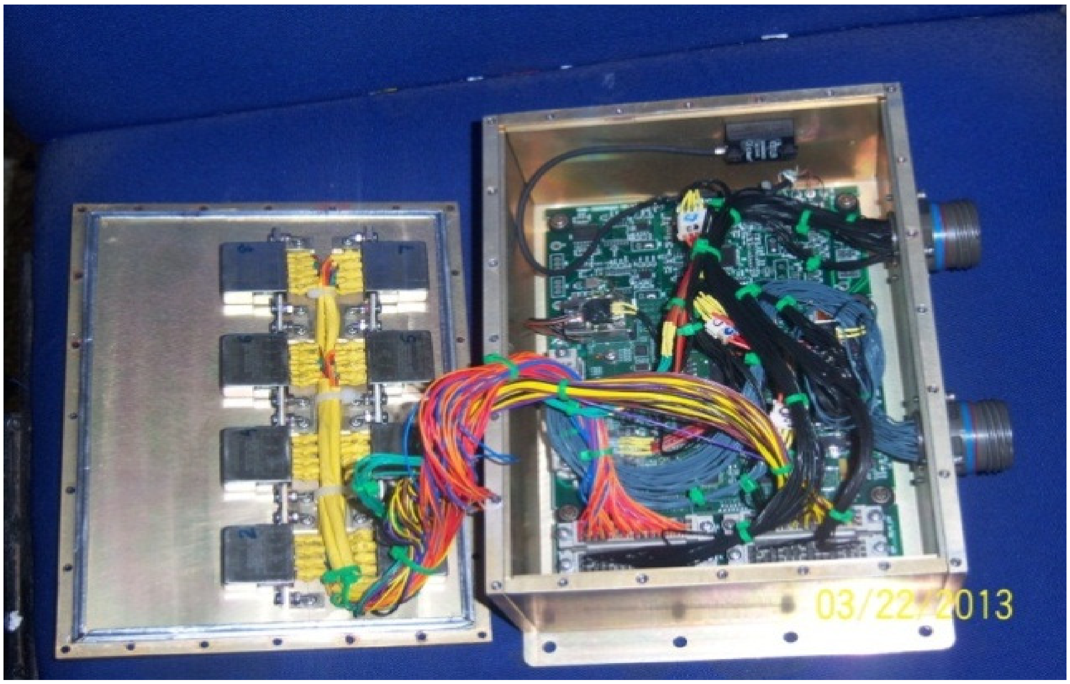

Figure 4.2: System realized for experimentation & implementation

samples at 2 kHz from 3 different accelerometers and save data in flash memory for 20 sec. The picture and the block diagram are shown in figures 4.2 and4.3. Use of 3 accelerometers helped us in getting consistent data in one trial itself. To find the effect of use of different brands of accelerometers and different types of mountings, three different accelerometers are used. While two of the sensors were mounted on the printed circuit board, third sensor was mounted on the wall of the housing with anti-vibration mounts. This also brought out in table 4.1. Having a number of sensors also leaves scope for data fusion. The board was also capable of invoking interrupt on occurrence of position marker pulses. The distance is derived by double integration of acceleration. Provision was made to pick up signal from pre-programmed location so as to apply position fix. As an extension of this work, trigger based time, distance, velocity and acceleration was generated so as to fire next set of rockets, deploy a parachute and check for sustained acceleration. There was a provision to check start of motion using an umbilical connector which gets snapped off as the motion started. The values of acceleration were recorded with a pre-trigger time of 80ms. However, the data acquired had error and distance so derived deviated from true value due to number of factors, which are explained later.

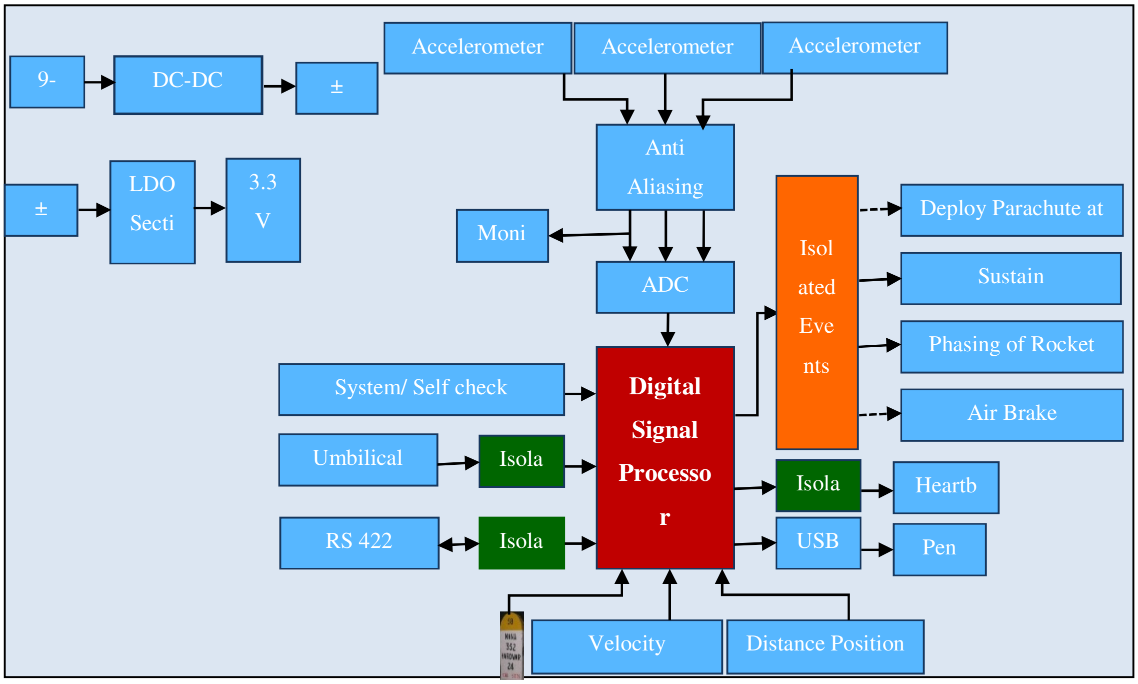

Figure 4.3: Block diagram of the onboard system to acquire and record signals from 2 sensors.

4.2.2 Accelerometers and Their Configuration

Three different MEMS based accelerometers, namely A1,A2 and A3, were deployed under similar test conditions. All the three accelerometer were of different brands. The brief relevant specifications, as converted to comparable units, of these three sensors are given in table 4.1.A drift in accelerometer output severely affects the accuracy of measurement of velocity and distance. Therefore, accelerometers with MEMS capacitive technology, having low drift, were chosen. Moreover, these accelerometers do not require complex high impedance accelerometer cables, which are so essential in piezo-electric accelerometers [62].

Table 4.1: Comparative brief specifications of three accelerometers used simultaneously while conducting experiments			
Name	A1	A2	A3
Make	Kistler	Analog Devices	Freescale
Type (Single Axis)	Capacitive MEMS	Capacitive MEMS	Capacitive MEMS
Range (g)	±50	±55	±22.5
Sensitivity (mV/g)	80	38	100
AmplifierGain	1	2	2
Bandwidth (Hz)	1000 (±5%)	400 (3dB)	400 (3dB)
Noise density (Typical)	0.625 (0-100Hz) mg/√Hz	1.4 - 3 mg/√ Hz	1.1 mg/√ Hz
Mounting	Chassis mounted	Soldered on PCB	Soldered on PCB

From table 4.1 it is clear that the inherent sensitivity of accelerometers A2 and A3 is 38 and 100 mV/g respectively. A2 has low sensitivity and A3 has a low range. Therefore, a gain of 2 has been provided in the amplifier section. The data obtained for these channels has double the value. This also enables us to convert the accelerometers A2 and A3 output of 0 to 5V to ±5V. The sensor A1 has an output of

±5V and did not require any change in the gain. With this change, all the output values of amplifiers matched the input range of analog to digital converter. While the sensor A1 was mounted on chassis, the other two sensors, namely A2 and A3, were soldered on the PCB. Since each trial required firing of as many as eight expensive rockets, only two trials could be conducted to acquire data. But, adequate data was obtained as three accelerometers were deployed in each trial.

4.2.3 Experimental Setup to Generate Reference Readings

There was a requirement to obtain distances travelled with time with more accuracy and relate it with the distances derived from accelerometers. Magneto-Inductive pickups were used to mark the distances at regular interval of sled travel. Magnet and inductive pick-ups used are as described by the authors of paper [61] and further elaborated in Chapter III. The same sets of sensors were organized in two different arrangements and output from both the setups was recorded by each system separately. In one case, the coil was on the ground and magnet was on the moving sled. The output of coils was multiplexed in 10 different channels and the picked up signals propagated to a computer, which was about 1.2 km away in this set of trials. The setup is explained in section 3.8.3.2. The distance between the coils was measured with a precision of 1 mm. In the second arrangement the magnets were on the ground and coil was on the moving sled. A specially designed card acquired the signals at 50 kHz sampling rate. The signals were stored in the onboard flash memory. Such a system is explained in section 3.8.3.3. The interval between incoming pulses and the distance between the magnets from both the setups were combined together and a profile of the distance versus time was generated which acted as the reference values. The worst case relative error in this arrangement is given by equation (4.1).

$$Relative\ error = [(\Delta s/S_{min}) + (\Delta t/T_{min})]\ X\ 100\ \% \qquad (4.1)$$

Here, Δs is error in measurement of distance S_{min}, S_{min} is the minimum distance between two sensors, Δt is the error in measurement of time T_{min}, it is the minimum time between two pulses from inductive pick up. The accuracy of the system when recording was by onboard system was found to be 0.046% and when the recording was by ground based system the accuracy was found to be 0.24%.

The distance vs time profile so measured acted as the reference for comparison of correctness of distances calculated from measured values of acceleration. The reference readings are shown as blue coloured graph in figure 4.4. There were gaps in the data obtained using both the systems. Therefore, the reference readings of onboard as well as ground based system were merged and more consistent graph was obtained.

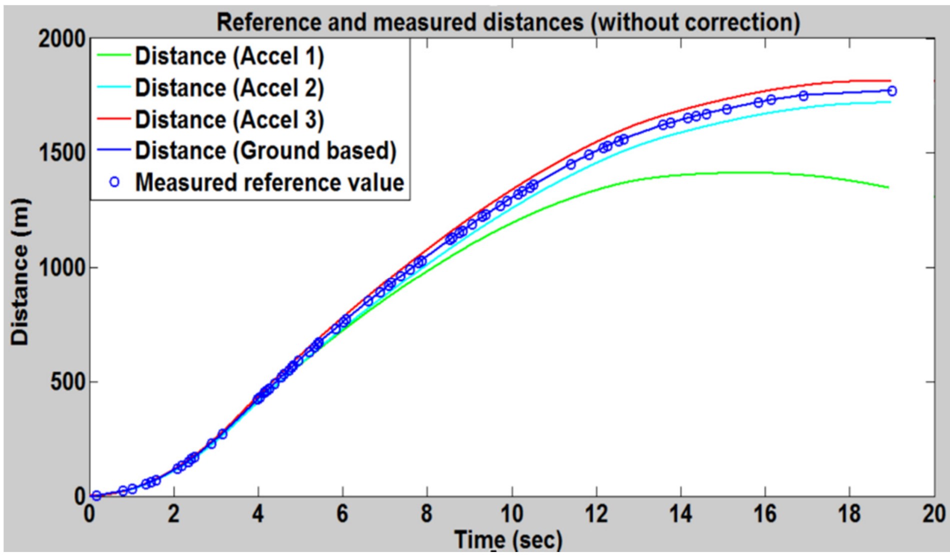

Figure 4.4: Reference vs Measured distance with time

4.2.4 Correcting Acceleration and Distance data

The acceleration data was acquired during high speed sled run using the system explained in section 4.2.1. The plot of data from accelerometer A3 is shown in figure 4.5. There are two distinct phases of acceleration. This was due to two sets of rockets being fired. Second set is fired after the first set had burnt out. This can be observed in the acceleration profiles obtained from each sensor. With such a scheme it becomes possible to achieve higher velocity and yet maintain a low level of 'g'. The distance traversed was determined by double numerical integration of the acceleration. Before numerical integration, bias correction and filtering was carried out. This process had to be done as data was noisy and exhibited a significant bias level. These details are explained in the section 4.3.1.2.

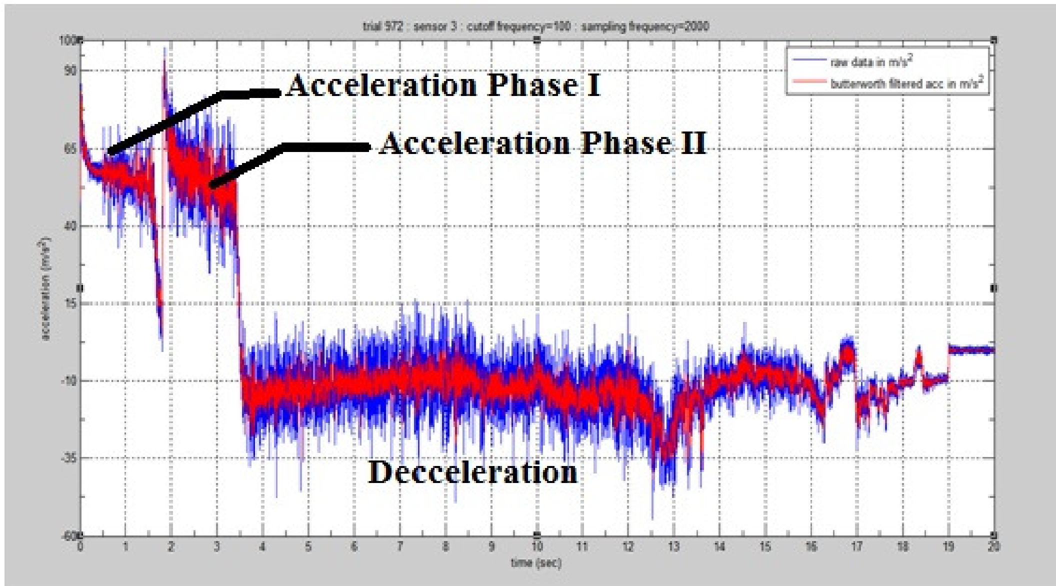

Fig 4.5: Acceleration profile of data acquired using accelerometer A3.

There was a major deviation of distance derived from accelerometer A1. The errors so found are consolidated and tabulated in section 4.4.2.The plot in figure 4.5 shows that even after filtering the graph is not in the acceptable condition. There is scope for a lot of improvement. The following section describes the host of methods followed to bring about the desired improvements. It was felt that errors need to be removed by following systematic approaches, which are explained in next section.

4.2.5 Steps to Improve Upon the Acquired Acceleration Data

The deviation of results from true value can be due to offset, thermal drift, vibration during motion and method of integration. Following is the list of steps taken to improve the accuracy of measurement.

- Bias correction to remove the error due to offset
- Some of the AC noise was removed by anti-aliasing and low pass Butterworth filter. Still, the filtered acceleration had some AC noise component along with the desired AC and DC signal values. They cannot be separated further as they lie in the same frequency band.

- Double integration of the acceleration using trapezoidal method of integration was done in order to obtain the distance. The distance signal so obtained consisted of DC noise component along with the desired DC signal values.
- This DC noise was further reduced by subtracting the double integrated stationary sensor RMS noise. The RMS noise so found had dimensions of distance and was the DC equivalent of the AC noise in stationary accelerometer.
- To remove the leftover DC noise completely, which arises due to vibration during motion, a correction coefficient is determined by generating the reference distance markers. Now the position fix was applied.
- Corrected course was determined from start time (t0). This was achieved by numerical differentiation of corrected distance to determine velocity and acceleration. Corrected course is used for further estimation of distances until requirement of next position fix occurs.

4.2.6 Capping and Filtering

During the sled motion, noise is first removed using a capping factor. The spikes which appear in the acquired signal and are not there in the physical phenomenon are limited by the capping factor. In the application under study, it is possible to estimate the maximum change of acceleration that would occur in the trial to be conducted. This is achieved using the thrust and drag during sled motion and is not in the scope of this research. The capping function is based on the outcome of estimated value of acceleration. It was estimated that if the change of acceleration is more than the estimated value, it must be due to noise. So a capping function was developed and implemented to limit the noise.

Let C_f be the capping factor calculated from maximum estimated value of acceleration or deceleration, the capping factor CS is given by equation

$$C_s = \frac{(a_2 - a_1)}{(t_2 - t_1)} \text{ x } t_s, \tag{4.2}$$

If $C_s > C_f$

$$a_2 = a_1 + C_f \tag{4.3}$$

where, a_2 is the acceleration at time t_2 and a_1 is the acceleration at time t_1. ts is the interval at which acceleration signal is sampled. It may be noted that maximum change of acceleration is observed on full burn of a rocket propellant. This is in fact the deceleration.

In case the difference between current reading and previous reading of acceleration is more than capping factor, then we replace current reading of acceleration with previous reading plus capping factor keeping in view the sign of change. To further reduce the noise there are two types of filters implemented in the system. An anti-aliasing filter of 1 kHz, which is implemented in the hardware, acts as the low pass filter. In addition a 2nd order Butterworth filter in the software restricts the bandwidth to 100 Hz.

4.2.7 Bias Correction and Issues

The fixed bias error is the sensor output observed in the sensor even when there is no physical input [53]. In signal conditioner output of each accelerometer, zero acceleration does not correspond to zero volts output. It results in significant error while deriving the distance. Therefore, a bias correction becomes mandatory.

The sled is propelled by firing rockets. The start of motion event is sensed by a snap off connector which disconnects on sled motion and starts the recording. However, it was found that the electrical disconnection happened after 23 ms of the physical motion of sled. This was due to travel time of connector pins in the shell. This resulted in initial loss of data of rise time of acceleration and caused creeping in of error at very first stage which affected all the distances derived by double integration during the entire travel time. As a remedial measure, the feasible pre-trigger of 40ms was provided which enabled start of recording before the start event was sensed. The first 40ms of acquired signals are shown figure 4.6. In this record first N=34 samples (17ms) of pre trigger period was found to be quiescent period and was averaged to determine bias level.

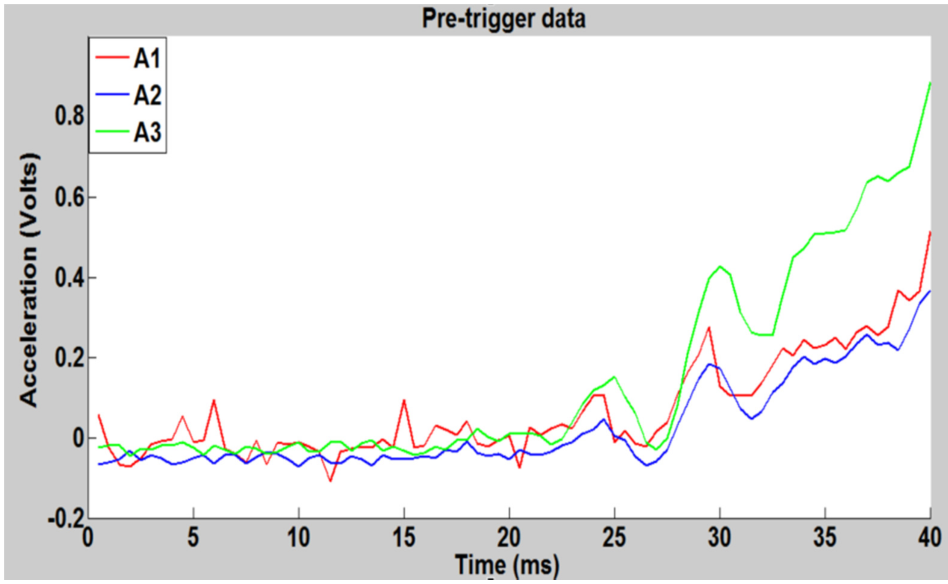

Figure 4.6: Pretrigger acceleration of first 40ms

To correct the bias, it was subtracted from each ith sample of acceleration (accel)

$$\boldsymbol{a}(i) = accel(i) - \frac{1}{N}\sum_{n=1}^{N} a(n) \qquad (4.4)$$

where, $a(n)$ is the value of acceleration samples during the quiescent period and $\boldsymbol{a}(i)$ is the bias corrected sample of acceleration.

4.2.8 Derivation of Distance from Samples of Acceleration

The distance travelled is obtained from acceleration samples by using Eulers method of double integration applied on bias corrected discrete acceleration samples,

$$v(i) = v(i-1) + [t(i) - t(i-1)]a(i) \qquad (4.5)$$

$$s(i) = s(i-1) + [t(i) - t(i-1)]v(i) \qquad (4.6)$$

Where $s(i)$, $v(i)$ and $a(i)$ are the samples of distance, velocity and acceleration at instance $t(i)$. The error in measurement of s and v was more as the integration time increased while using (4.5) and (4.6). To reduce the measurement error, trapezoidal integration given by (4.7) and (4.8) was applied to the bias corrected samples

$$v(i) = v(i-1) + \frac{1}{2}[t(i) - t(i-1)][\,a(i-1) + a(i)\,] \qquad (4.7)$$

$$s(i) = s(i-1) + \frac{1}{2}[t(i) - t(i-1)][v(i-1) + v(i)] \qquad (4.8)$$

As mentioned above, a number of methods are available for numerical integration. We have chosen trapezoidal rule because of its simplicity and good approximation. Also, our sampling rate is very high that results in high accuracy of trapezoidal method. The resulting improvements are discussed in section 4.4.1.

4.2.9 RMS noise Erms(N) when Accelerometer is Stationary

The measured value differs from the reference values due to various reasons. Some of the prominent reasons are listed section 4.1.1. Having corrected bias and passing the signal through low pass filter, the next attempt is to handle noise observed when accelerometer is stationary. It was found that the accelerometer exhibits noise even when it is not in motion. The value of noise and the double integrated values were found to vary from sensor to sensor. This aspect was confirmed by keeping sensor and the acquisition system over the vibration free bench. The system described in section 4.2.1 is capable of recording for 20sec. Therefore, as shown in figure 4.7, the values were recorded for 20 sec. The values of noise density (σ_c) in $m/s^{3/2}$ as interpreted from data sheets of accelerometers are σ_c = 0.000625x9.806 for A1; σ_c = 0.0014x9.806 for A2 and σ_c = 0.0011x9.806 for A3. These values have been used in the calculations of RMS value of noise $E_{rms}(N)$.

The graph in figure 4.7 is obtained after correcting the offset, followed by double integration of the measured acceleration using trapezoidal method of numerical integration and using the equations mentioned in Appendix A to find distance. The value of distance so derived after using $E_{rms}(N)$ is plotted in figure 4.7in red colour.

Reversal of Direction

The graph of figure 4.7 is also helpful in determining reversal of direction of sled. If there is acceleration, deceleration followed by zero acceleration and then a deceleration (ref fig 4.11), it can be assumed that sled has reversed direction. If double integrated value of measurement is more that the value as shown in figure 4.7, it can be assumed that sled has reversed direction. The magnitude of error signal which the deceleration signal due to reversal has to overcome will depend upon the integration time.

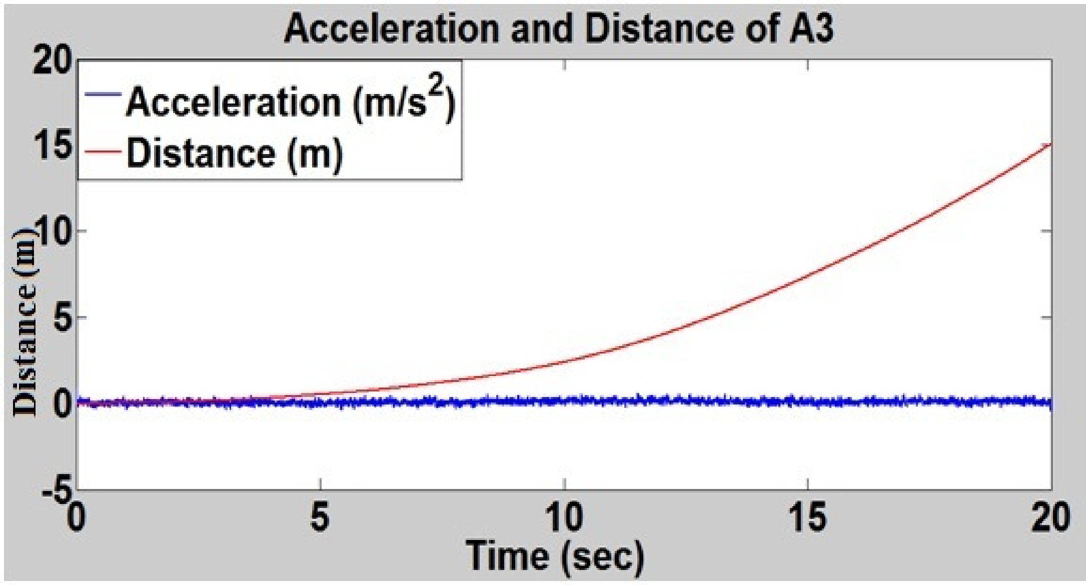

Figure 4.7: Distance measured after removing noise added

4.2.10 Method of determining position fix

It was observed that as the travel time increased, the deviation of actual position from true position also gets increased. The position fix (true position) confirms the actual position during a journey. To determine the actual position, a magnet is fixed on the ground at the pre-determined distance and an inductive pickup is kept on the moving sled [61]. As the sled passes the pre-determined distance, the position marker pulse is generated which invokes an interrupt in the recording system of figure 4.2. The time of arrival of the position marker pulse gets recorded. All the past and current measurements are corrected until the next position fix is obtained. The correction due to position fix to all the samples recorded is applied and is described in the next section.

Application of position fix and course correction

The position marker mentioned in preceding section gives location of the sled which is more accurate than the one measured by the proposed system and acts as the reference distance. A correction co-efficient (k) is determined at point of fix and is applied thereafter until the next fix. The value of E_{rms}, as elaborated in Appendix A, is obtained for every sample. The multiplication of k with E_{rms} is a measure of the correction to be applied at every sample.

Let s(n) be the distance obtained by double integration of measured acceleration at point of fix. It is also the bias corrected or filtered value in case the same has been considered in the calculation and sr(n) be the distance obtained from the reference position marker described in the preceding section. The correction coefficient (k) is calculated as

$$k = 2 \times \frac{s(n) - s_r(n)}{E_{rms}(N)} \tag{4.9}$$

Here 'n' signifies the sample number and 'N' signifies total number of samples that have been used in the calculation of this parameter. It may be noted that the value of k will be different for measured, bias corrected and filtered cases of samples.

From Newton's second law of motion,

$$s = ut + 1/2\ at^2 \tag{4.10}$$

Similarly, the corrected distance $s_c(n)$ at any sample n is calculated as

$$s_c(n) = s(n) + \frac{1}{2} k E_{rms}(n) \tag{4.11}$$

Here, $\frac{1}{2}$ k $E_{rms}(n)$ has the dimensions of distance and is a measure of the correction required to be applied in all samples of s(n) where the position fix is applied till the latest point of pre-determined distance. The value of s(n) will be based on whether bias correction or filtered acceleration has been considered. Further, the corrected velocity and acceleration are determined by numerical differentiation of $s_c(n)$. It was found that two such position marker pulses were adequate to reduce and bring the error in distance within tolerable limits. The corrected distance graphs are shown in figure 4.8, where position fix is applied at 4.2 sec and 8.76 sec.

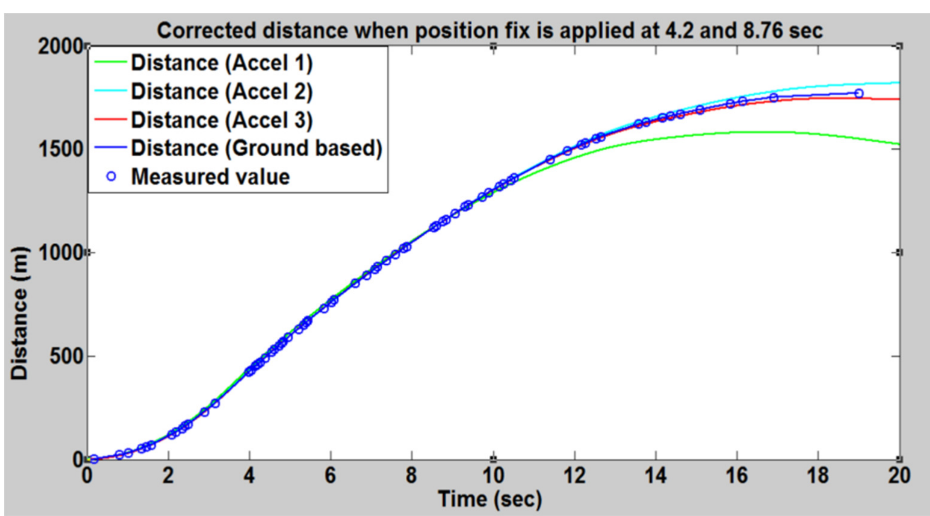

Figure 4.8: Corrected distance measurement with position fix

4.2.11 Improvement due to trapezoidal method over the Euler's method of integration

The improvement in distance measured by using trapezoidal method over Euler's method of integration is shown in figure 4.9 for sensor A2. The improvement is found to increase with time and its maximum value is 0.231 m at endpoint where the sled is stopped. Similar results were obtained for all the three deployed sensors , wherein the resulting distance using trapezoidal method was 0.2 to 0.231 m more close to the reference value at end point where the sled stopped. It reconfirms the fact that trapezoidal method gives better results. This was due to the fact that the Euler's method follows the area under the curve in steps of rectangles. The trapezoidal method follows the area under the curve in steps of rectangles and the additional area in triangles, which makes closely follow the curved path and gives more accurate integrated value. Therefore, trapezoidal method was used for further work presented in this study.

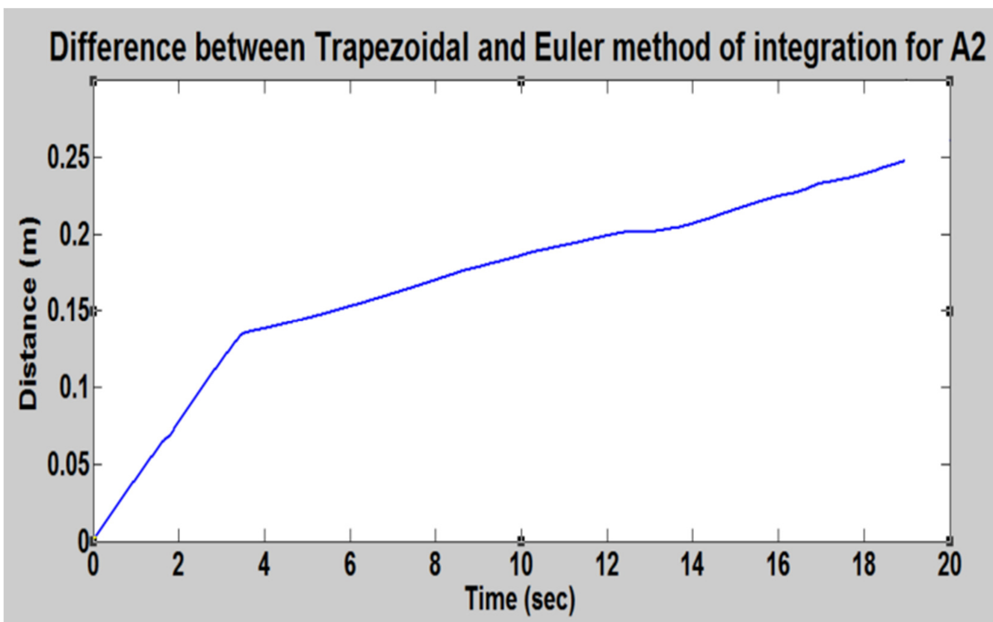

Figure 4.9: Difference in Trapezoidal and Euler methods of measured distance

4.2.12 Error Calculation and Consolidated Tabulation

The list of various measures taken to mitigate the error, percentage improvement for each measure taken for the three accelerator used in the experiments, is listed in Table 4.2. The value of s(n) is modified for different cases of bias correction or filtering in (4.11). Further, using equation 4.11, the error in distance is calculated as follows

$$\text{Percentage}Error(\%)\text{in distance} = \frac{s_r(n) - s_c(n)}{s_r(n)} \times 100 \qquad (4.12)$$

Table 4.2: Results of experiments in terms of % error in distance

Sl. No.	Description	% Error in dist. at 4.2 sec	% Error in dist. at 8.76 s	% Error in dist at 19.1 s
ACCELEROMETER 1				
A1.1	No correction is done	7.032	13.192	43.186
A1.2	Only bias correction is done	3.519	7.069	24.262
A1.3	With capping and bias correction	3.519	7.069	24.262
A1.4	With Capping, biasing and filtering	3.515	7.066	24.257
A1.5	Only RMS noise is subtracted	3.478	7.019	24.159
A1.6	Position fix at 4.2 sec	0	2.813	15.381
A1.7	Position fix at 8.76 sec	-2.326	0	9.510
A1.8	Position fix at 19.1 sec	-6.095	-4.557	0
A1.9	Position fix at 4.2 & 8.76 sec	-3.282	0	12.627
ACCELEROMETER 2				
A2.1	No correction is done	16.338	25.974	72.148
A2.2	Only bias correction is done	3.489	3.577	2.927
A2.3	With capping and bias correction	3.489	3.579	2.927
A2.4	With Capping, biasing and filtering	3.489	3.579	2.927
A2.5	Only RMS noise is subtracted	3.446	3.527	2.818
A2.6	Position fix at 4.2 sec	0	-0.640	-5.877
A2.7	Position fix at 8.76 sec	0.529	0	-4.542
A2.8	Position fix at 19.1 sec	2.329	2.176	0
A2.9	Position fix at 4.2 & 8.76 sec	-0.418	0	-2.451
ACCELEROMETER 3				
A3.1	No correction is done	-0.453	1.658	11.036
A3.2	Only bias correction is done	-2.956	-2.704	-2.448
A3.3	With capping and bias correction	-2.956	-2.704	-2.448
A3.4	With Capping, biasing and filtering	-2.954	-2.703	-2.447
A3.5	Only RMS noise is subtracted	-2.939	-2.685	-2.4068
A3.6	Position fix at 4.2 sec	0	0.870	5.010
A3.7	Position fix at 8.76 sec	-0.7192	0	3.196
A3.8	Position fix at 19.1 sec	-1.986	-1.531	0
A3.9	Position fix at 4.2 & 8.76 sec	0.082	0	1.517

4.2.13 Discussion

The following discussion presents the effects of various factors affecting the results of distance measured

(a) Mounting of sensors

It is evident from rows A1.2, A2.2 and A3.2, of Table 4.2, the error in measurement of distance is highest due to sensor A1. The noise picked up by sensor accelerometer A1 is highest, although A1 has least noise density (Table 4.1). Higher bandwidth of sensor A1 has and method of mounting of sensor has contributed to this error. The fact also manifests itself in figure 4.4 where the deviation of measured distance from reference value due to sensor A1 is highest. The sensor A1 was mounted on chassis using two M3x14 mm bolts. It may be noted that while A1 was mounted on the chassis and the accelerometer A2 and A3 were soldered on PCB. The PCB was further supported on shock mounts.

(b) Capping & Filtering

These were some of the measures tried to improve results of measurements but with not much success. It has been found that the use of the Butterworth low pass filter does not improve the accuracy of measurement of distance. The observations in rows A1.3 and A1.4, A2.3 and A2.4 and A3.3 and A3.4 of Table 4.2 indicate that there is negligible improvement over the rows A1.2, A2.2 and A3.2. These results also indicate that capping, which is explained in section 4.3.1.1, also did not improve the results.

(c)Method of integration

The trapezoidal method resulted in an improvement of up to 0.23 m at end point over the Euler's method (Figure 4.9). Thus, the effect of this measure did improve the results but the effect was not so significant.

(d)Error due to noise when not in motion

One full paper [49] has delved at length onnoise in the stationary accelerometer and its effect. But as seen in rows A1.5, A2.5 and A2.5 of table 4.2, it is found that the contribution of percentage error due to noise, which is present even when sensor is stationary, is very little.

(e) Significance of bias correction in error correction

In rows A1.1 and A1.2, rows A2.1 and A2.2, and rows A3.1 and A3.2, of the table 4.2 show that the effect of bias correction plays a vital role in reducing the error. Acquisition during motionless period plays an important role in the determining the fixed bias. Number of sample recorded when sled is stationary, just before and after the motion should be increased to at least 20 sec each. It will help in better estimation of level of bias and further improve the results due to bias correction.

(f) Significance ofposition fix in error reduction

With reference to rows A1.6 to A1.9, A2.6 to A2.9 and A3.6 to A3.9 of table 4.2, the position fix significantly reduces the percentage error. It is also pertinent to mention here that it is advantageous to apply fix in distance and not in velocity or acceleration. This is due to two reasons. One, due to the fact that after double integration the error is near DC and a constant correction coefficient can be applied to correct the error. Secondly, the precise reference distance markers can be generated in this application, which is not possible with velocity or acceleration.

4.3 Multi Sensor Data Fusion

Multi-disciplinary research in data fusion is driven by the requirements of diverse applications and is an active area of research[63]. Inthis thesis data fusion was proposed as one of the methods for further studiesand as stated in already published research[61]. The study has now been completed and is presented in this chapter. The major advantage of this study is that the results obtained by method of multi sensor data fusion are comparable to the results obtained by taking a position fix and yet without deploying any hardware in the field for obtaining any position fix.The study begins by processing signals obtained from accelerometers data with the steps mentioned below

- Conversion of units.
- Bias correction.
- Filtering.
- Numerical Integration.
- Sensor Fusion.

4.3.1 Conversion of Units

The samples acquired from sensor are in the unit of mV. These are converted to SI units. To convert the acquired data sample $W(n)$in mV to $X(n)$sequence in SI units, i.e. in m/s2 following equation is used

$$X(n) = (W(n) * 9.8)/(Sc * Ga) \quad (4.13)$$

Where, SC and Ga are the sensitivity constant in mV/g and the amplifier gain (unit less) respectively which are mentioned in table 4.1.

4.3.2 Bias Correction

It has been observed that even when there is no motion of the sled, i.e. if accelerometers are initialized while the system is in static condition; it still gives non-zero values of acceleration. These values are random and result in noise. It has a DC bias which if not corrected in the beginning itself, will result in large scale error. The method mentioned in section 4.3.1.2 is used for the purpose, which is in fact

$$Y(n) = X(n) - \bar{X} \quad (4.14)$$

That is,

$$\text{Required}_{\text{data}} = \text{Measured}_{\text{value}} - \text{Average}_{\text{value}}$$

Here, Requireddatais the bias corrected sequence.

4.3.3 Median filter – a pre-processing step

The median filter is a nonlinear digital filtering technique, often used to remove noise. Such noise reduction is a typical pre-processing step to improve the results of later processing. The median filter refers to the replacement of a point by the median value of the series in a segment and its working principle is illustrated in figure 4.10. Here L denotes the number of samples to be passed through preprocessing filter.

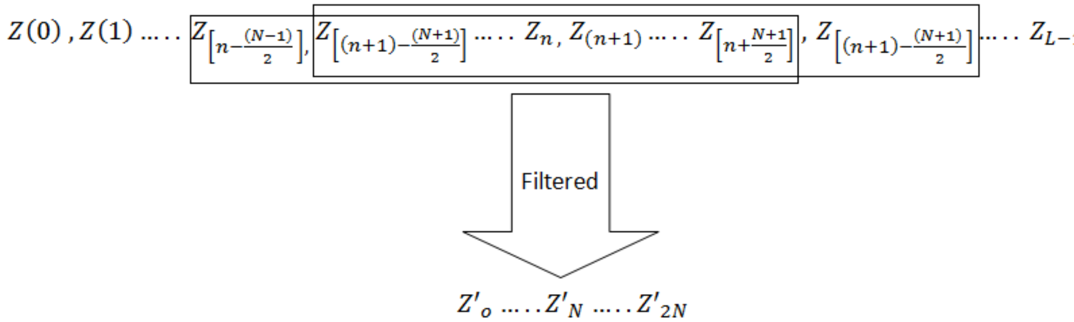

Figure 4.10: Method of obtaining moving window median filter

Z(0)-Z(L-1) refers to the complete data series. A moving window with odd number of elements is taken. So, a moving window of length 2N+1 forms the segment Z(n-(2N+1)/2) - Z(n+(2N+1)/2), which is subjected to pre-processing filter. Now, we obtain a temporary array by sorting segment Z(n-(2N+1)/2) - Z(n+(2N+1)/2) in ascending or descending order. The middle of point in the segment is replaced by the middle point of the temporary array.

The filtering process continues when new segment is obtained by removing the earliest point at the back and inserting the latest (new) point to the front of the original segment, i.e., Z(n-(2N+1)/2) - Z(n+(2N+1)/2). The window moves over the whole data series Z(0)-Z(L-1) to smooth out acceleration signals. Z'(n) is the desired filtered data.

The following graph in figure 4.11 shows the application of median filter. The blue graph shows that the accelerometer data without application of the median filter and the black one represents the output of median filter.

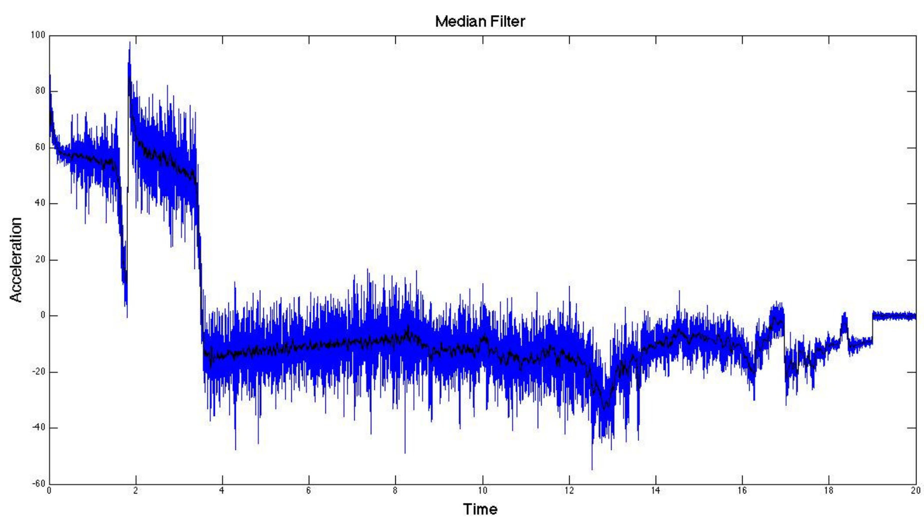

Figure 4.11: Application of median filter to pre-processed data

4.3.4 Variances of Different Sensors

To achieve data fusion of different sensors, we need to express the uncertainty in data from each sensor so as meet the challenge of data fusion [63]. Following section describes the method adapted for arriving at the variances. If number of observations is more than 20, the standard deviation is given by

Let deviation d = xi - $\overline{X}$,

Where xi is the observations in form of samples of acceleration,

$\overline{X}$ is the arithmetic mean of observations,

n is the number of observations

$$S.D.\ \sigma = \sum\sqrt{d^2/n} \quad (4.15)$$

The average value $\overline{X}$ approaches the true value as the number of measurements in the average approaches infinity. Finding the true value is impractical, so we settle for the best value given by the average. The average value is also called the mean value. Random fluctuations are described by the normal distribution, or Gaussian distribution, or the bell curve.

The variances are calculated from the data just before the sled motion starts, i.e. noise recorded by accelerometer prior to system run. First 17 ms of data shown in figure 4.6 was used for this purpose as this was data just before the motion began. The values of the variances calculated were as follows

Variance of Sensor 1 $\sigma_{z_1}^2$= 30.7718 (4.16)

Variance of Sensor 2 $\sigma_{z_2}^2$= 9.0369 (4.17)

Variance of Sensor 3 $\sigma_{z_3}^2$= 4.8 (4.18)

A variance measures how far a set of numbers is spread out. A variance of zero indicates that all the values are identical. Variance is always non-negative value. A small variance indicates that the data tends to be very close to the expected value and hence to each other, while a high variance indicates that the data has broader spread out around the mean. Since, the variance of sensor 1 is much higher than the variance from sensor 2 and sensors 3, the measurements obtained from it are much less reliable than the measurements from other two sensors.

4.3.5 Data fusion

At this point we had three measurements to estimate the best value of acceleration and hence the position. But the question was how to combine these values so as to obtain a single value which is closest to the true value. The concepts mentioned in reference [46] were adapted to be applied to the new application of determining kinematic parameters of sled run. Multi-sensor data fusion is a technique which enables combining of data from several sensors so as to obtain a composite picture which is better that the information from individual sensor. In recent years the data fusion research community has achieved substantial advances. Still emulation of data fusion capability and capacity of human brain is farfetched phenomenon [63].

Appling the information available in [46], the conditional probability density based on measurements from accelerometer a1 and a2 are plotted in figure 4.12. The figure depicts higher level of uncertainty due to a1, that is large value of σ , than the plot of a2. Data from sensor a1 and sensor a2 is fused such that we get graph a. The desired result is obtained if uncertainty due to a is lower than a1 or a2.

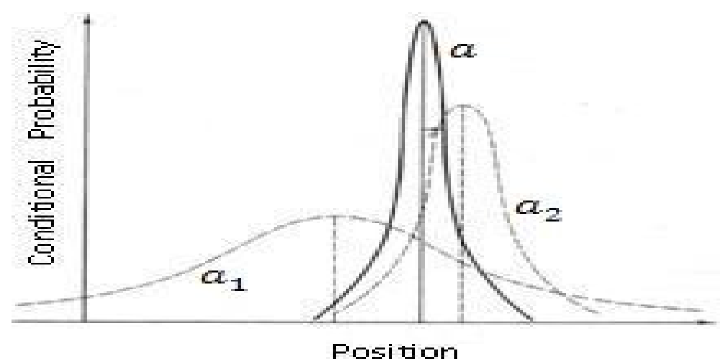

Figure 4.12 Concept of Conditional probability density due to sensor *a1, a2* and after fusion of both into *a*.

Now putting the values of variances from equations 4.16 and 4.17 in equation 4.19 and 4.20 mean μ_1 corresponding to each sample, as shown in graph a in figure 4.12, is

$$\mu_1 = \left[\frac{\sigma_{z_2}^2}{(\sigma_{z_1}^2 + \sigma_{z_2}^2)}\right] z_1 + \left[\frac{\sigma_{z_1}^2}{(\sigma_{z_1}^2 + \sigma_{z_2}^2)}\right] z_2 \qquad (4.19)$$

$$\frac{1}{\sigma_{12}^2} = \left(\frac{1}{\sigma_{z_1}^2}\right) + \left(\frac{1}{\sigma_{z_2}^2}\right) \tag{4.20}$$

This shows that uncertainty σ_{12}^2 after fusion of $\sigma_{z_1}^2$ and $\sigma_{z_2}^2$ will be lower than the least. The outcome of fusion of two sensors is further combined with the third sensor as follows

$$\mu = \left[\frac{\sigma_{z_3}^2}{(\sigma_{12}^2 + \sigma_{z_3}^2)}\right]\mu_1 + \left[\frac{\sigma_{12}^2}{(\sigma_{12}^2 + \sigma_{z_3}^2)}\right] z_3 \tag{4.21}$$

$$\frac{1}{\sigma^2} = \left(\frac{1}{\sigma_{12}^2}\right) + \left(\frac{1}{\sigma_{z_3}^2}\right) \tag{4.22}$$

Here z_3 are the measurements by the sensor 3

μ is the mean due to all three sensors

σ^2 is the resultant uncertainty

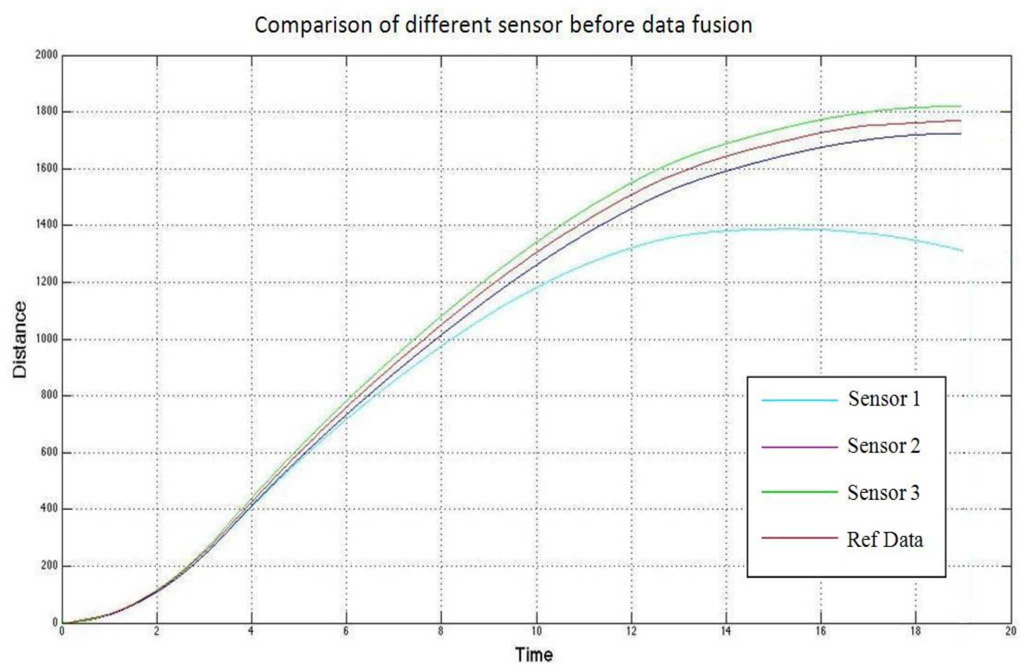

Figure 4.13 : Plot of distances from sensors with respect to the reference reading before the data fusion

The values of acceleration are converted to distance domain. The values are converted to distance domain because the accurate reference values in the domain are available for comparison. Trapezoidal method of integration was used for this purpose. The double integration is used to arrive at the distance. The results are shown in figure

4.13 depicting graphs of distance derived from sensor 1, sensor 2 and sensor 3 in comparison with the reference readings mentioned as Ref Data. Now the fused data is generated using equations 4.19 to 4.22. The graph of fuse data is plotted in comparison to the values of figure 4.13. The resultant values are shown in figure 4.14.

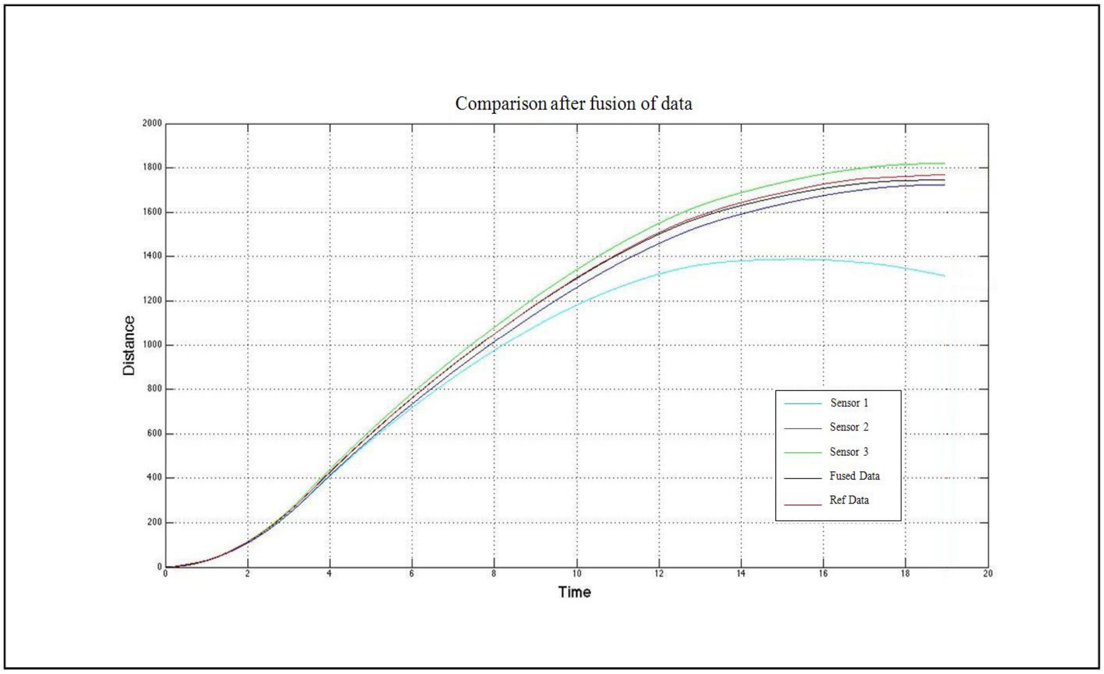

Figure 4.14: The distances after fusion nearly coincide with the reference distances, whereas the distances due to individual sensors have large deviation.

4.3.6 Discussions

The results were compiled by passing data through following processes

- No correction – Errors were found in the acquired data
- Bias correction carried out – The bias level was subtracted from the acquired data
- Median Filter – Median filter was applied to data acquired from each sensor. This was a preprocessing step, before the data fusion could be carried out.
- Data fusion – Data fusion of data from all sensors, after passing through pre-processing steps, was carried out
- The results so obtained , after consideration of fusion of data, are tabulated in table 4.3 below

Table 4.3: Results of accelerometers ACCELEROMETER 1					
Sl. No.	Description		% Error in distance at 4.2 sec	% Error in distance at 8.76 s	% Error in distance at 19.1 s
A1.1	No correction is done		7	13.2	43.2
A1.2	Only bias correction is done		3.68	7.3	25.1
A1.3	Filtering is also done		4.4	7.9	26
A1.4	Fusion is carried out		-0.28	0.087	1.52
ACCELEROMETER 2					
A2.1	No correction is done		16.3	26	72.2
A2.2	Only bias correction is done		3.62	3.74	3.5
A2.3	Filtering is also done		3.47	3.39	2.6
A2.4	Fusion is carried out		-0.28	0.087	1.52
ACCELEROMETER 3					
A3.1	No correction is done		-0.46	1.65	11.07
A3.2	Only bias correction is done		-2.88	-2.6	-2.14
A3.3	Filtering is also done		-2.93	-2.87	-2.77
A3.4	Fusion is carried out		-0.28	0.087	1.52

4.4 Summary of the chapter

We have experimented and evaluated results of use of three different MEMS based accelerometers of different makes under identical conditions when propelled at high velocities.

In the application under study, an unconventional reference system was developed which has an accuracy of 4.6 mm in distance. GPS based reference systems are predominantly used and are not better than the proposed reference system. The WAAS-enabled GPS is stated to have an accuracy of 110 mm.

An embedded system was developed to conduct experiments. Various errors contributing to measurement of velocity and distance at supersonic speeds have been identified and discussed in this chapter. Technique of data fusion was developed which resulted in accuracy comparable with the method of position fix. Major advantage of data fusion is that no additional hardware need be carried with the onboard system.

Chapter 5

5 Measurement of velocity based on pressure

The study so far focused on determining velocity using two different primary measurements. In Chapter 3 we have described the technique based on distance time measurement. The Chapter 4 describes the measurement of acceleration as the primary measurement for finding velocity and distance. Further several techniques were explored and pressure as primary measurement was identified as suitable and feasible technique for RTRS applications. Therefore, the study was extended to cover various aspects of measurement of pressure leading to velocity of sled. The study was supported by number of experiments wherein the technique was applied for the first time in such an application. The objective 1.2(b) mentions that two out of three techniques be proposed for use in future at RTRS.

The **velocity of fluid flow relative to sled is a measure of the velocity of sled.** The pressure due to fluid flow increases when it is brought to rest by an obstruction. A probe named Pitot tube is used to study such a phenomenon. The tube was named after Henri Pitot in 1732, who was studying the flow of water [27]. The basic principle of the Pitot and Pitot static tube is that the pressure of a flowing fluid will increase when it is brought to rest at a stagnation point of the probe [64]. The difference between the stagnation pressure and the static pressure is related to the dynamic pressure which is proportional to the square of the velocity for incompressible flow. **At low velocities the density of air does not change and the flow is considered incompressible. So if we can measure the raised pressure, the velocity can be derived from it.**

Typical application of a Pitot tube is the measurement of velocity of an aircraft [64]. Design of Pitot for measurement of velocity in wind tunnels of NASA has also been reported [65]. The velocity measurement from different flows is discussed next.

5.1 Theory of determining velocity in different flow regimes

Knowledge of fluid dynamics is required to effectively utilize the velocity measurement capability of Pitot tube. As shown in figure 5.1, when a body moves through air flow, the fast moving flow comes to a rest on the nose of the body. The point where it happens is called stagnation point. The pressure at this point rises and is called stagnation pressure. The stagnation pressure is obtained from the Pitot probe mounted on the moving article such as an aircraft or a sled. The static pressure, which is due to random motion of air particles, is sensed by a static pressure hole elsewhere on the aircraft. Sometimes the static and total / stagnation pressure are sensed using the same tube, that is, Pitot static tube senses both the stagnation pressure and the static pressure. **Static pressure is the one we would feel when moving along with flow. On the other hand stagnation pressure is the pressure that would exist if flow were slowed down isentropically to zero velocity.** It is experienced when the body moves against the flow.

Dynamic pressure is the difference between total pressure and static pressure. The value of dynamic pressure is the measure of velocity. The variation in velocity changes the pressure, but compression of flow field also changes the pressure. It is imperative to understand the flow field for accurate measurement of velocity. This field can be incompressible at low velocities, subsonic compressible or supersonic. The description of these flow fields for different ranges of sonic velocities are given in the following section [64].

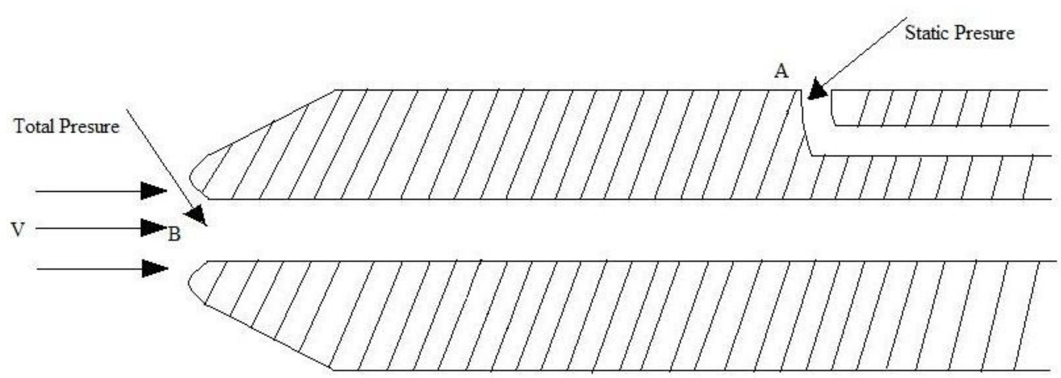

Figure 5.1 A representative simplified view of ports for sensing total and static pressures.

5.1.1 Velocity is less than 30% of sonic velocity

A flow can be considered incompressible if its velocity is less than 30% of its sonic velocity. For measurement of static pressure, surface which is parallel to flow is used. So, only random motion of air is measured at point A of figure 5.1. Total pressure is measured at point B, as shown in figure 5.1. The inlet is aligned parallel to flow, so that particles of air flow are isentropically decelerated to zero velocity. For such a fluid, the Bernoulli equation describes the relationship between the velocity and pressure along a streamline [66],

$$p_0 = p_s + \frac{1}{2}\rho v^2 \tag{5.1}$$

Where p_0 is the total pressure

p_s is the static pressure

v is the velocity of sled relative to flow

ρ is the density of the medium through which body moves

The relationship between the velocity and the measured total pressure is derived as follows

$$or \qquad v = \sqrt{\frac{2}{\rho}(p_0 - p_s)} \tag{5.2}$$

.

Here, the density of the medium is given by $\rho = \frac{p_s}{RT_s}$ (5.3)

Where R is the specific gas constant, its value for air at standard conditions is 287J/kg K.

T_s is the ambient temperature as measured on the day of trial, which is taken as 300°K for sake of calculation. The static pressure is value of pressure measured on barometer at the trial site and is taken as $p_s = 96500\ N/m^2$. Density of medium through which the sled moves becomes

$$\rho = \frac{96500}{287x300}$$

$$= 1.1207\ kg/m^3$$

$$v = \sqrt{\frac{2}{1.1207}(p_0 - 96500)}$$

$$or \qquad v = 1.336\sqrt{(p_0 - 96500)}\ {}^{m}/_{s} \tag{5.4}$$

Value of pressure measured, at point B of figure 5.1, on port for total pressure p_0 is put into equation 5.4 to obtain the velocity, that is , when it is less than 30% of sonic velocity.

5.1.2 Velocities greater than 30% and less than 100% of the sonic velocity

For flow velocities greater than 30% of the sonic velocity, the fluid is to be treated as compressible. In this section we will be working in velocity regime where in the relative velocity of flow and sled will be between 30% and 100%.

When a Pitot tube is exposed to a subsonic compressible flow, fluid traveling along the streamline that ends on the Pitot tube's stagnation point is continuously compressed. It manifests itself at point B in figure 5.1. If we assume that the flow decelerated and compressed from the free-stream state isentropically, the velocity-pressure relationship for the Pitot tube is given by following Bernoulli's equation [66],

$$\frac{v^2}{2} + \frac{\gamma}{\gamma - 1}\frac{p_s}{\rho_s} = \frac{\gamma}{\gamma - 1}\frac{p_0}{\rho_0} \tag{5.5}$$

Where the description of symbols p_s & $p_0$are as described in section 5.4.1.

γ gamma is a constant. Its value depends upon the ratio of specific heat at constant pressure to the specific heat at constant volume and it's value for air at standard conditions is taken as 1.4

ρ_0 is the density of fluid at point of stagnation

ρ_s is the density of ambient air where trial is conducted

Now deriving the expression so as to find the velocity v as a funtion of total pressure p_0,

$$p_0 = \frac{\gamma - 1}{\gamma}\rho_0\left(\frac{v^2}{2} + \frac{\gamma}{\gamma - 1}\frac{p_s}{\rho_s}\right) \tag{5.6}$$

$$p_0 = \left(\frac{\gamma - 1}{\gamma}\frac{\rho_0 v^2}{2}\right) + \rho_0\frac{p_s}{\rho_s} \tag{5.7}$$

Dividing both sides by p_s, we get

$$\frac{p_0}{p_s} = \frac{\rho_0}{\rho_s}\left[\frac{1}{2}\left(\frac{\gamma - 1}{\gamma}\right)\frac{\rho_s v^2}{p_s} + 1\right] \tag{5.8}$$

$$\frac{p_0}{p_s}\frac{1}{\frac{\rho_0}{\rho_s}} = \frac{1}{2}\left(\frac{\gamma-1}{\gamma}\right)\frac{\rho_s v^2}{p_s} + 1 \quad (5.9)$$

Since $\frac{\rho_0}{\rho_s} = (\frac{p_0}{p_s})^{1/\gamma}$

$$(\frac{p_0}{p_s})^{\gamma-1/\gamma} = \frac{1}{2}\left(\frac{\gamma-1}{\gamma}\right)\frac{\rho_s v^2}{p_s} + 1 \quad (5.10)$$

$$v = \sqrt{\left(\left(\frac{p_0}{p_s}\right)^{\gamma-1/\gamma} - 1\right)\left(\frac{2\gamma}{\gamma-1}\right)\frac{p_s}{\rho_s}} \quad (5.12)$$

Putting $p_s = 96500\ N/m^2, \rho_s = 1.1207\ kg/m^3 \&\ \gamma = 1.4, weget$

$$v = 776.37\sqrt{(\frac{p_0}{96500})^{0.2857} - 1} \quad (5.13)$$

Now total pressure p_0, at point B of figure 5.1, measured by the pressure transducer in Pitot tube is put in equation 5.13 to get the velocity of sled under compressible flow.

5.1.3 Supersonic Velocities

At supersonic velocities the flow field is supersonic compressible flow. For supersonic flow having Mach number M > 1, the fluid element travelling along streamline A, B & C terminates at the Pitot tube's stagnation point C, which is at the mouth of Pitot tube (Figure 5.2).

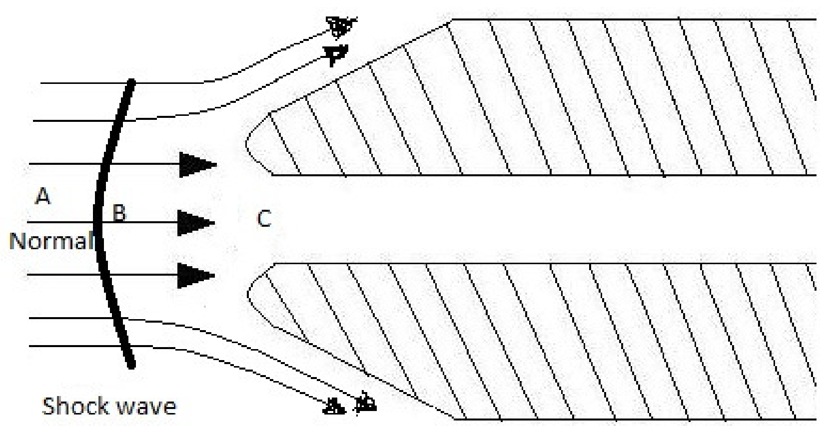

Figure 5.2 Pitot tube in supersonic flow

As shown in figure 5.2, the free stream is supersonic, which is obstructed by the Pitot tube. This causes a bow like shock wave formation ahead of tube. Fluid element at A travels normal to shock wave along A, B & C. Fluid element traveling along this streamline is first decelerated non-isentropically to a subsonic speed and then decelerated isentropically to zero velocity at the stagnation point C.

5.1.3.1 Reduction in measured pressure due to shock wave

The pressure measured at point C of figure 5.2, for supersonic flow is less than the pressure at point C for subsonic flow due to formation of shock wave. On the other hand, the pressure at point A is a measure of the velocity. Unlike the case of subsonic flow, the relationship between pressure and velocity does not exist. We find a relationship between total pressure and Mach number at C and extend it to determine the velocity at A.

The equations 5.14, 5.15 and 5.16, as given in ref [64], describe relation between pressures at different points with respect to the Mach number, viz, ahead of point A and behind the point B and C of figure 5.2 the shock wave.

$$\frac{p_2}{p_1} = 1 + \frac{2\gamma}{\gamma+1}\left(M_1^2 - 1\right) = \frac{1-\gamma+2\gamma M_1^2}{\gamma+1} \quad (5.14)$$

$$\frac{p_{02}}{p_2} = \left(1 + \frac{\gamma-1}{2} M_2^2\right)^{\frac{\gamma}{\gamma-1}} \quad (5.15)$$

$$M_2^2 = \frac{1 + \frac{\gamma-1}{2} M_1^2}{\gamma M_1^2 - \frac{(\gamma-1)}{2}} \quad (5.16)$$

Here p_{02} is the total pressure at stagnation point C and is as measured by the pressure transducer in the Pitot tube when shock wave has formed.

p2 is the static pressure we feel when we ride along with air at local flow velocity when no shock wave is formed, as is the case at sub-sonic velocity.

γ is a constant with value 1.4 for air.

For a normal shock wave, M1 is Mach number of the flow ahead of shock wave (point A of figure 5.2) and M2 is the Mach number behind the shock wave (at point C in figure 5.2). Equation 5.16 shows that Mach number behind the wave is a function of Mach number ahead of the shock wave. These equations 5.14, 5.15 and 5.16 are used to derive an expression of Mach number in terms of the total pressure which will further lead to determining the velocity. Putting value of M1 from equation 5.16 in equation 5.15 we get

$$\frac{p_{02}}{p_2} = \left[1 + \frac{\gamma-1}{2}\left[\frac{1+\frac{\gamma-1}{2}M_1^2}{2\gamma M_1^2 - \frac{(\gamma-1)}{2}}\right]\right]^{\frac{\gamma}{\gamma-1}} = \left[1 + (\gamma-1)\left[\frac{2+(\gamma-1)M_1^2}{4\gamma M_1^2 - 2(\gamma-1)}\right]\right]^{\frac{\gamma}{\gamma-1}} \quad (5.17)$$

$$= \left[\frac{4\gamma M_1^2 - 2(\gamma-1) + 2(\gamma-1) + (\gamma-1)^2 M_1^2}{4\gamma M_1^2 - 2(\gamma-1)}\right]^{\frac{\gamma}{\gamma-1}} \quad (5.18)$$

$$= \left[\frac{4\gamma M_1^2 + (\gamma^2 - 2\gamma + 1) \quad M_1^2}{4\gamma M_1^2 - 2(\gamma-1)}\right]^{\frac{\gamma}{\gamma-1}} = \left[\frac{(\gamma^2 + 2\gamma + 1) \quad M_1^2}{4\gamma M_1^2 - 2(\gamma-1)}\right]^{\frac{\gamma}{\gamma-1}} \quad (5.19)$$

or $$\frac{p_{02}}{p_1} = \left[\frac{(\gamma+1)^2 M_1^2}{4\gamma M_1^2 - 2(\gamma-1)}\right]^{\frac{\gamma}{\gamma-1}} \quad (5.20)$$

Multiplying equations 5.20 and equation (5.7), we get

$$\frac{p_{02}}{p_1} = \frac{p_{02}}{p_2} \times \frac{p_2}{p_1} = \left[\frac{(\gamma+1)^2 M_1^2}{4\gamma M_1^2 - 2(\gamma-1)}\right]^{\frac{\gamma}{\gamma-1}} \times \left[\frac{1-\gamma+2YM_1^2}{\gamma+1}\right] \quad (5.21)$$

or $$\frac{p_{02}}{p_1} = \left[\frac{(\gamma+1)^2 M_1^2}{4\gamma M_1^2 - 2(\gamma-1)}\right]^{\frac{\gamma}{\gamma-1}} \times \left[\frac{1-\gamma+2YM_1^2}{\gamma+1}\right] \quad (5.22)$$

$$= \left[\frac{(\gamma+1)^2 M_1^2}{2[(1-\gamma)+2\gamma M_1^2]}\right]^{\frac{\gamma}{\gamma-1}} \times \left[\frac{1-\gamma+2YM_1^2}{\gamma+1}\right] \quad (5.23)$$

This has taken the form of Rayeigh Pitot Tube Formula. For air as medium, the value of $\gamma\ is$ 1.14. So,

$$\frac{p_{02}}{p_1} = \left[\frac{(2.4)^2 M_1^2}{2[(-0.4) + 2.8M_1^2]}\right]^{3.5} \times \left[\frac{(0.4) + 2.8M_1^2}{2.4}\right] \quad (5.24)$$

$$= \frac{[5.76M_1^2]^{3.5}}{(2^{3.5})[(-0.4)+2.8M_1^2]^{3.5-1}} \times \left[\frac{1}{2.4}\right] \quad (5.25)$$

$$= \frac{16.89M_1^7}{[(-0.4)+2.8M_1^2]^{2.5}} \quad (5.26)$$

$$0.059\frac{p_{02}}{p_1} = \frac{M_1^7}{[(-0.4)+2.8M_1^2]^{\frac{5}{2}}} \quad (5.27)$$

Squaring both sides of equation 5.27 and expanding $[2.8M_1^2 - 0.4]^5$ by binomial distribution, we get

$$[3.481 \times 10^{-3}]\left[\frac{p_{02}}{p_1}\right]^2 = \frac{M_1^{14}}{[-0.01024 + 0.3584M_1^2 - 5.0176M_1^4 + 35.1232\ M_1^6 - 122.9M_1^8 + (M_1^{10} \times 172.1)]}$$

$$-0.01024M^{-14} + 0.3584M_1^{-12} - 5.0176M_1^{-10} + 35.123M_1^{-8} - 122.9M_1^{-6} + 172.1M_1^{-4} = \left[\frac{p_1}{p_{02}}\right]^2 287.3 \quad (5.28)$$

or

$$287.27\left[\frac{p_1}{p_{02}}\right]^2 = \left[-0.01024M^{-14} + 0.3584M_1^{-12} - 5.0176M_1^{-10} + 35.123M_1^{-8} - 122.9M_1^{-6} + 172.1M_1^{-4}\right] \quad (5.29)$$

This is the desired simplified equation. Putting the value of p_{02}, which is measured by the pressure transducer on total pressure port and p1 is the pressure of the free stream as given by a barometer at ambient pressure, we obtain the Mach number of M_1 of the free stream by numerical method. The value of velocity can now be obtained from this Mach number.

5.1.3.2 Determining Velocity

Knowing the Mach number from equation 5.27, we can determine velocity by first finding out the velocity of sound in the medium in which the sled travels. The velocity of sound a, as given in [64], is

$$a = \sqrt{\gamma RT} \quad (5.30)$$

Where

R is specific gas constant; its value for air at standard conditions is 287 J/kg K

γ is a constant, its value depends upon the ratio of specific heat at constant pressure to the specific heat at constant volume and for air at standard conditions it's value is 1.4

T is gas temperature, which in this case will be the temperature of the ambient air.

The velocity 'v' of sled using equations 5.29 and equations 5.30 is given by

$$v = M_1 a \quad (5.31)$$

The value of M_1 found from equation 5.29 and 'a' from equation 5.30 is put in equation 5.31, so as to determine the velocity of sled. That is the desired velocity of sled at supersonic speed.

5.2 Pitot based sensor system

As Pitot tube has been in use in aeronautical applications for very long, it was felt that it would be prudent to deploy it for measurement of velocity of rocket sled. Such a system is suitable for velocity regimes in which the experiments are conducted at RTRS with additional advantage of having continuous data. The sensor developed in this study, for measurement of velocity based on pressure comprised of three main parts, namely

- Pitot tube
- coupler and
- boom

5.2.1 Pitot tube

The Pitot was meant to give stagnation pressure and the static pressure. Figure 5.1 shows a simplified diagram of Pitot tube where in ports for total pressure and static pressure are shown. Stagnation pressure is in fact the total pressure comprising of dynamic pressure due to velocity and the static pressure due to atmosphere. Point A is chosen such that there is no turbulence around the port. It is shown as point A in the figure 5.1. The stagnation pressure develops at point B. Both these points are located within the Pitot tube of figure 5.3.

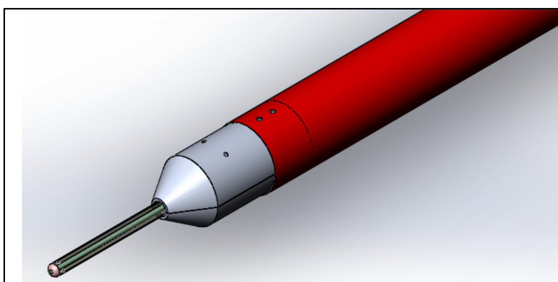

Figure 5.3: Pictorial view of Pitot, Pitot coupler and Pitot boom. The model is shown in left picture and its hardware realization on the right hand side for adaptation to the sled.

The Pitot sensor system was first modeled as shown in figure 5.3 and then fabricated.

5.2.1.1 Pitot static pressure

The tubes recording static pressure and stagnation pressure are frequently combined into one instrument known as a Pitot-static tube. Static pressure is the one we feel when moving along with the flow. The salient points of such a tube are

- There is an error in static pressure due to flow field created by probe itself.
- The ‘static’ tube surrounds the ‘total head’ tube and two or more small holes are drilled radially through the outer wall into the annular space.
- Total pressure (p0) is usually developed to high degree of accuracy.

- An error in differential pressure Δqc usually exists because of Δp, an error in the static pressure (p) measurement. This is because air flow over the body creates a flow field where pressure varies widely from one point to another and this variation is different for different configurations.

- The dynamic pressure is derived from total pressure and static pressure. An error in measurement of static pressure results in error in dynamic pressure and hence the error in velocity.
- The location of these 'static pressure holes' is important.

5.2.1.2 **Pitot total pressure**

The fluid element travelling with free stream comes to rest at point C as shown in figure 5.2. The elevated total pressure at this point is measured by the pressure transducer at total pressure port. Measurement of total pressure can be accomplished accurately considering a number of factors that influence the total pressure measurement in Pitot tube. The description of these factors is given in [64].

5.2.2 Coupler

The pressures at point A and B of figure 5.1 needs to be transferred to pressure transducers.

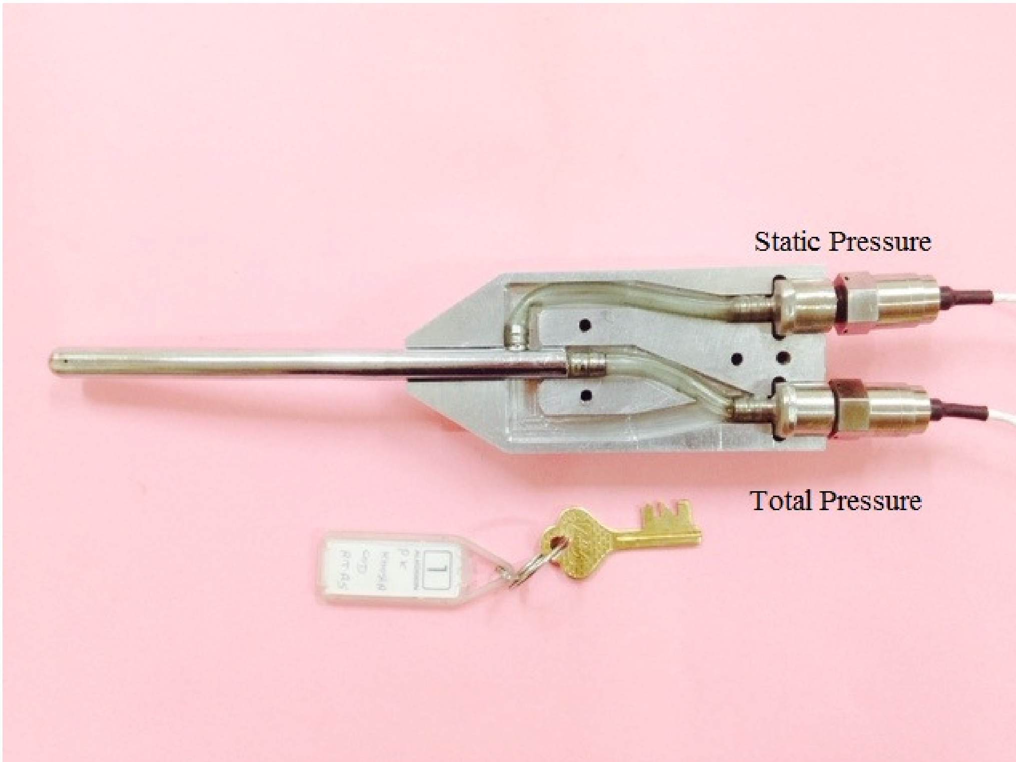

Figure 5.4 : Pitot with ports and pressure transducers fitted for measurement of static and total pressure

Additionally an arrangement is required to attach it to a boom which will extend the Pitot ahead of sled. The proposed coupler was specifically designed to meet this requirement. The coupler so developed and fabricated is shown in figure 5.4. The specifications of the pressure transducers shown in this figure at right hand are given in table 5.1.

5.2.3 Boom

On the moving sled, the Pitot should be located such that it moves through free air stream. This requires extending the Pitot tube ahead of the sled so that it operates in unobstructed air stream. The coupler serves the purpose of interfacing the Pitot tube on one side and boom on the other side. The boom is shown as a red colored fixture in figure 5.3.

5.3 Integration

All the three parts, namely, Pitot tube, coupler and the boom are assembled and integrated with the sled. The Pitot tube is mounted on sled in such a way (figure 5.5) that the flow of air stream is not disturbed by any other member of the moving body.

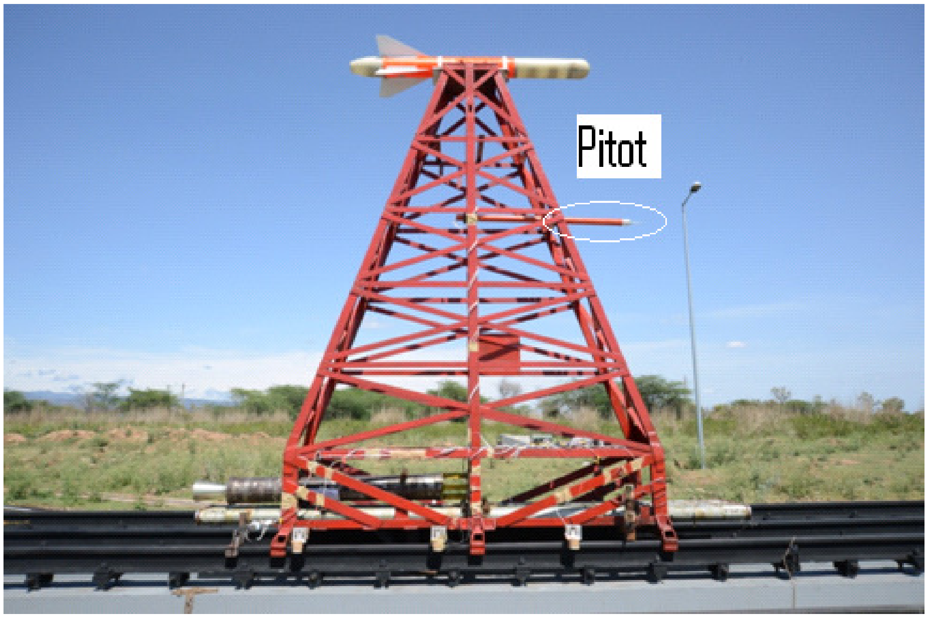

Figure 5.5: Mounting of Pitot in the rocket sled in an experiment. Motion of sled is from left to right.

As per the practice in this study, more than one experiment is conducted in different configuration. Figure 5.6 shows yet another implementation of developed methodology. The Pitot sensor system was identical in the trials shown in figure 5.5 and figure 5.6. The main difference is that in figure 5.5 the motion is from left to right and in figure 5.6, the motion is from right to left.

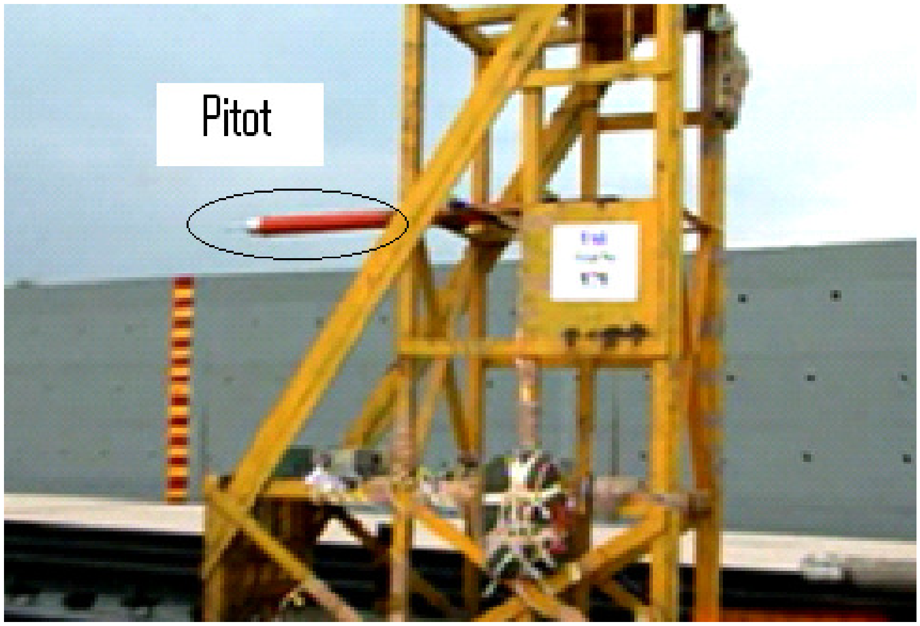

Figure 5.6: Integration of Pitot sensor system with the sled while the motion is from right to left.

5.4 Velocimeter for Rocket Sled

Having developed the Pitot tube sensor which could be deployed on the sled, the experimental setup was rigged up. Provision was made to record the output on the velocimeter card. This required development of a card which was capable of recording signals from all the three techniques developed under this research. That is, to acquire and record signals from magneto-inductive sensors, accelerometer and the pressure transducers of Pitot. The card also provided excitation to accelerometer and the pressure transducers. The block diagram of the system is shown in figure 5.7. The channel for measurement of pressure was added to the hardware depicted in figure 3.14.

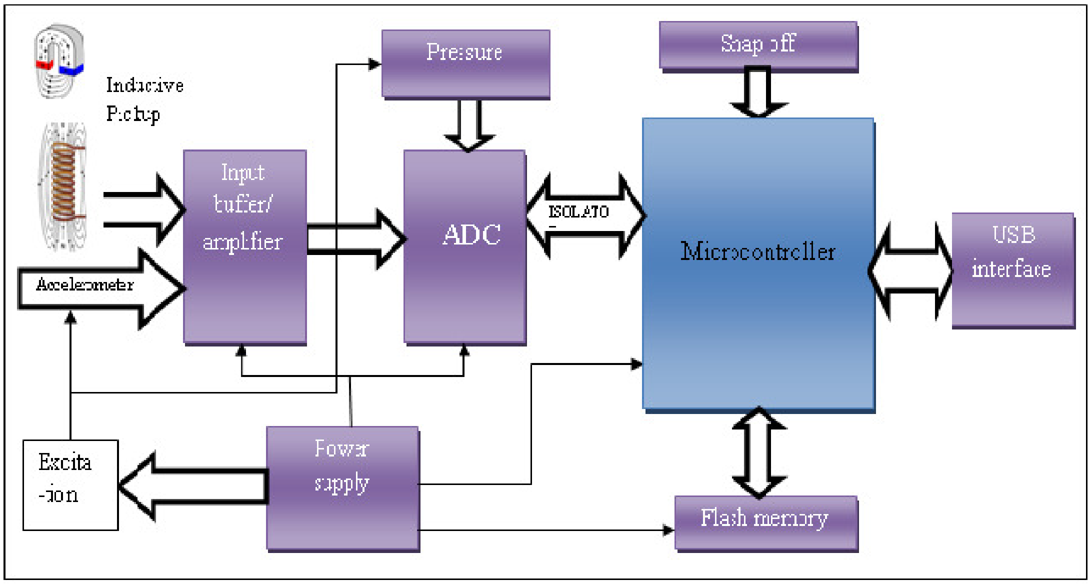

Figure 5.7: Velocimeter developed as a product for measurement of velocity using all the three different primary measurements.

Table 5.1: Brief specifications of pressure transducer used on ports of Pitot		
S.No	Parameter	Value
	Range	7 bar (100 psi)
	Sensitivity	720 mV/bar
	Bandwidth	DC - 5 kHz
	Sensing Principle	Wheatstone Bridge
	Make	Kulite

The broad specifications of the pressure transducer and hardware deployed in the experiment the ports for static pressure and total pressure are shown in Table 5.1. Figure 6.xin chapter 6 shows the populated PCB of velocimetry card realized for acquiring velocity using three different primary measurements. The hardware so realized was used for conducting experiments explained in the next section.

5.5 Experiments

Based on the theory described in this chapter and the systems realized, two experiments were conducted to determine velocity. Setup shown in the picture in figure 5.5 was used to conduct experiment. Two pressure transducers shown in figure

5.4 were used to sense pressures. Total pressure and the static pressure recorded are shown in figure 5.8.

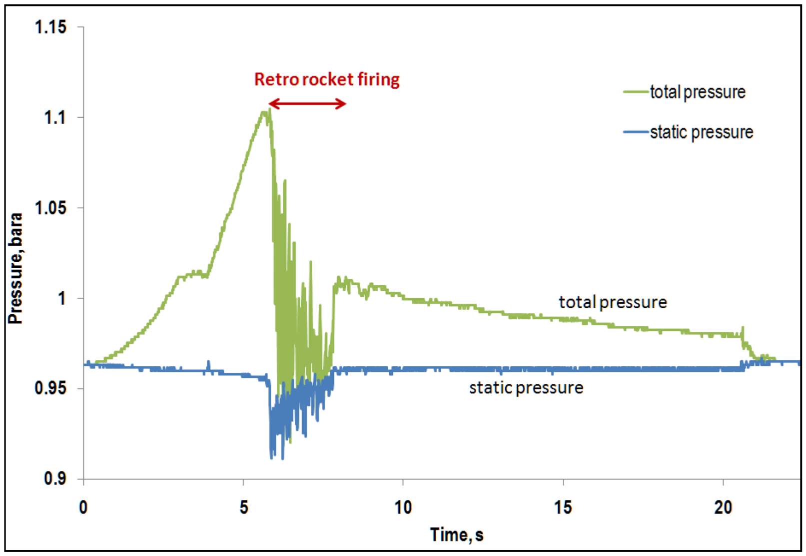

Figure 5.8: Plot of total pressure and static pressure recorded using Pitot tube

The static pressure does not remain constant. The value of static pressure measured by Pitot is influenced by axial location of orifice along tube, shape of nose section of tube, size and shape of turbulence on rear portion of the tube, size and configuration of orifice and location on projectile body. Therefore, static pressure measured by Pitot was not used in the computation of velocity. Instead, ambient pressure was taken as the static pressure, as the sled run is along a level rail track and the pressure in the test terrain will not change.

This was the case of sub-sonic velocity and the velocity derived from pressure is shown in figure 5.9. A step at point 'A' as shown in figure 5.9 occurs when first phase of rockets providing thrust have burnt out and the second stage has been ignited. The noise was observed between point B and C also. It can be attributed to two factors. One, the retro rockets which provide thrust in the opposite direction so as to apply brakes to the sled was used in this region.

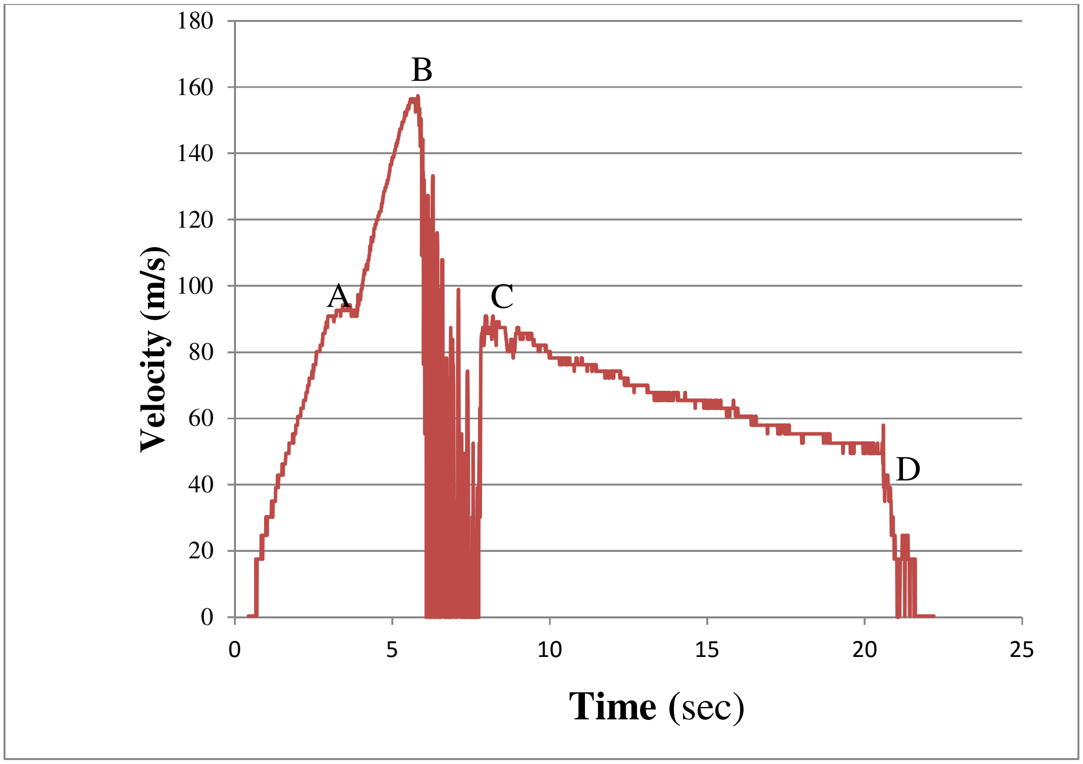

Figure 5.9: Velocity derived from pressure plotted in figure 5.8

The plume of this rocket as shown in Figure 5.10 could have affected the flow field seen by Pitot tube. The second possible reason can be increased level of vibration in this region that affects the electronics and causes noise. The hardware could log data for 20 sec, so record after D is not available.

Figure 5.10: Plume due to retro-rockets, which affects the measurement of total pressure, was seen on the right end

Another experiment was conducted in which the retro rocket was not used. Setup shown in the picture in figure 5.6 was used to conduct experiment. Two pressure transducers shown in figure 5.4 were used to sense pressures. The plot of total pressure, static pressure and the ambient pressure is shown in figure 5.11. In this experiment also the graph of static pressure was not constant. The ambient pressure was taken as the static for calculation of velocity.

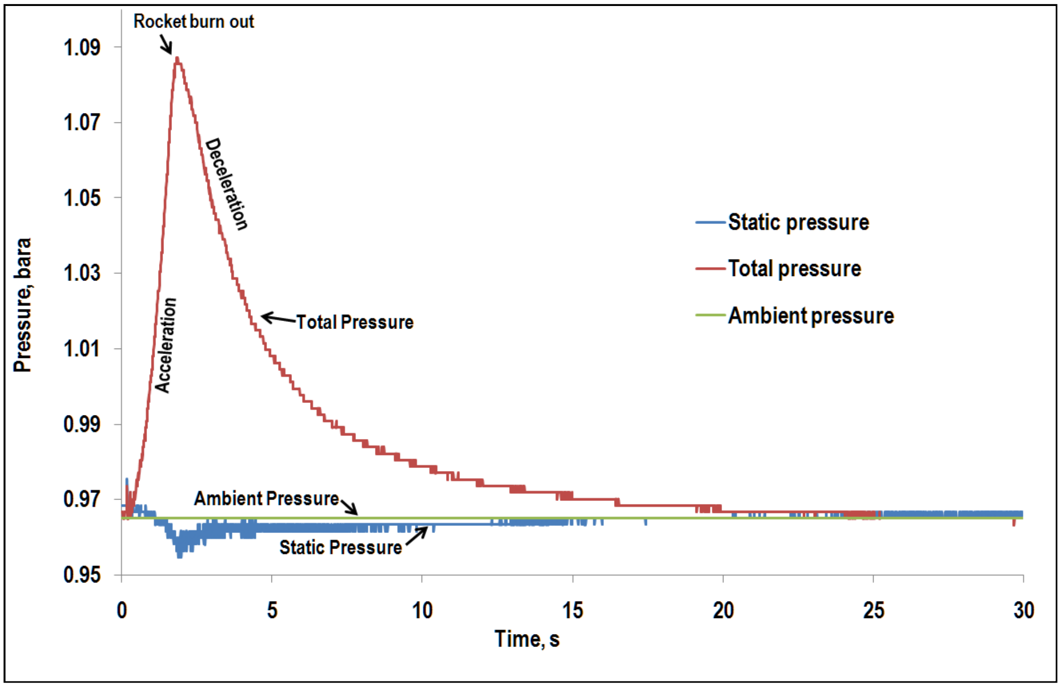

Figure 5.11: Variation in pressure in another trial where retro rocket was not fired

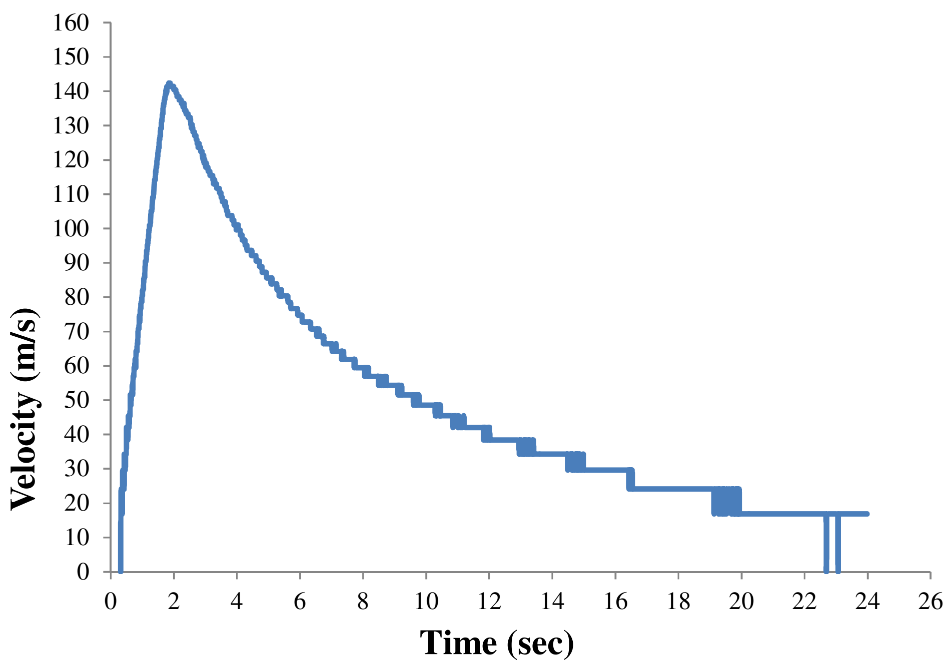

Figure 5.12: Velocity derived from pressure plotted in figure 5.12

The velocity so obtained is shown in figure 5.12. No noise was observed in this case as compared to the previous experiment. In this case steps were observed in the plot, which are attributed to inadequate amplifier gain at the output of pressure transducers.

5.6 Summary of the chapter

Pitot tube has been deployed for measurement of velocity of supersonic rocket sled for the first time. No single equation establishes relationship between the pressure and the velocity. So equations to be considered for determining velocity under different flow regimes have been discussed. A relationship between total pressure and Mach number was established, which further leads to velocity. While measuring the static pressure with Pitot tube, significant errors have been reported in the literature as well as observed in the experiments that have been conducted in this study. We have been able to find the velocity without taking into consideration the static pressure measured by the Pitot tube. This method can be deployed in all the ground based applications where Pitot is put to use. Limitation for sled borne application has also been identified. A Pitot tube based device capable of measuring total pressure and static pressure were developed, fabricated and deployed in the experiments. The velocity was derived and the results presented.

Chapter 6

Comparison of techniques, Conclusion and Future Scope of Work

6.1 Introduction

This thesis presents work on determining velocity using three different primary measurements, namely, distance, acceleration and pressure. Testimony of a successful research is the realization of a product based on the outcome of studies. The embedded system shown in figure 6.1 has been realized in such a manner that it can measure distance-time, acceleration and pressure. The same is recorded in on-board flash memory and it derives velocity from recorded values.

Figure 6.1: Velocity derived from pressure plotted in figure 5.12

This system does not have a DSP processor, similar to the one explained in chapter 4. Being an offline activity, the computational load is shifted to desktop PC. The brief discussion and conclusion of the studies is explained below.

6.2 Research on Distance and Time Based Velocity

The research described in Chapter 3, focuses on the improvements in the magneto-inductive pick up and determines velocity based on distance and time. In an experiment, result of which are tabulated in table 3.1, it was found that the existing sensor will not be able to detect signals if the velocity increases beyond 500 m/s. Usual thinking would have been to increase the number of turns of inductive pick-up so as to increase the amplitude of the output. But, the research findings entailed decreasing number of turns. A mathematical model of the existing sensor as described by equations (3.4-3.5)was developed as shown in figure 3.7. Based on this model, the reasons for fall in amplitude were explained in section 3.1 and an improved sensor was proposed. The result of improvement is evident from the experimental result presented in figure 3.18. For ready reference it is reproduced in figure 6.2. It shows that under identical conditions the proposed sensor output recorded was 1.13 V against amplitude of 0.25V of existing sensor in an experiment of sled run at 303 m/s. That was the highest feasible velocity achieved in an experiment.

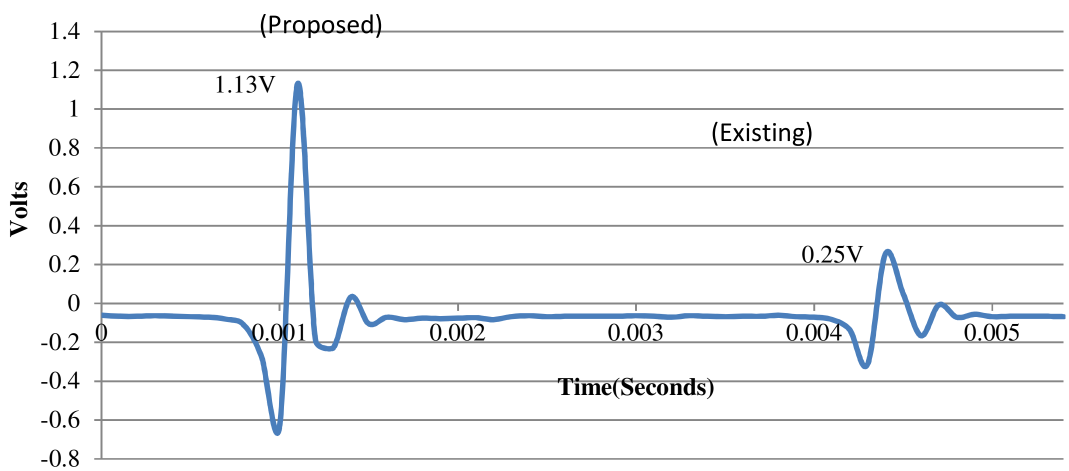

Figure 6.2: Comparative output of proposed and existing sensor at 303 m/s (1091 km/hr)

The improved sensor was realized in larger numbers and a system was implemented so as to be deployable in a sled run experiment. The method of communication of signals to control room is also shown in figure 3.17. The results of experiments plotted in figure 3.14 and figure 3.19 are based on signals acquired using proposed sensors.

Such a system offers higher level of precision as compared to the other two techniques. As explained in section 3.10.3, the relative error was found to be 0.046%.In this system the absolute values of distances are available and the system has been considered as reference system for comparison of results of other two techniques, too.

6.3 Comparative Study of Velocity Derived from Acceleration Based Systems Versus Distance-Time Based Systems

It was found that acceleration can be another measureable parameter which can lead to accurate velocity of high speed sled. If the output of accelerometer is integrated, the value of velocity so obtained has large error and is not directly usable. Chapter 4 explained this aspect of research. A number of factors which contribute to errors and issues in the present problem were identified. The methodology of obtaining corrected position and velocity was established. Three accelerometers of different makes were deployed in every experiment. This offered several advantages such as more data from a single trial, evaluating effects of sensors of different makes and allowing data fusion which leads to position. It is pertinent to mention that each trial requires months of preparation. Values of position at different points were considered as reference data as accurate values of position data was available along the track. A number of operations need to be performed over the acquired data so as to improve the accuracy of final velocity.

The techniques to reduce these errors have also been implemented practically and the results are presented. It has been found that the error in measurement can be reduced by using bias correction, use of position fix, proper mounting of sensors and by trapezoidal rule of integration. In this study, the trapezoidal method has been observed to give minimum error and the result was found to be 0.2 m closer to the reference value for all the three sensors deployed in the experiment as compared to the Euler's method of integration. Most significant improvement was observed on position fix. The accuracy of the order of 1.5% was achieved with one of the sensors. Figure 6.3 shows difference between experimental velocity data from reference magneto-inductive system and velocity data from acceleration based system as a percentage of velocity from magneto-inductive system. It evident from the figure 6.3 that the difference between the two sets has remained within 2.5% of the velocity measured by magneto-inductive system. As the focus of this research was higher velocities, velocities below 80 m/s have not been considered.

The study substantiates the fact that the choice of accelerometers with low drift low noise density and properly designed anti-vibration mounts will give better results. The methodology of quantification of errors presented here can be followed for study of other possible errors, too.

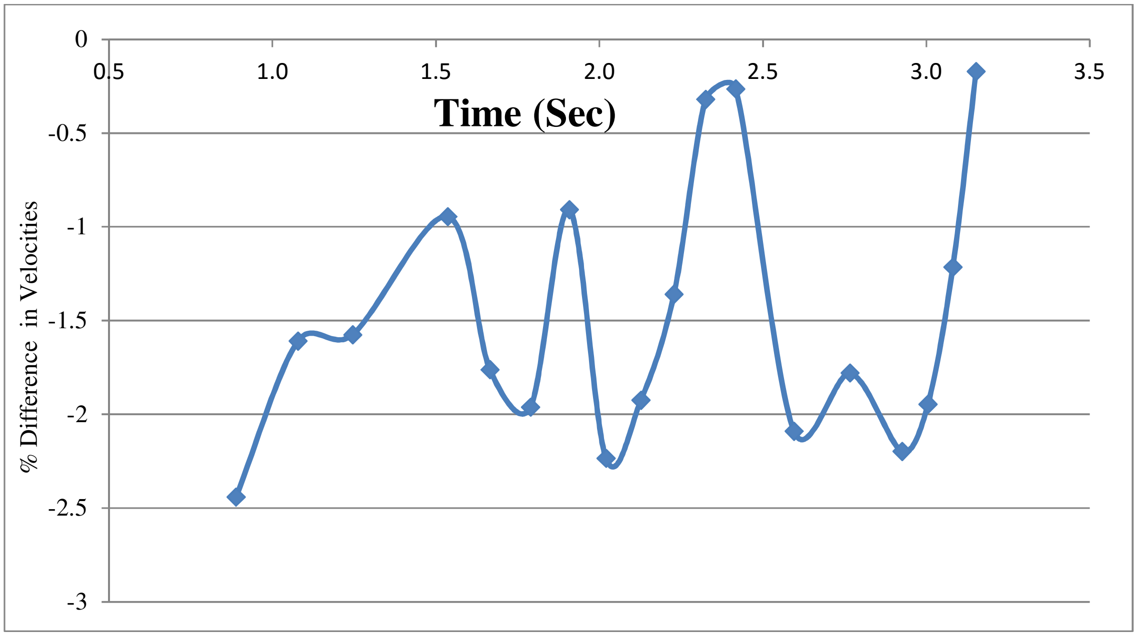

Figure 6.3: Percentage Difference between experimental velocity data from reference magneto-inductive system and acceleration based system

Fusion of data from number of sensors was also carried out and a methodology was evolved by application of existing principles to a new application. The results obtained were comparable to the methods presented in position fix based method. The major advantage of fusion of data over position fix was that no additional hardware is required to sense position, when sled is running at supersonic speed. It is pertinent to mention here that carrying additional hardware in high speed onboard systems is a penalty.

6.4 Comparative Velocity Derived from Pressure Versus Distance-Time Based Systems

The study of velocity based on pressure, was explained in chapter 5. Its comparison with the reference system was studied in two different experiments. The comparative graph of first experiment is shown in figure 6.4. The flow field in front of Pitot was disturbed due to firing of retro rockets for applying brakes to the sled. Therefore, the velocity between the times 6 to 8 sec was noisy. The percentage difference between the two set of values from velocimeter and the Pitot is potted in figure 6.5.

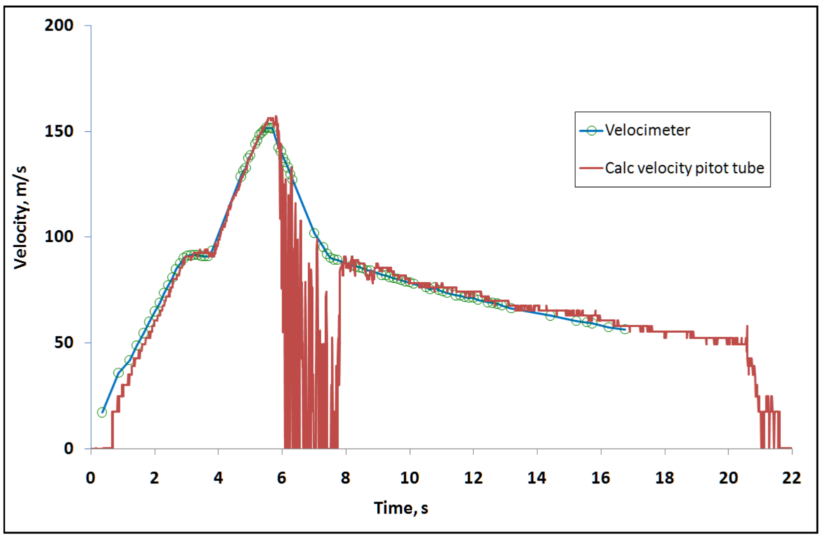

Figure 6.4: Comparative results of velocimeter and Pitot

The values of differences are omitted while flow field was disturbed. The percentage difference was found to be between +2.9% and -5.5%. Another experiment was conducted to check consistency and to check the signals while no retro rockets were fired. Figure 6.6 is the graph of the comparative velocity from distance based and pressure based values. It does not show any disturbance in the flow field and hence the velocities were in agreement with the expectation.

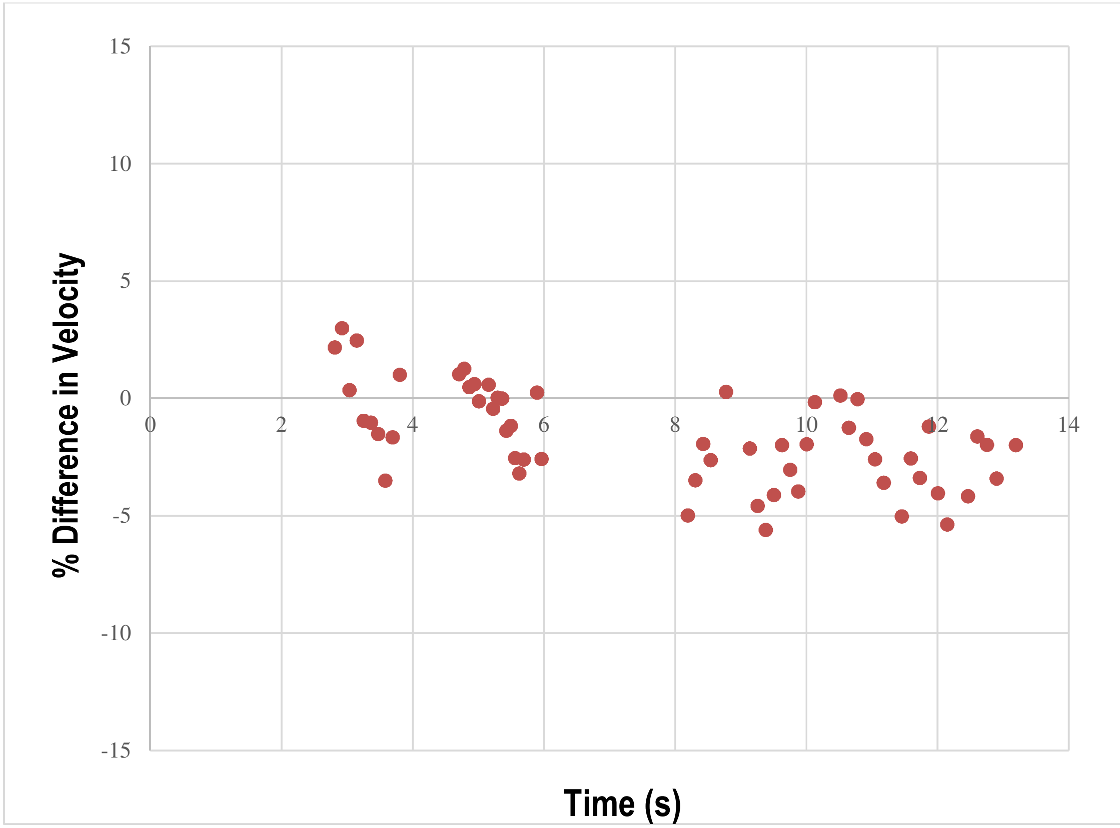

Figure 6.5: Percentage difference in velocities between velocimeter and Pitot based as shown in figure 6.4

The values of percentage difference between distance based and pressure based values, which are plotted in figure 6.6, was determined. These values are shown in figure 6.7. The band of spread is found to be between 5.7% and -2.5%. The spread in this experiment is 8.2% as compared to the spread of 8.4% in the previous experiment. The focus of this study being higher velocities, comparison below velocity of 80m/s has not been attempted.

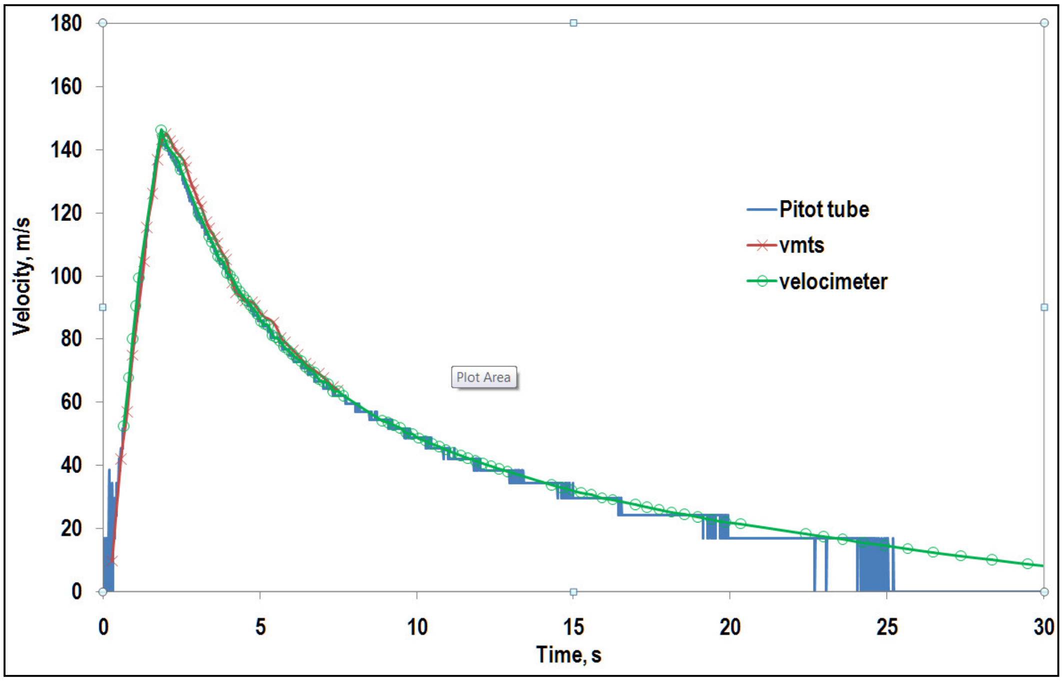

Figure 6.6: VMTS and Velocimeter are the values of velocity from distance based system while velocity from Pitot based system is plotted in blue colour.

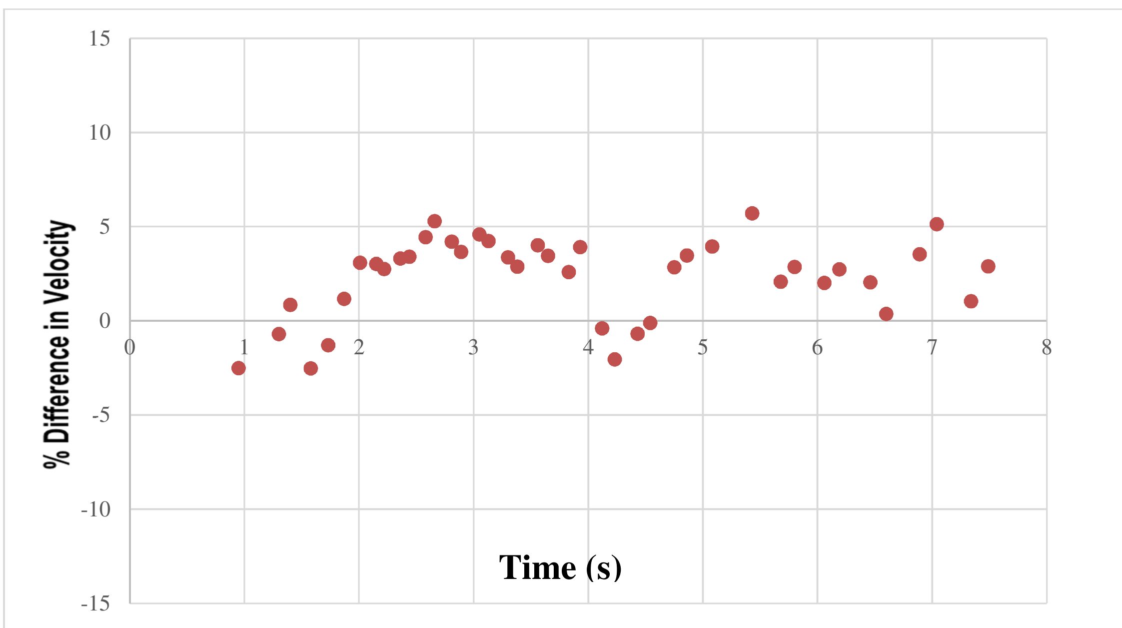

Figure 6.7: Percentage difference in velocities depicted in figure 6.6

6.5 Qualitative comparison of three proposed techniques

The table below highlights various aspects of three different techniques:

Table 6.1: Qualitative comparison of three proposed techniques

S. No	Attribute	Magneto-Inductive	Acceleration Based	Pressure Based
1.	**Number of Samples**	No of samples available are equal to the sensors deployed	No of samples available depend upon the sampling rate.	No of samples available depend upon the sampling rate.
2.	**Primary Data**	Primary data is distance which is differentiated to obtain velocity. It increases the level of noise.	Primary data is acceleration which is integrated to obtain velocity. It reduces the level of noise.	The velocity is proportional to difference of pressures and does not affect the noise.
3.	**Data Points**	Maximum 400 data points are available in sled application.	Data points are in tens of thousands based on sampling rate	Data points are in tens of thousands based on sampling rate
4.	**Accuracy of distances**	Accurate discrete distances are available	Distances are prone to errors and error reduction techniques are to be employed	Distance obtained is not as accurate as the one in magneto-inductive system
5.	**Derivation of Velocity from primary data**	Velocity derived is noisy due to processes of	Velocity is smooth due to integration process	Velocity is directly available as neither integration nor

		interpolation and differentiation		differentiation is required. Square root of pressure difference gives velocity.
6.	**Installation cost**	Initial installation cost and effort is high	Installation cost and effort is low	Installation cost and effort is higher than acceleration system but much lower than magneto-inductive systems
7.	**Online/Offline**	Information is available to the user in real time	Available offline	Available offline
8.	**Triggering and control**	Parameter based triggering and control of onboard systems is not feasible when used as a ground based system.	Parameter based triggering and easier to realise	Parameter based triggering and control is feasible
9.	**Control of cameras and recording devices**	Parameter based triggering of ground based cameras and other ground based recording devices is feasible	Parameter based triggering of ground based cameras and other ground based recording devices is not feasible	Parameter based triggering of ground based cameras and other ground based recording devices is not feasible

10.	**Ground based or Onboard system**	Essentially a ground based system. Only a permanent magnet is required to be on mobile sled. When used as a velocimeter, it is an onboard system.	It has to be an on-board system	It is an onboard system
11.	**Range of sensor for measurement of high velocity**	Sensor has been improved for measurements at supersonic velocity	Range of sensor is the only limitation for operation at supersonic velocity	The formula for deriving of velocity from pressure will be different at supersonic velocity
12.	**Complexity of system**	Having initial installation, the operation in every experiment is easy and requires least effort, irrespective of the sled used	Needs to be installed before every experiment as the sled is different in different experiments	Installation is most complex before every experiment
13.	**Primary Measurement Accuracy**	Distance being primary measurement, the accuracy in distance domain	Acceleration being primary measurement, the accuracy in acceleration	Pressure is primary measurement and velocity is proportional to difference of

		will be maximum.	domain will be maximum.	pressures, accuracy in velocity domain will be maximum.
14.	**Calibration requirement**	Primary measurement is position and absolute distances between positions on the ground can be measured, precise calibration and hence accuracy in distance domain will be maximum.	Can be calibrated with respect to magnet-inductive system.	Can be calibrated with respect to magnet-inductive system.

6.6 Conclusion

The objective of this research was to develop three different techniques for measurement of supersonic sled, which has been fulfilled. Based on outcome of this research a system has been realized which can simultaneously measure the velocity based on position, acceleration and pressure as the primary measurements.

The magneto-inductive sensor has been improved and it has been established that using this sensor supersonic velocities can also be measured. This sensor senses the position of sled during its high speed travel. The positions are pre-calibrated. It was found that the relative error in velocity with one of such systems was 0.046%. The approach to identifying the problem and bringing about the improvement will be of immense value other similar work. It has been experimentally found that the amplitude of signal obtained from proposed sensor is higher than the amplitude from existing sensor.

Challenges in obtaining velocity from acceleration have been widely covered in chapter 4. Error quantification & mitigation, positions fix and data fusion techniques have been developed. Various applications utilizing MEMs accelerometers will benefit from the techniques proposed in this chapter. The study is a step towards improving our system level understanding and bringing MEMS accelerometers in the domain of applications which demand better accuracy and traditionally use expensive accelerometers. It was found that the percentage difference in velocity data from magneto-inductive system and the acceleration based system was within 2.5%.

Further, the work on measurement of velocity using pressure gave fairly good results. This is the only technique where the velocity was found to be directly proportional to the measured parameter. Its adaption to sled application was attempted for the first time and it posed several challenges. When retro rocket is fired to reverse the direction of sled, the rocket plume, disturbs the flow of air into the Pitot and causes noisy data and prevents measurement of velocity. It was found that the percentage difference in velocity data from magneto-inductive system and the pressure based system was within 8.4%.

Table 6.1 shows that each technique has some advantages and disadvantages and provides information that will help in choosing technique for different applications.

The magneto-inductive system was found to be most suitable and acceleration based measurements provided the next best option.

6.7 Future challenges

The qualitative comparison of three techniques is given in table 6.1. It is amply clear that each technique has some advantages and disadvantages.

- Challenges in magneto inductive system the effect of change in sensor impedance with velocity will have effect on coupling of signal with the transmission line.
- There will also be effect of loading of impedance by other sensors, especially, at lower velocities.
- The effect of change in reference for calculation of time will generate error, albeit small, which needs to be quantified.
- Finding the instantaneous velocity from single pulse will be a challenge and this study will be a step in that direction.
- In the study based of acceleration, the methodology of quantification of errors holds good for other possible errors, but study does not specifically investigate the errors due to misalignment of sensor axis, variation due to vehicle dynamics, non-linearity of scale factor, cross coupling effect and error due to temperature sensitivity etc. When position fix is applied, these errors also get compensated. The study of these individual factors can also be attempted on lines similar to the ones proposed in this thesis.
- In the study based on pressure finding a flow field free of turbulence and locating a sensor can be a challenge and solution researched.
- Work on fusion of data from all three proposed techniques will be of immense value in futuristic systems.

7 References

[1]J. F. Meyers and H. Komine, "Doppler global velocimetry: a new way to look at velocity,", *Laser Anemometry*, vol. 1, pp. 289-296, 1991.

[2] D. J. Jie*et al.*,"All-fiber displacement interference velocity measurement system data processing method research based on S-transformation,"in *2nd IEEE Int. Conf. on Computer Science and Information Technology, ICCSIT 2009*,2009, pp. 48-51.

[3] H. Zheng et al, "Advantages in using multi-frequency driving to enhance ultrasound contrast microbubble non-linearities for optimizing echo particle image velocimetry techniques," in *Int. Symp. on Biomedical Imaging: Nano to Macro, 2004, IEEE*,2004, pp. 500-503.

[4] D. Starratt et al. "An efficient method for continuous measurement of projectile motion in ballistic impact experiments." *International J. of Impact Engineering,* vol. 24, no. 2, pp. 155-170, 2000.

[5] Phillips, D. B., M. P. Lee, F. C. Speirits, S. M. Barnett, S. H. Simpson, M. P. J. Lavery, M. J. Padgett, G. M. Gibson ,et al. "Rotational Doppler velocimetry to probe the angular velocity of spinning microparticles," *Physical Review A,*vol. 90, no. 1, pp. 011801, 2014.

[6]F. J. Beutler, L. L.Rauch*et al*, " Precision Measurement of Supersonic Rocket Sled Velocity,*" J. of Jet Propulsion,* vol. 27, no. 9, , pp. 1021-1024 Sept. 1957.

[7] F. J. Beutler, "Precision Measurement of Supersonic Rocket Sled Velocity-Part II,*"J. of Jet Propulsion*, vol. 28, no. 12, pp. 809-816, 1958.

[8] J.Stirtonand B. Glatt, "Hybrid Velocity Data for the Velocity Measuring System of the Supersonic Naval Ordnance Research Track,*" Proc. of the IRE*, vol. 47, no. 5, pp. 963-969, 1959.

[9] W. Naumann, K. Engberg, and R. D. Hogg,J. Hunka, andG. Oliver, "Rocket Sled Improved Velocity Measuring System Feasibility Study,"Defense Technical Information Center, DITC document, 1980.

[10] P.P. Dubeyand P. Borkar, "Review on techniques for traffic jam detection and congestion avoidance," *Electronics and Communication Systems (ICECS)*, 2nd Int. Conf. on. IEEE, 2015, pp. 434-440.

[11] G. John, "Advances in inductive position sensor technology," *Sensor Review*, vol. 30, no. 2, pp.142 – 147, 2010.

[12] J. Lenz and A. S. Edelstein, "Magnetic sensors and their applications,"*IEEE Sensors J.,*vol.6, no. 3, pp 631-649, June 2006.

[13] Edelen Russ, "Behind the scenes: SNORT instrumentation," Air Time, Nav Air Ranges, Rep. vol. III, issue I, pp. 9-17, 2007.

[14] E. R. Laithwaite, "Adapting a linear induction motor for the acceleration of large masses to high velocities,"*IEE Proc.-Electric Power Applications,* vol. 142, no. 4, pp. 262-268, 1995.

[15] S. T. Jeng and L. Chu, "A high-definition traffic performance monitoring system with the Inductive Loop Detector signature technology,"*in Int. Conf. on Intelligent Transportation Systems (ITSC), IEEE 17th,* 2014, pp. 1820-1825.

[16] Y.Y. Jung et al, "Position Sensing System for Magnet Based Autonomous Vehicle and Robot Using 1-Dimensional Magnetic Field Sensor Array,"*Int. Joint Conf SICE-ICASE,* IEEE,2006, pp. 187-192.

[17] I.M. Chhabra,"Ring Laser Gyroscope" paper presented at *5th All India Combined Rajbhasha Scientific and Technical Conf.* held on 18-19 Feb'2010 at RCI, Hyderabad, India, 2010.

[18] R. Periyasamy, A. Mishra, S. Anand, and A. C. Ammini. "Foot pressure distribution variation in pre-obese and non-obese adult subject while standing," *The Foot,*vol. 22, no. 4, pp. 276-282, 2012.

[19] J. Bryzek, "Emergence of a $ Trillion MEMS sensor market," *Proc. SensorCon*, Santa Clara, 2012.

[20] E. Levenberg, "Inferring pavement properties using an embedded accelerometer," *International J. of Transportation Science and Technology*, vol. 1, no. 3,pp. 229-246, 2012.

[21] M. Lele and G. Jason, "Evaluation of solid state accelerometer sensor for effective position estimation," in *9th World Congress on Intelligent Control and Automation (WCICA)*, Taipei, Taiwan, IEEE, 2011, pp. 959-964.

[22] H. Liu and G. Pang, "Evaluation of a Low Cost Solid-state Accelerometer as a Distance Measuring Sensor for Vehicle Positioning System." In *IEEE proc. of Int. Conf. onIntelligent Transportation Systems*,Tokyo, 1999, pp. 435-440.

[23] El Faouzi, *et al*,"Data fusion in intelligent transportation systems: Progress and challenges–A survey," *Information Fusion*, vol. 12, no. 1, pp 4-10, 2011.

[24]O.P.Sahu, A.K.Gupta, “Measurement of Distance and Medium Velocity Using Frequency Modulated Sound/Ultrasound” *IEEE Transaction on I and M*,vol. 57, no. 4, pp. 838-42, 2007.

[25]Heirich, Oliver, et al. “Bayesian train localization method extended by 3D geometric railway track observations from inertial sensors.”*Information Fusion (FUSION), 2012 15th Int. Conf. on*. IEEE, 2012, pp. 426-423.

[26] R. C. Kalonia, et al. "Multiple laser-based high-speed digital shadowgraphy system for small caliber projectile-target interaction studies.*"Optical Engineering* vol. 53, no. 3, 2014.

[27] M.Sahu*et al*, "Critical appraisal of various techniques used for velocity Distribution in open channel flow," *Proc. of 9th Int. Conf. on Hydro-Science and Engineering (ICHE 2010)*, IIT Madras, Chennai, 2010.

[28]A. S. Mulmule, M. S.Tirumkudulu and K. Ramamurthi, “Instability of a moving liquid sheet in the presence of acoustic forcing,"*Physics of Fluids (1994-present)*vol. 22, no. 2, pp. 022101,2010.

[29] R. J. Klopfonstein ,“Air velocity and flow measurement using a Pitot tube,” *ISA Transactions*, vol. 37, no. 4, pp. 257-263, 1998.

[30]S. Padhy and S. Panigrahi,” Measuring projectile velocity using shock wave pressure sensor,”*Defence Science Journal*, vol. 64, no. 6, pp. 499-501, Nov. 2014

[31] R. C., Kalonia, M.Gautam, Amod Kumar, R. K. Varma, Manpreet Singh, V. S. Sethi, "Laser-based projectile speed measurement system." *Optical Engineering,* vol. 46, no. 4, pp. 044303-044303, 2007.

[32]W. G. Proud, S. M. Walley, D. M. Williamson, A. L. Collins, and J. W. Addiss, "Recent trends in research on energetic materials at Cambridge," Central European J. of Energetic Materials,vol. 6, no.1, pp. 67-102, 2009.

[33] W. G. Proud, "The measurement of hot-spots in granulated ammonium nitrate," in *AIP conf. proc*.,2002, no. 2, pp. 1081-1086.

[34] Rajeev Agrawal, S. Kalyanasundaram, V. Ramachandran, V. Raman, "Directional Distance-based Location Update Mechanism Using Knowledge of Mobility Patterns”. Scholar.google.co.in

[35]Baibak, Timothy, Rajeev Agrawal, "AC 2007-495: programming games to learn algorithms," Available: www.scholar.google.co.in, 2007.

[36]S. Kumar, S. C. Sharma and B. Suman, "Classification and evaluation of mobility metrics for mobility model movement patterns in mobile Ad-Hoc networks," in *Int. j. on applications of graph theory in wireless ad hoc and sensor networks (GRAPH-HOC,)* vol. 3, 2011.

[37] J. G. Stuart, "Electric Initiator ESD Hazard, "*8th Int. High Energy Materials Conf. & Exhibit (HEMCE-2011), 2011.*

[38] D. Turnbull *et al*"Soft Sled Test Capability at the Holloman High Speed Test Track." U.S. Air Force T&E Days 2010 Nashville, Tennessee, rep. AIAA 2010-1708,2 - 4 February 2010.

[39] D. Nakata, et al, "Research and Development of High Speed Test Track Facility in Japan,"*In Aerospace Expo. ,*Nashville, Tennessee, 2012, pp. 1-11.

[40] E.Akeila, Z.Salcic and A. Swain,"Reducing low-cost INS error accumulation in distance estimation using self-resetting," *IEEE Trans. Instrumentation and Measurement,* vol. 6, no. 1,pp. 177-184, Jan. 2014.

[41] S. Tumanski,"Induction coil sensors – a review," *Measurement Science and Technololgy*, vol. 18, no. 3, pp. R31,2007.

[42] A. Leuzinger and A. Taylor,"Magneto-Inductive Technology Overview," *white paper by PNI Sensor Corporation,* Feb 2010.

[43] V. Leus, S. Taylor,"*Experimental* Evidence for the Magneto-kinematic Effect," in *Progress in Electromagnetic Research Seminar (PIERS) Proc.*Moscow, Russia, 2012, pp. 1040-1048.

[44] Leus, Vladimir A. "Magneto-Kinematical and Electro-Kinematical Fields," *Progress in Electromagnetics Research* M, vol. 32, pp. 27-41, July 2013.

[45]P. K. Khosla, R. Khanna and S. P. Sood, "Analysis of Magneto-inductive System for rocket Sled Velocity Measurement Beyond Mach 1.5," *Defence Science Journal*, vol. 64, no. 2, pp. 143-151, Mar. 2014.

[46] P.S.Maybeck, "Introduction" in *Stochastic, models, estimation and control*, vol. I, New York: Academic Press, 1979, pp. 2 and 11.

[47] JorgJerosch and Jürgen Heisel, "Management der Arthrose: Innovative Therapiekonzepte (in German)". in *DeutscherÄrzteverlag*. ISBN 978-3-7691-0599-5, pp 107, Retrieved 2011.

[48] Y.K. Thong, M.S. Woolfson, J.A. Crowe, B. R. Hayes-Gill,R.E. Challis, "Dependence of inertial measurements of distance on accelerometer noise," in *Measurement Science and Technology,* vol.13, no. 8**,** pp. 1163-1172, 2002.

[49] Y.K. Thong, M.S. Woolfson, J.A. Crowe, B.R. Hayes-Gill, D. A. Jones, "Numerical double integration of acceleration measurementsin noise," in Measurement, vol.36, no. 1, pp. 73–92, 2004.

[50] L. Hoff, O. J. Elle, M. Grimnes, S.Halvorsen, H. J. Alker, E. Fosse,*"*Measurementsof Heart Motion using Accelerometers,"*IEEE Proc. of sensors,* vol. 3, pp. 1353-1354, 2004.

[51] S. Nikbakht, M. Mazlom, A. Khayatian,*"Evaluation* of Solid State Accelerometer Sensor for Position Estimation,*" IEEE Int. Conf. on industrial technology,* Hong Kong, 2005, pp.729-723.

[52] C. Verplaetse, "Inertial proprioceptive devices,Self-motion sensing toys and tools," in *IBM Systems J.*, vol. 35, no. 3 and 4, pp. 639-650,1996.

[53] Y. Hirao, S. Kunimatsu,T. Hamamoto,*"*Wireless Measurement System for Ground-borne Vibration and Vibration Amplifications in Buildings,*"Mapan*, vol. 27, no. 4, pp. 231-239, 2012.

[54] C.Tan, S. Park, "Design of Accelerometer-Based Inertial
Navigation Systems,*"* in IEEE Transactions On Instrumentation And Measurementvol. 54, no. 6, 2005.

[55] P.Neto*et al*, "3-D position estimation from inertial sensing: minimizing the error from the process of double integration of accelerations,*"*Annu. Conf. of the IEEE Industrial Electronics Society IECON, Vienna, Austria, 2013, pp. 4024-4029.

[56] G.A. Aydemir and A. Saranli, "Characterization and calibration of MEMS inertial sensors for state and parameter estimation applications,*"* in Measurement J.,vol.45 no. 5, pp.1210–1225.

[57] K. N. Suryanarayana Rao, "GAGAN – The Indian satellite based augmentation system,*"*in Indian Journal of Radio and Space Physics vol. 36, no. 4, pp. 293-302.

[58]Indian Space Projects,*"*GAGAN Satellite Based Navigation System," Available:http://isp.justthe80.com/space-applications/gagan, Jan. 2014.

[59] Indian Defence Secretary, “GAGAN will be put in place by end of 2014,” in The Hindu (News Paper), 14th Dec, 2013.

[60] T.H. Whitte and A.M. Wilson, “Accuracy of WAAS-enabled GPS for the determination of position and speed over ground*,” in J. of Biomechanics,*vol.38, no. 8, pp. 1717-1722, 2005.

[61] P. K. Khosla, R. Khanna and S. P. Sood, "Quantification and Mitigation of Errors in the Inertial Measurements of Distance,*" MAPAN – Journal of Metrological Society of India*, vol. 30, no.1, pp. 49-57, 2015.

[62] V. N. Ojha, S. K. Sharma, S. K. Singhal, G. S. Lamba, “Insulation Resistance Measurement of High Impedance Accelerometer Cables,*” in MAPAN—J. of Metrology Society of India* vol. 19, No. 1-2, pp. 117-120, 2004.

[63]B.Khaleghi, A. Khamis, F. O. Karray, S. N. Raazvi, "Multisensor data fusion: A review of the state-of-the-art," in *Information Fusion* vol. 14, no. 1, pp. 28-44, 2013.

[64] J.D. Anderson Jr, “Normal Shock Waves and Related Topics,” in *Fundamentals of Aerodynamics,* 5th ed., New York, McGraw Hill Education (India), 2013, ch. 8, pp. 529-548.

[65] A. R. Porro, “Pressure probe designs for dynamic pressure measurements in a supersonic flow field,” *19th Int. Congr. on ICIASF* 2001 *Instrumentation in Aerospace Simulation Facilities, 20001*, IEEE, 2001, pp. 417-426.

[66] E. Ower and R. C.Pankhurst, “Bernoulli’s theorem and its application to the measurement of flow velocity,” in the Measurement of air flow, 5th ed., Elsevier, 2014, pp. 10-15.

[67] Y. Tani, Y. Yokota, M. Yayota, O. Masato, “Automatic recognition and classification of cattle chewing activity by an acoustic monitoring method with a single-axis acceleration sensor,” in *Computers and Electronics in Agriculture*, vol. 92, pp. 54–65, March 2013.